For Reference

NOT TO BE TAKEN FROM THIS ROOM

Ex libris
universitatis
albertaensis

QUAECUMQUE VERA

Grad Studies

THE UNIVERSITY OF ALBERTA

RELEASE FORM

NAME OF AUTHOR Brenda J. Hutcheon-Johnson

TITLE OF THESIS Interactions of Gadolinium and Platinum Ions with the Crystalline and Solution States of Phosphorylase

DEGREE FOR WHICH THESIS WAS PRESENTED Master of Science

YEAR THIS DEGREE GRANTED Spring 1977

Permission is hereby granted to the UNIVERSITY OF ALBERTA LIBRARY to reproduce single copies of this thesis and to lend or sell such copies for private, scholarly or scientific research purposes only.

The author reserves other publication rights, and neither the thesis nor extensive extracts from it may be printed or otherwise reproduced without the author's written permission.

THE UNIVERSITY OF ALBERTA

INTERACTIONS OF GADOLINIUM AND PLATINUM IONS WITH THE CRYSTALLINE AND SOLUTION STATES OF PHOSPHORYLASE

by

Ⓒ BRENDA J. HUTCHEON-JOHNSON

A THESIS

SUBMITTED TO THE FACULTY OF GRADUATE STUDIES AND RESEARCH
IN PARTIAL FULFILLMENT OF THE REQUIREMENTS FOR THE DEGREE
OF MASTER OF SCIENCE

DEPARTMENT OF BIOCHEMISTRY

EDMONTON, ALBERTA

SPRING, 1977

Digitized by the Internet Archive
in 2023 with funding from
University of Alberta Library

https://archive.org/details/Hutcheon1977

THE UNIVERSITY OF ALBERTA

FACULTY OF GRADUATE STUDIES AND RESEARCH

The undersigned certify that they have read, and recommend to the Faculty of Graduate Studies and Research for acceptance, a thesis entitled INTERACTIONS OF GADOLINIUM AND PLATINUM IONS WITH THE CRYSTALLINE AND SOLUTION STATES OF PHOSPHORYLASE submitted by BRENDA HUTCHEON-JOHNSON in partial fulfillment of the requirements for the degree of Master of Science.

ABSTRACT

The physico-chemical characteristics of metallocomplexes of glycogen phosphorylase in both the solution and crystalline states of the enzyme were examined to establish the degree of structural correlation between these two physical forms. One metal derivative, platinumdiamminodichloride, was selected for investigation due to the covalent nature of its complex formation, its ligand specificity and its prior use as a heavy atom derivative in the x-ray maps of both phosphorylases _a_ and _b_. The paramagnetic character of gadolinium trichloride salts in conjunction with the large changes Gd induces in phosphorylase properties, supported the use of this lanthanide element as a second derivative.

Metal induced perturbations of the enzyme were indicated by activity, sedimentation velocity, spectral and chemical modification studies. The occupancy of metal sites was examined with titration curves, n.m.r. techniques, atomic absorption analyses and spectrophotometric assays.

In the solution state, Pt derivatives of phosphorylase exhibit monomerization, inactivation, PLP perturbation and the loss of a titratable sulfhydryl group in either the N or the A peptide. The solution site was compatible in several aspects with the environment of Pt site 1 which was determined from x-ray analyses. Although evidence exists for a second Pt site, correlations with the crystalline state are tenuous.

Three unique types of metal coordination sites were found with Gd derivatives of phosphorylase in the solution state. The highest affinity site alters the alpha aggregation and coenzyme sites. The secondary locus promotes tetramerization of phosphorylase _a_ and nucleo-

tide-phosphorylase b complexes, while retaining the integrity of both the active and the coenzyme sites. The lowest affinity Gd site(s) promotes gross protein conformational changes as evidenced by the loss of AMP homotropic cooperativity, polydisperse molecular weights, enhanced reactivity of Cys residues with DTNB and PCMB, inactivation and increases in the absorbance at 415 nm. Based on these properties, the Gd sites established from x-ray analyses, are tentatively matched with the highest affinity solution site correlating with Gd site 1 and the secondary solution locus with Gd site 2.

ACKNOWLEDGEMENTS

The development of this thesis involved contributions directly or indirectly from several individuals. Assistance extended by Mr. Gerry McQuaid and Dr. Brian Sykes with both the technical and theoretical problems encountered in the n.m.r. experiments was greatly appreciated. In addition I would like to thank Mr. Kim Oikawa for his contributions to the polarized light studies and Mr. Morris Aarbo for the ultracentrifugation runs that he conducted in connection with this work.

I am also indebted to Dr. J. Sygusch and Dr. R. Fletterick for information regarding the current status of the x-ray structure of phosphorylase. Preliminary studies concerning Gd and carbodiimide interactions with phosphorylase, which were conducted by Dr. O. Avramovic-Zikic, served as a starting point for this research.

I wish to extend my appreciation to the several members of Dr. N.B. Madsen's research group who were constantly striving to improve my laboratory techniques. In particular I wish to mention Mrs. Shirley Shechosky, who contributed willingly to this work with advice on several matters concerning phosphorylase purification and characterization. I also wish to thank Mrs. Nancy Murray who gallantly undertook the typing of this manuscript.

Finally I wish to convey to my supervisor, Dr. N.B. Madsen, my deep appreciation for the time, effort and patience he has so willingly donated during the course of this study.

TABLE OF CONTENTS

PAGE

ABSTRACT iv

ACKNOWLEDGEMENTS vi

TABLE OF CONTENTS vii

LIST OF FIGURES x

LIST OF TABLES xiii

LIST OF ABBREVIATIONS xiv

CHAPTER I INTRODUCTION 1

CHAPTER II METHODS AND MATERIALS

- A. Materials 5
- B. Methods
  - 1. Protein Preparation 5
  - 2. Platinum Analytical Techniques
    - a. QDT/$SnCl_2$ Method 7
    - b. Atomic Absorption 8
  - 3. Spectral and Ultracentrifugal Studies 8
  - 4. Preparation of Pyridoxal Analogues 9
  - 5. Polarized Light Techniques 9
  - 6. Phosphorous N.M.R. Spectroscopy 9
  - 7. Water Proton Relaxation Enhancement 10

CHAPTER III INTERACTIONS OF PAC WITH PHOSPHORYLASE b

- A. Introduction
- B. Results
  - 1. PAC Coordination to Phosphorylase b in the Solution State
    - a. Number of Metal Binding Sites

        i. Atomic Absorption.................................. 13
        ii. Spectrophotometric................................ 13
      b. Metal Titration.. 14
      c. Inactivation Studies................................... 14
      d. Ligand Protection of the Enzyme from Metal Induced Inactivation.. 20
      e. Fluorescence Spectra................................... 27
      f. Polarized Light Studies................................ 27
      g. Sulfhydryl Reactivity.................................. 30
      h. Sedimentation Velocity Profile......................... 32
    2. PAC Coordination to Phosphorylase _b_ in the Crystalline State
      a. Number of Metal Binding Sites.......................... 35
      b. Activity Studies with Crosslinked Crystals............. 38
      c. Activity Studies with Solubilized Crystals of the Metalloprotein................................ 39
  C. Discussion.. 40

CHAPTER IV INTERACTIONS OF GADOLINIUM IONS WITH PHOSPHORYLASE

  A. Introduction.. 46
  B. Results
    1. Gd Interactions with Phosphorylase in the Solution State
      a. Reaction Conditions.................................... 49
      b. Number of Metal Binding Sites
        i. Metal Titration Curve.............................. 50
        ii. Water Proton Relaxation........................... 57
      c. Perturbations of Phosphorylase Induced upon Gd Occupation of the Low Affinity Site

i. Activity Studies.................................. 63

ii. Coenzyme Characteristics

Absorbance and Fluorescence Spectra............. 66

Solvent Accessability........................... 74

iii. Reversibility of Metal Binding................. 76

iv. Ligand Protection Studies....................... 77

v. Sulfhydryl Reactivity........................... 83

d. Perturbation of Phosphorylase Induced upon Gd Occupation of the High Affinity Site

i. Activity and Spectral Studies................... 88

ii. Sedimentation Velocity Studies.................. 91

iii. Coenzyme Characteristics........................ 95

iv. Reversibility of Metal Binding.................. 97

v. Sulfhydryl Reactivity........................... 99

2. Gd Interactions with Phosphorylase in the Crystalline State

a. Activity Studies with Crosslinked Crystals......... 99

C. Discussion.. 101

BIBLIOGRAPHY... 110

APPENDIX I Calculations for Water Proton Relaxation Data........ 115

APPENDIX II Calculations for Polarized Light Data.............. 117

APPENDIX III The Crick Magdoff Equation for Approximating the Fractional Change in Intensity Expected upon Heavy Atom Binding to a Protein Molecule...... 119

APPENDIX IV Summary of the Observed Properties of Metallo-complexes of Phosphorylase....................... 120

LIST OF FIGURES

Figure Page

1 Activity titration curve of phosphorylase _b_ equilibrated with varying concentrations of PAC........................ 16

2 Spectral titration curve of phosphorylase _b_ equilibrated with varying concentrations of PAC........................ 18

3 Time study of inactivation upon incubation of phosphorylase _a_ with PAC... 22

4 Glucose-1-phosphate protection of phosphorylase _b_ from PAC induced inactivation................................. 24

5 AMP homocooperativity within the PAC-phosphorylase _b_ complex.. 26

6 Time studies of the rate of inactivation and fluorescence quenching upon formation of PAC-phosphorylase _b_ complexes.. 29

7 Sulfhydryl reactivity of PAC-phosphorylase _b_ with DTNB..... 34

8 Sedimentation velocity profile of phosphorylase _b_ reacted with PAC... 36

9 Activity titration curve of phosphorylase _b_ equilibrated with varying concentrations of Gd......................... 52

10 Spectral titration curve at 415 nm of phosphorylase _b_ equilibrated with varying concentrations of Gd............. 54

11 Spectral titration curve at 330 nm of phosphorylase _b_ equilibrated with varying concentrations of Gd............. 56

12 Enhancement of water proton relaxation upon titration of phosphorylase _b_ with Gd................................. 59

13 Enhancement of water proton relaxation upon titration of a constant Gd concentration with phosphorylase _b_.......... 62

Figure Page

14 Time study of inactivation and enhancement of 415 nm absorbance upon reaction of 2.7 mM Gd with phosphorylase _a_.................................. 65

15 Time studies of inactivation and 415 nm peak intensity enhancement upon reaction of 2 mM Gd with phosphorylase _b_.. 68

16 Spectral scan during the formation of the Gd-phosphorylase _b_ complex.................................. 70

17 Rate of alteration of the 415 nm peak intensity upon occupation of the low affinity Gd site in phosphorylase _b_.. 73

18 Protection study involving Gd induced inactivation of phosphorylase _b_ with 50 mM glucose........................ 80

19 Sedimentation velocity study of nucleotide complexes of phosphorylase _b_ reacted with 2 mM Gd...................... 82

20 Protection study involving Gd induced inactivation of phosphorylase _b_ in the presence of nucleotides or glucose-1-phosphate.................................. 85

21 Sulfhydryl reactivity of Gd-phosphorylase _b_ with PCMB...... 87

22 Time studies of changes in the 330 nm and 415 nm peak intensities upon occupation of the primary Gd site........ 90

23 Log plot of the change in absorbance with wavelength of phosphorylase _b_ reacted with an equimolar concentration of Gd.................................. 93

24 Sedimentation velocity study of phosphorylase _b_ in the presence and absence of 1 mM AMP reacted with an equimolar concentration of Gd.................................. 94

25 Phosphorous n.m.r. spectra of native phosphorylase _b_ within the solution state.................................. 96

Figure Page

26 Phosphorous n.m.r. spectra of phosphorylase _b_ upon occupation of the primary Gd site within the solution state........ 98

LIST OF TABLES

Table Page

1 Analyses of Lineweaver Burk plots of the PAC-phosphorylase _b_ complex.. 19

2 Secondary structural parameters obtained from polarized light studies.. 31

3 Analytical determinations of the number of PAC binding sites per phosphorylase monomer........................... 37

4 Coordinates of metal derivatives determined from x-ray crystallographic studies of phosphorylase _a_ and _b_.......... 41

5 Chelation of Gd by phosphate functional groups............. 107

LIST OF ABREVIATIONS

AMP	adenosine-5'-phosphoric acid
ATP	adenosine-5'-triphosphate
BES	N,N-bis-(2-hydroxyethyl)-2-aminoethanesulfonic acid
CD	circular dichroism
DMF	dimethyl foramide
DTNB	5,5'-dithiobis-(2-nitrobenzoic acid)
DTT	dithiothreitol
EDTA	ethylenediaminetetraacetic acid
EMTS	ethylmercurithiosalicylic acid
G-1-P	D-glucose-1-phosphate
IAM	iodoacetamide
IMP	inosine-5'-phosphoric acid
(m')	reduced mean residue rotation
MES	2-(N-morpholino)ethane sulfonic acid
NMR	nuclear magnetic resonance
OAc	acetate
O.D.	absorbance
ORD	optical rotary dispersion
PAC	platinumdiamminodichloride
PCMB	p-chloromercuribenzoate
P_i	inorganic phosphate
PLP	pyridoxal-5'-phosphate
QDT	quinoxaline dithiol

Ƶ	occupancy factor which refers to the number of electrons per heavy atom evidenced on an electron density map
λ_c	Drude dispersion constant
	correlation time
ε	molar absorbtivity
ε^*	observed enhancement of water proton relaxation
$\Delta\nu_T$	total linewidth of a nuclear resonance peak

Chapter I

Introduction

A dominant method of analyzing the structure of biological macromolecules, x-ray crystallography, examines a molecule in the solid state. However most biochemical techniques are orientated towards the solution state of a molecule. Questions naturally arise concerning the extent of correlation between molecular structures under crystal lattice restraints and those within solution. To approach this question, metal derivatives of glycogen phosphorylase (E.C.2.4.1.1.) were utilized. By examining the physico-chemical properties of the metallo complex of the enzyme from the perspective of the protein environment of the metal site, determined from x-ray crystallographic maps, the degree of similarity between the two physical states of phosphorylase could be assessed.

Before proceeding with current developments concerning this topic, a few characteristics of the enzyme will be mentioned to facilitate subsequent data interpretation. For a detailed and comprehensive review of this enzyme, the reader is referred to the excellent article published by Graves and Wang (1). Glycogen phosphorylase in vivo catalyzes the phosphorolysis of α-1,4-glycosidic bonds in polysaccharide chains, releasing G-1-P and a dextrin chain shortened by one glucose residue. Since, in vitro, the reaction is reversible, subsequent activity assays monitored the release of inorganic phosphate. Although kinetic analyses have established the rapid equilibrium random bi bi mechanism of catalysis (2), the actual structure and function of active site amino acids have yet to be elucidated. Phosphorylase exists as two interconvertable forms linked by enzymes governing the phosphorylation state of Ser 14.

Phosphorylase a in the absence of effectors expresses activity, whereas phosphorylase b, which lacks this phosphate moeity, requires AMP or IMP or certain AMP analogues for catalytic efficiency.

Both forms of the enzyme are most active in the dimeric state, although tetrameric phosphorylase a may possess some degree of activity (3). The dimer-tetramer equilibrium is governed primarily by substrates and AMP, whereas subunit dissociation is increased upon incubation with the allosteric inhibitor ATP or upon chemical modification of the enzyme's sulfhydryl groups (4). The molecular weight of each subunit has been assessed as 9.25×10^4 (5).

The absorption peaks observed at 330 nm and 415 nm in a spectral scan of phosphorylase are attributed to the coenzyme, pyridoxal -5'-phosphate. Evidence from model studies (1), iodide fluorescence quenching (6) and ethylene glycol experiments (7) have assigned this vitamin B_6 analogue to a partially closed hydrophobic pocket within the native enzyme. The accessability of PLP to solvent is governed by allosteric modifiers and subunit interactions (8). The theories of most groups coincide on the designation of the 415 nm absorption band to a schiff base formed between PLP and an ε amino group of a lysine residue. Since reduction of this imine bond results in a 40 to 60% loss of activity, implication of this bond in the catalytic mechanism was ruled out. However resolution of the coenzyme results in enzyme inactivation and monomerization.

The assignment of the tautomeric structures of PLP in the native and chemically modified enzyme remains in controversy. A recent paper by Feldman and coworkers (9) outlines the current status of the situation. Basically this group postulates along with Graves et al (7), that the

increase in the 415 nm optical density observed with the enzyme at low temperatures or pH or high ionic strengths is due to an increased exposure of the coenzyme in the schiff base form to water molecules. In the native state, within a partially closed pocket, the PLP exists as a zwitterionic schiff base with an unprotonated 3 hydroxyl group absorbing at 330 nm. The alternate approach of Honikel and Kent attributes the shift in peak intensity to a reflection of an equilibrium change between a substituted aldimine (10) or a carbinolamine (11), and the schiff base. Admittedly the absorption spectra of 3-O-methyl PLP and the chemical shifts induced in the model systems in both polar and apolar solvents upon schiff base formation argues in favour of the former proposal, however its reconciliation with the following fluorescence data is more questionable. Honikel found that the quantum yields of PLP reacted with lysine in 95% dioxane/water were too low relative to native phosphorylase. The yield could be increased by acidification. If the coenzyme existed solely as the schiff base, protonation of the 3 hydroxyl group of PLP at lower pH values would further decrease the quantum yield. Conversely the increase in the hydronium ion concentration would shift the equilibrium of the carbinolamine in favour of the schiff base resulting in fluorescence enhancement upon excitation at 415 nm. These concepts will be expanded further in subsequent sections.

Although metal ions are not involved in the catalytic mechanism directly, such divalent cations as Mn(II), Mg(II), Ca(II), Sr(II) and Ba(II) are required for enzyme crystallization (10). With phosphorylase _b_, tetramerization occurred only in the presence of AMP and millimolar concentrations of certain metal ions (12). This may be attributed to the increased affinity of phosphorylase _b_ for AMP in the presence of high

concentrations of Mg(II) (13). In 1971, the Oxford group utilized the paramagnetic properties of Mn(II) to study its interactions with phosphorylase b in the presence and absence of substrates and modifiers (14). The sigmoidal response of the water proton relaxation enhancement to increasing concentrations of AMP in conjunction with later P^{31} n.m.r. results suggests the close proximity of this high affinity metal site to the active site. The second site for Mn binding exhibits an apparent dissociation constant in the same range as metal concentrations required to promote tetramerization.

Some evidence has recently been published concerning the relationship between protein orientation in the crystalline and the solution states of phosphorylase. Kasvinsky (15) conducted activity studies with crosslinked tetragonal crystals of both phosphorylase a and b utilizing maltoheptaose as a glycogen substitute to overcome the crystal's inherent diffusion problems. Although the activities are significantly lower than the corresponding solution form, crystalline phosphorylase is definitely functional catalytically, as the K_m values of both substrates, G-1-P and maltoheptaose, are comparable in both physical states of the enzyme. In addition the distance calculated by Radda and coworkers (16) between G-1-P and AMP utilizing the paramagnetic effects of Mn in the phosphorylase b quaternary complex concurred with the crystallographic distances determined with phosphorylase a (17). Both approaches are indicative of conformational similarities between the two physical states in the region of the active site.

Chapter II

Materials and Methods

A. Materials

The metals platinumdiaminodichloride, $GdCl_3 \cdot 6H_2O$ and $LaCl_3$ were purchased from Pfaltz and Bauer Inc., Ventron and Fischer Scientific respectively. Pyridoxal and PLP were received from Sigma as were p-chloromercuribenzoate, DTNB and glutaraldehyde. Reagents for the carbodiimide modification, glycine ethyl ester • HCl and N-ethyl-N'-(3-dimethylaminopropyl) carbodiimide were obtained from Aldrich and ICN Pharmaceuticals respectively. Substrates glucose-1-phosphate and AMP were obtained from British Drug Houses and Terochem Laboratories Ltd. Glycogen was freed of AMP by passage through the chloride resin Dowex AG 1-X8. Quinoxalinedithiol was obtained from Eastman Laboratories. All buffer reagents were purchased from standard biochemical supply houses and were of the highest purity available.

B. Methods

1. Protein Preparation

Crystals of glycogen phosphorylase b and a were prepared from rabbit skeletal muscle via the respective methods of Fischer and Krebs (18); Krebs and Love (19). In both techniques, DTT was substituted for cysteine. The enzyme was recrystallized at least three times prior to use. Calculations from the phenylhydrazine assay of Wada and Snell (20) were used to determine the extent of $NaBH_4$ reduction of phosphorylase b in media of high ionic strength (21).

Prior to metal addition, phosphorylase was passed through a Sephadex G-25 column equilibrated with the appropriate buffer.

Tetragonal microcrystals of the enzyme were obtained by the method outlined by Kasvinsky (15). Repeated centrifugation at 100 rpm and resuspension in buffer A (10 mM BES, 1 mM EDTA, 5 mM DTT, 50 mM glucose, 10 mM $Mg(OAc)_2$ pH 6.8) for phosphorylase a or in buffer B (10 mM BES, 1 mM EDTA, 5 mM DTT, 2 mM IMP, 10 mM $Mg(OAc)_2$ pH 6.8) for phosphorylase b were used to size the microcrystal suspensions. Since activity studies with native crystals led to their solubilization, glutaraldehyde was used as a crosslinking reagent. Aliquots of 1×10^{-2} % glutaraldehyde were added at zero and 40 min to the crystal suspension. After a 60 min incubation at 25°C , the reaction was quenched by repeated washings with IMP and EDTA free buffer B in the case of phosphorylase b and EDTA free buffer A for phosphorylase a. It was necessary to remove excess nucleotide as Gd reacted via the phosphate group to form insoluble adducts (22). After soaking in either 10 mM Gd or 1 mM PAC overnight at 16°C , the crystals were washed to remove excess metal and resuspended in buffers A or B.

Enzyme activity was monitored in the direction of glycogen synthesis. The assays outlined by Cori et al (23) and Hedrick (24) were used to follow P_i production at 30°C. Substrate solutions at pH 6.8 contained 2 mM AMP, 2% glycogen, 32 mM glucose-1-phosphate for the former method and 2 mM AMP, 2% glycogen and 0.15 M glucose-1-phosphate for the latter. Equal volumes of substrate and buffer containing 3-5 micrograms of enzyme were combined to initiate the activity assays. The utilization of concentrations of G-1-P exceeding saturating levels, as in the Hedrick method, resulted in the linear production of P_i or zero

order kinetics.

Aliquots from a microcrystal suspension containing approximately 0.2 mg of protein per ml of substrate were assayed for P_i production at 30°C. by the method of Gold (25). In accordance with substrate permeability and diffusion difficulties encountered by the enzyme in the solid state, maltodextrins ranging from 3 to 7 glucose moieties in length were substituted for glycogen. The substrate for phosphorylase _b_ crystals contained 2 mM IMP, 25 mM glucose-1-phosphate, 1 mg/ml maltodextrins, 10 mM BES, 1 mM DTT at pH 6.8. In phosphorylase _a_ assays, 50 mM glucose was substituted for 2 mM IMP in the above solution.

Protein concentration was determined by the absorbance at 280 nm with a value of $E^{1\%}_{1\ cm}$ 13.2 (26). Microcrystals hydrolyzed in 0.1 M NaOH for 12 hr at 70°C and chemically perturbed phosphorylase were assayed according to Lowry _et al_ (30). When necessary, mercaptan interference was removed by the method of Ross (28), prior to Lowry analyses.

2. Platinum Analytical Techniques

Protein samples containing 5 to 30 X 10^{-5} M Pt were hydrolyzed in 6 N HCl at 110°C for 25 hr. The vacuum dried samples were dissolved in the appropriate solvent for each assay.

a. QDT/$SnCl_2$ method

The metalloprotein pellet was dissolved in 0.5 ml of 5.8 N HCl prior to the addition of 0.1 ml of 10% $SnCl_2$/5.8 N HCl. After the addition of 1 ml of dimethylformamide, the tube was cooled to room temperature before adding 0.2 ml of 1% quinoxalinedithiol (QDT) in dimethylformamide. After shaking, the volume was adjusted to 2.2 ml.

Absorbance at 624 nm was recorded after 1.5 hr of colour development (29). The optical densities decreased after standing for 25 hr , but their relative intensities were retained.

b. atomic absorption

Atomic absorption data was collected on a Pie Unicam instrument model SP90A. The sample pellet was dissolved in 0.1 M HCl and aspirated into an acetylene/air flame. Gas flow was maintained at 1.25 l/min , while air flow was 5 l/min and the current was 9.9 milliamperes. Platinum absorption at 285.2 nm with a slit width of 0.031 nm was standardized against $PtCl_4$ stock solutions. $LaCl_3$ at 2000 ppm was added to each sample to decrease ionic interference (30).

3. Spectral and Ultracentrifugation Studies

Sedimentation velocity studies were conducted at a speed of 56,000 to 59,000 rpm in a Beckman Spinco Model E ultracentrifuge equipped with schlieren optics. The Kel-F centerpiece was maintained at 20°C.

A Zeiss PMQII spectrophotometer equilibrated at 30°C or 25°C monitored changes in the 330 nm and the 415 nm absorption peaks. Spectral scans were recorded on a Durram prism grating spectrophotometer model D200.

The excitation and emission spectra were recorded on a Turner 210 absolute spectrofluorimeter, with samples absorbing at less than 0.1 O.D. at the excitation wavelength. Fluorescence yields were calculated by dividing the area under the emission peak by the concentration of the molecular species absorbing at the excitation wavelength.

4. Preparation of PLP-Val Schiff Base

Model studies with pyridoxal and PLP were conducted at pH 6.8 in 30 mM BES in the presence and absence of 18.5 mM Gd. Pyridoxal phosphate valine was prepared by incubating 0.2 mM PLP and 2 mM Val in absolute methanol at 30°C for 3 hr (31). Gadolinium was added at a concentration of 5×10^{-5} M and incubated for 15 min prior to spectral analyses.

5. Polarized Light Technique

Optical data were collected on a Cary 60 spectropolarimeter a CD attachment regulated at 25°C. The metalloprotein was prepared by incubating phosphorylase b at 5 mg/ml in 10 mM BES, 1 mM DTT, 1 mM EDTA at pH 6.8 with a ten molar excess of PAC for 12 hr at 25°C. The native and modified enzyme were dialyzed against two changes of the above buffer for 16 hr. ORD and CD spectra were monitored over the respective ranges of 600 nm to 300 nm and 250 nm to 205 nm which are troughs corresponding to the peptide backbone. Linear regression analyses of Yang-Moffat plots (32) generated a_o and b_o values which were used in calculating the fractions of alpha helix, beta sheet and random coiled structures as outlined in Appendix 2. The coefficients determined by Chen *et al* (33) were used to convert the ellipticity parameters to the secondary structural components.

6. Phosphorous N.M.R. Spectroscopy

Spectra of phosphorous resonances were recorded at 109.3 MHz (6.34 Telsa) with a HX 270 Bruker N.M.R. spectrometer. Each spectrum represented a 5000 Hz sweep width of 52,000 transients. Each transient was observed during a 0.41 sec aquisition time with a 1.3 sec delay between 45^o pulses.

Proton decoupling with 5 W. continuous wave was used to simplify the spectrum. Data was weighted with a line broadening of 100 Hz. Phosphoric acid was used as a chemical shift reference and the sample temperature was maintained at $300^{\circ}K$.

Measurements were obtained with 2 ml samples containing a 6.9×10^{-4} M concentration of AMP free phosphorylase b in 30 mM BES, 3 mM DTT pH 6.8. Due to its ability to chelate Gd, EDTA was not present in the buffer, however special precautions were undertaken to minimize paramagnetic contamination. The metalloprotein was formed upon the addition of 5.5×10^{-4} M $GdCl_3$ to an NMR tube of 10 mm diameter containing the native enzyme.

7. Water Proton Relaxation

The logitudinal relaxation rate of water protons was determined by using a non-linear least squares fit of pulse heights to tau values to calculate the tau null value described by Carr and Purcell (34). A Varian NMR spectrometer operating at 40.5 MHz was used and the temperature of the 0.5 ml sample was $25^{\circ}C$. Phosphorylase b freed of AMP as described previously was buffered in 30 mM BES, 3 mM DTT pH 6.8. Data were collected between 1 to 2 hr after Gd addition and were analyzed as outlined in Appendix I.

Chapter III

Interactions of PAC With Phosphorylase b

A. Introduction

Platinumdiamminodichloride, PAC, was used as a heavy metal derivative in the x-ray diffraction studies of phosphorylase a (17) and phosphorylase b (35). The chemistry of this metal differs markedly from the lanthanide elements. Platinum, a d-transition metal, which has an ionic radius of 0.52 A^o, exhibits an oxidation state of +2 in the PAC complex. PAC exists primarily as a square planar structure coordinating four ligands via dsp^2 hybridization. The amino group coordinates to the metal by donating an electron pair in the nitrogen's sp^3 orbital to a vacant subshell on the metal (36). Since this sigma bond is more stable than the forces coordinating the chloride ligands, nucleophilic substitution occurs preferentially at the chloride sites. PAC is a bifunctional reagent with the distance between substitution sites dependent on its isomeric state. The cis isomer has two positions 3.3 A^o apart open to nucleophilic attack. Since the metal bound amine possesses no significant trans influence on the chloride platinum bond, substitution at the halide is the rate determining step.

In addition, nucleophilic attack is highly dependent on pH and the anionic species present in solution. At neutrality, the most reactive amino acids are Glu, Asp, Arg, Tyr, Cys, His and Met (37). As these amino acids become protonated, their reactivity with PAC decreases. Another study utilizing both equilibrium dialysis and chlorimetry to monitor the reaction of different amino acids with

cis (dipyridyldichloride) Pt(II) demonstrated the rapid reactivity of Cys and Met residues in the pH range 6-7 (38).

To elucidate the dynamic structure of the Pt-sulfur bond, NMR data were collected with cis-bis-(dibenzyl-sulfide)-dichloro Pt(II) (39). Their results indicate sulfur inversion about the metal without concomitant bond dissociation. The proposed inversion mechanism has sulfur retaining a distorted tetrahedral configuration while the Pt atom forms sigma bonds alternately with the two sulfur lone electron pairs.

Wade *et al* (40) compared the binding of PAC and NAD^+ in both the crystalline and solution states of malate dehydrogenase (MDH). Reference to x-ray crystallographic maps places the Pt sites on the protein solvent interface. The metalloprotein is inactive in solution with only a small percentage of activity reinstated after extensive dialysis or gel filtration. At a molar ratio of PAC to MDH of 300, the pseudo first order rate constant for inactivation is 2.3×10^{-2} $min.^{-1}$.

Evaluation of the ribonuclease-PAC complex in the solution state demonstrated pH induced metal specificity. At pH 8.0, the metal coordinates covalently to His 119, whereas at pH 5.5 a second site, Met 29, is preferred (41).

Although several other related papers have been published recently, the same basic principles are exemplified. PAC slowly forms covalent bonds with unprotonated surface functional groups of proteins.

B. Results

1. PAC Coordination to Phosphorylase *b* in the Solution State

a. Number of Metal Binding Sites

i. Atomic Absorption

Although atomic absorption possesses lower sensitivity than the succeeding spectrophotometric method, it is highly specific for Pt ions. To overcome the light scattering effect of macromolecules in solution, the metalloprotein was hydrolyzed and lyophilized prior to analysis as outlined in Methods. The freeze-dried sample was dissolved in a minimal amount of buffer containing $LaCl_3$. The lanthanum acted as an ion scavenger since anionic complexation with Pt decreased the concentration of Pt° and hence the detection limit.

Phosphorylase b was preincubated with a 10 molar excess of PAC for 24 hr at 25°C or until inactivation had ceased. Extensive dialysis removed the unreacted metal. Extrapolation from a standard Pt curve corrected for anomalous absorption with hydrolyzed native enzyme detected 2.2 ± 0.1 Pt binding sites per monomeric unit. This value is the average of four separate determinations.

ii. Spectrophotometric

A modification of the 2,3 Quinoxalinedithiol/$SnCl_2$ method developed by Janota and Ayres and outlined in Methods gave reproducible results with hydrolyzed and vacuum dried samples. Stannous chloride served to reduce Pt(IV) to Pt(II), the metal oxidation state which reacted with the sulfhydryl groups of QDT to produce a coloured adduct. Metalloprotein samples were prepared as outlined in Methods. Linear regression analyses of PAC standard curves corrected for anomalous protein interference were used to calculate the presence of 4.2 ± 0.5 Pt binding sites per subunit.

b. Metal Titration

The complexation of PAC with phosphorylase *b* in addition to promoting enzyme inactivation, altered the optical density of the coenzyme's characteristic absorption bands. To ascertain the specificity of metal binding, these parameters were assayed as a constant concentration of enzyme was titrated with the metal.

A plot of zero order activity relative to native values, Fig. 1, with a PAC to monomer mole ratio of 0.18 to 4.3 demonstrates a distinct inflection with a 1.8 molar excess of metal.

Figure 2 outlines the metal induced spectral changes. Enhancements in the peak intensities at 415 nm and 330 nm increase to a plateau with optical densities respectively 3.6 and 1.4 fold greater than the native enzyme. The fact that alterations in the spectra of the coenzyme preceeded inactivation indicates the involvement of either two or more unique PAC sites or a single site capable of inducing two conformational changes at different rates.

Increasing the metal to monomer mole ratio above ten results in immediate protein turbidity.

c. Inactivation Studies

Lineweaver Burk plots with varied concentrations of G-1-P in two different buffer systems, glycerophosphate and BES, confirmed the non-competitive inhibition of phosphorylase *b* by PAC. Prior to activity determinations, the enzyme was preincubated with either a 10:1:0 or a 10:1:25 mole ratio of PAC:monomer:Mg for 12 hr. at 30°C. The results from linear regression analyses are cited in Table 1.

Within experimental error, the presence of Mg had a negligible effect on the catalytic inefficiency induced by PAC, but it did confer a

Figure 1

Activity titration curve of phosphorylase b equilibrated with varying concentrations of PAC. Plot of the fraction of control activity retained under conditions of zero order kinetics *vs.* the molar ratio of PAC to monomer. The concentration of phosphorylase b was 8.5 X 10^{-5} M in 30 mM BES pH 6.8. Samples were assayed after a 19 hr. incubation at 25°C. with the indicated metal concentration. The x intercept was calculated via linear regression as 8.7 ± 0.1.

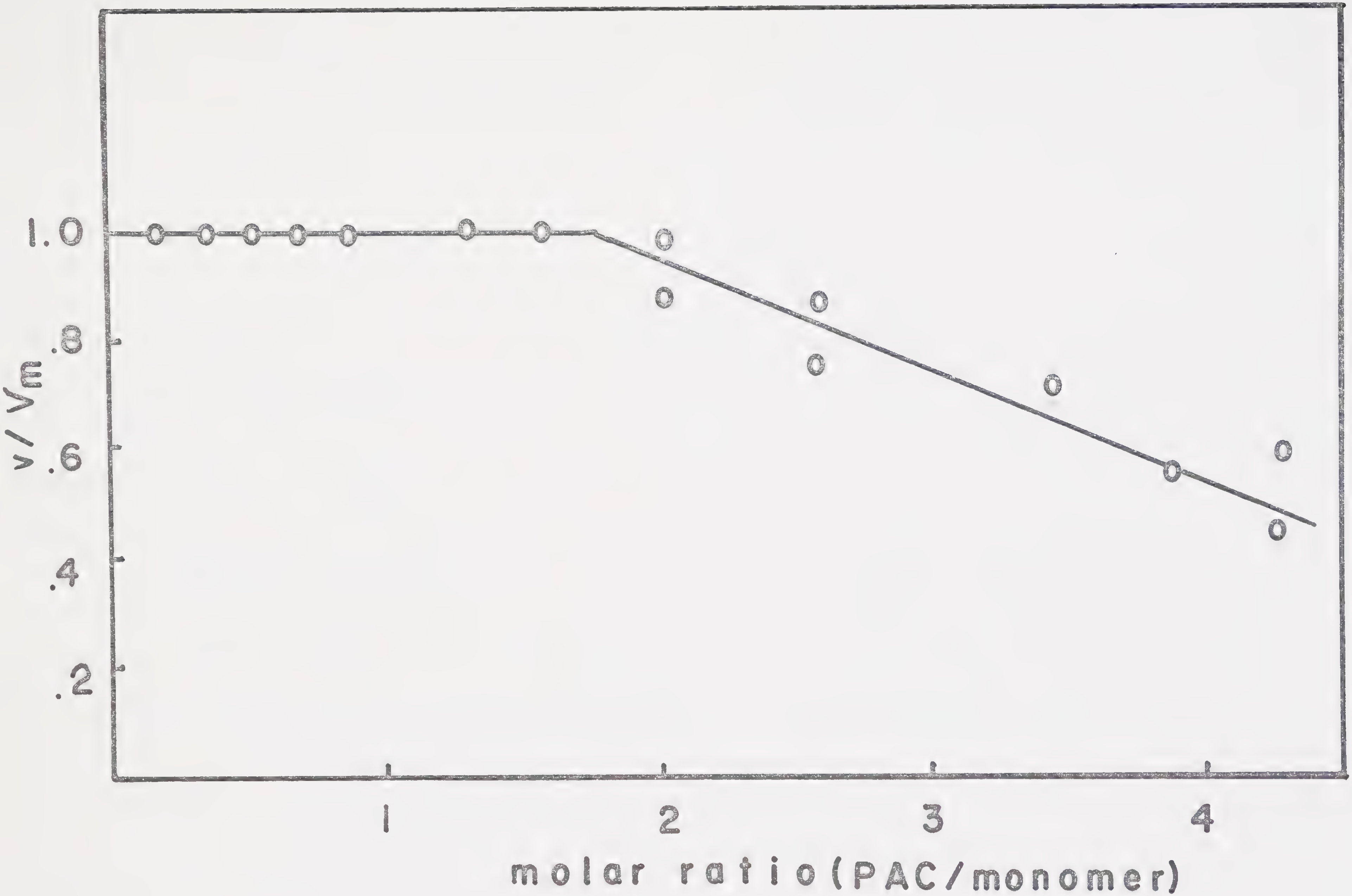
1.0
.8
.6
.4
.2
v/ Vm
1
2
3
4
molar ratio(PAC/monomer)

Figure 2

Spectral titration curve of phosphorylase _b_ equilibrated with varying concentrations of PAC. Plot of molar absorbtivity at 415 nm and 330 nm against the molar ratio of PAC to monomer. Reaction conditions were identical to those in Figure 1.

O——O molar absorption at 415 nm

X——X molar absorption at 330 nm

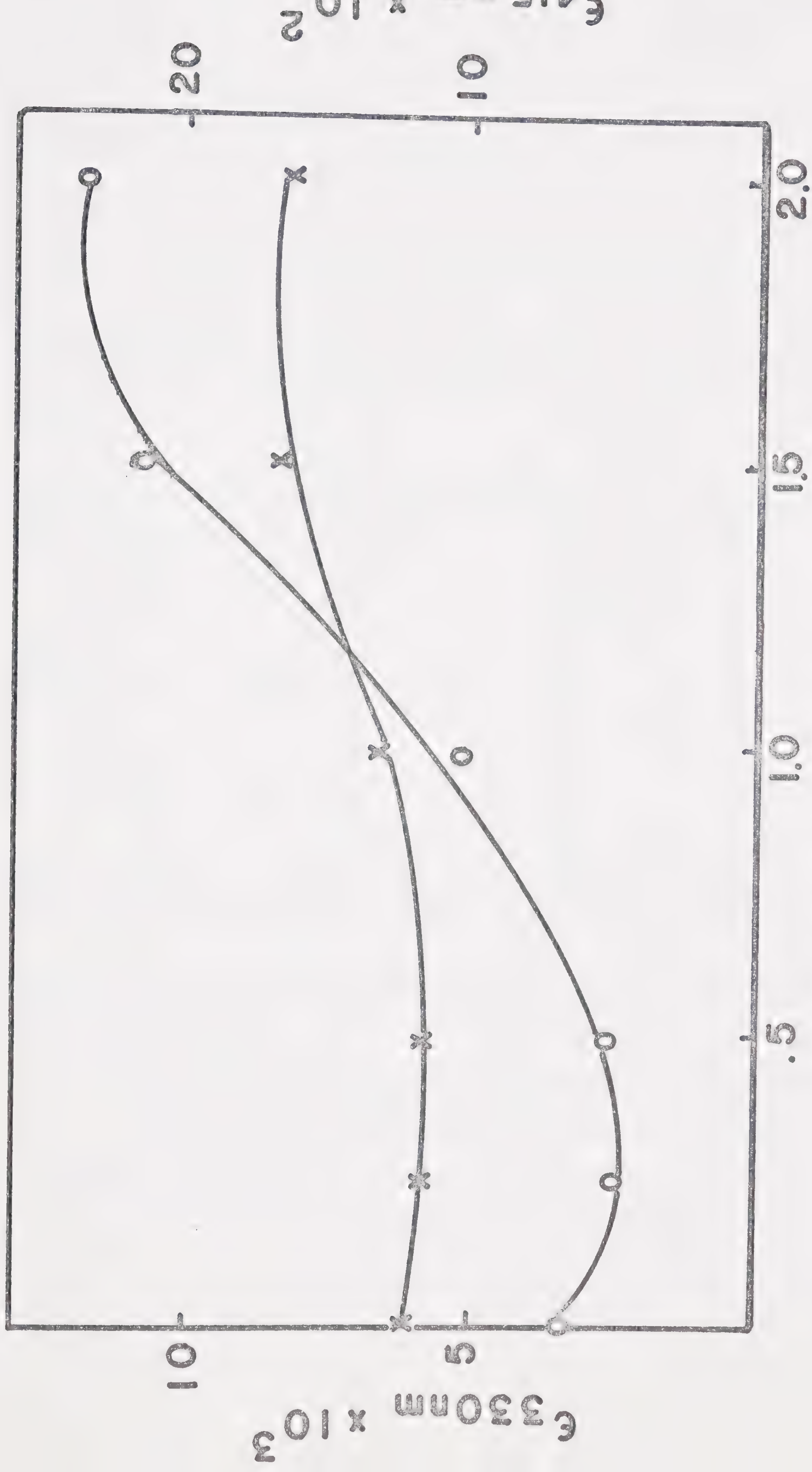
$\epsilon_{415nm} \times 10^2$
20
10
$\epsilon_{330nm} \times 10^3$
10
5
.5
1.0
1.5
2.0
Molar Ratio (PAC:monomer)

Table I

Kinetic Properties of PAC Modified Phosphorylase b

BUFFER	COMPLEX	PAC-b	STD. DEV.	PAC-Mg-b	STD. DEV.	native b	STD. DEV.
glycerophosphate	V_{max}	24.8	3.3	27.2	2.8	49.3	3.3
(20 mM)	K_m	4.0	0.6	4.9	0.6	3.0	0.5
BES	V_{max}	24.1	1.4			42.7	2.7
(30 mM)	K_m	4.8	0.3			3.3	0.6
reference (1)	V_{max}					65	
	K_m					3.0	

Phosphorylase b at a concentration of 5.2×10^{-5} M was preincubated with either 5.2×10^{-4} M PAC and 1.3×10^{-3} M Mg or 5.2×10^{-4} M PAC for 12 hr. at 30°C. prior to the determination of enzymatic activity at varying G-1-P concentrations in the presence of 1% glycogen, 1 mM AMP pH 6.8. Slopes and intercepts of double reciprocal plots of activity versus G-1-P concentrations were calculated via linear regression analyses.

slightly lower affinity of the enzyme for G-1-P. Glycerophosphate promotes binding of G-1-P to the metalloprotein relative to BES.

Phosphorylase a at a concentration of 5.2 X 10^{-5}M is inactivated upon incubation at 30°C with a 9.2 molar excess of PAC, as depicted in Figure 3. Spectrophotometric experiments with complexes of phosphorylase a reacted with PAC ions were discontinued due to the viscous, turbid protein suspension incurred upon incubation with the metal.

d. Ligand Protection of the Enzyme from Metal Induced Inactivation

Increasing the concentration of G-1-P from 16 to 60 mM results in a slight decrease in the reactivity of phosphorylase b with PAC as illustrated in Figure 4. Since the Lineweaver Burk plot indicates the noncompetitive inhibition of phosphorylase b by PAC, this protection is due solely to indirect modification by G-1-P of the Pt site involved in inducing inactivation.

Phosphorylase b at 4.7 mg/ml, was preincubated with 2.67 mM AMP for 20 min at 30°C before the addition of 0.5 mM PAC. The slight degree of protection observed could be attributed to PAC complexation at the unprotonated sites of the nucleotide rather than an AMP induced conformational change.

The effect of PAC binding on the homotropic cooperativity of AMP was examined in the double reciprocal plot in Figure 5. Phosphorylase b at a concentration of 9.2 X 10^{-5} M was incubated with either 13.8 X 10^{-5}M or 46 X 10^{-5} M PAC for 1.5 hr at 30°C in 30 mM BES pH 6.8, prior to activity determinations with 75 mM G-1-P, 1% glycogen and varied concentrations of AMP. The allosteric effect of the nucleotide remains intact at a metal to monomer mole ratio of 1.5, but is abolished with a 5 molar

Figure 3

Time study of inactivation of phosphorylase a upon incubation with PAC. Aliquots removed at set time intervals from a reaction system containing 5.2 X 10^{-5} M monomer and 47.8 X 10^{-5}M PAC in 30 mM BES pH 6.8, were assayed for activity in a substrate solution containing 16 mM G-1-P, 1% glycogen pH 6.8.

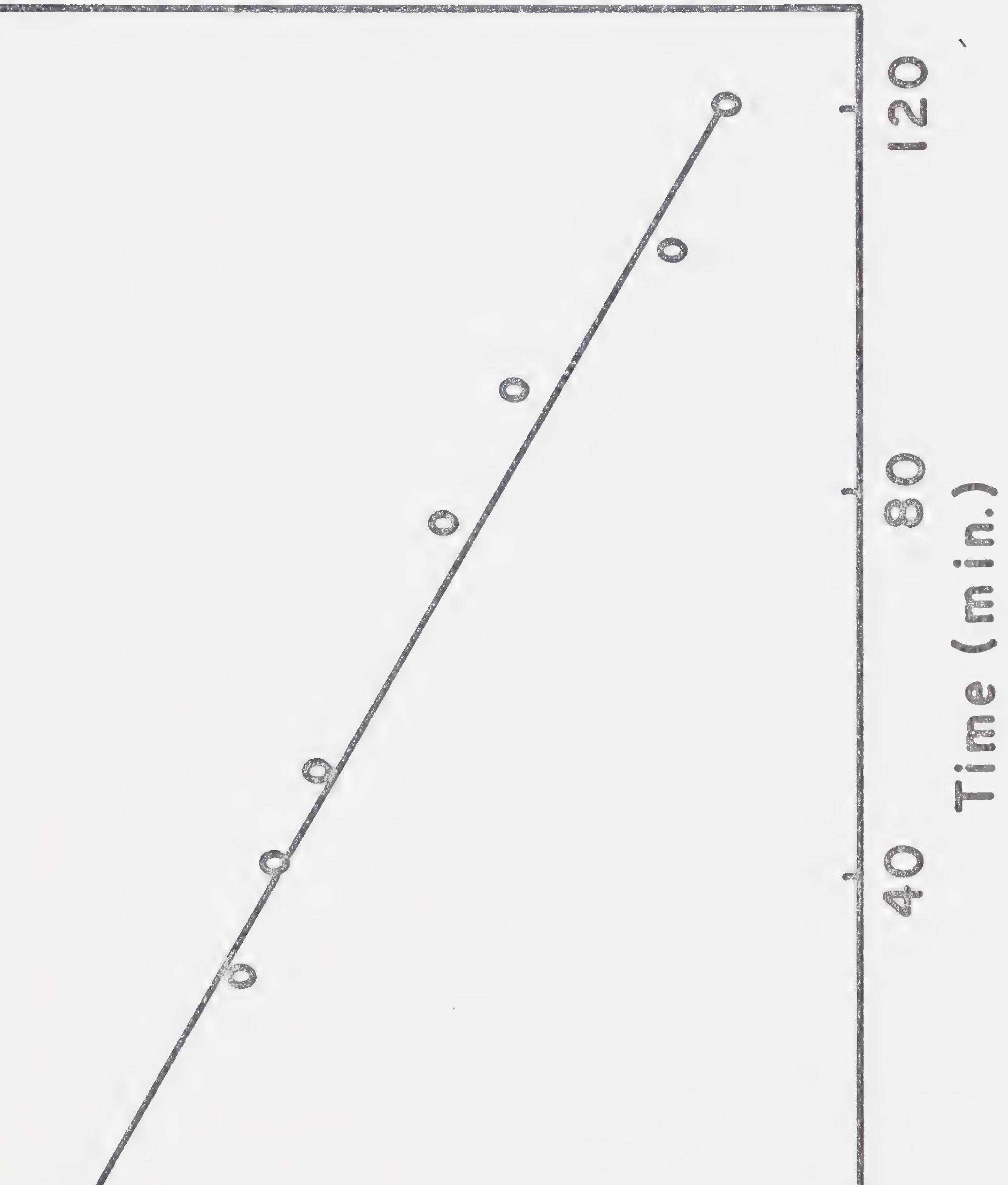
Activity (µmole/min/mg)
70
60
50
40
30
Time (min.)
40
80
120

Figure 4

Glucose-1-phosphate protection of phosphorylase _b_ from PAC induced inactivation. Plot of the slopes of the fraction of control activity retained against the molar ratio of PAC to monomer _vs_. the concentrations of glucose-1-phosphate. Phosphorylase _b_ at a concentration of 5.4 mg/ml was incubated with various concentrations of G-1-P for 30 min. at 30°C. prior to the addition of either a 0, 1, 5, 30 or 50 molar excess of PAC. Aliquots were assayed for activity after a 5 hr. incubation with metal. The buffer consisted of 20 mM glycerophosphate, 1 mM DTT pH 6.8. Error bars were calculated from linear regression analyses.

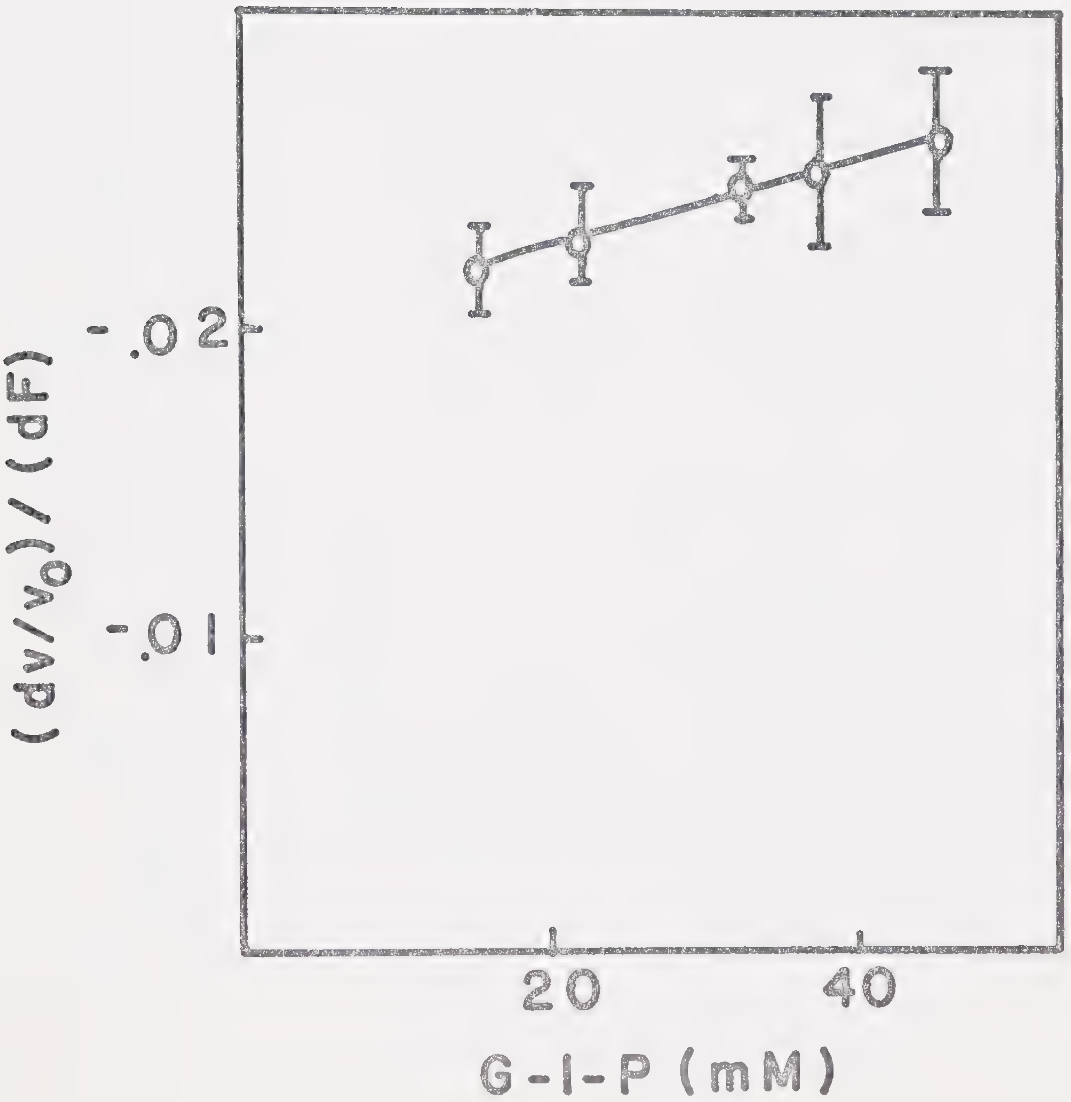
(dv/v$_0$)/(dF)
-.02
-.01
20
40
G-1-P (mM)

Figure 5

AMP homotropic cooperativity within the PAC-phosphorylase *b* complex. Plot of reciprocal activity in (umol/min/mg)$^{-1}$ *vs*. reciprocal AMP concentrations. Reaction conditions were outlined in the text.

O——O reciprocal activities in the absence of PAC or in the presence of a 1.5 molar excess of metal to monomer. V_{max} = 67 μm P_i/min/mg, K_m = 32 μM and n_H (from Hill plot) = 1.4 ± 0.1

X——X reciprocal activities obtained with phosphorylase *b* incubated with a 5 molar excess of PAC. V_{max} = 30.5 μm P_i/min/mg, K_m = 34 μM and n_H (from Hill plot) = 1.0 ± 0.1

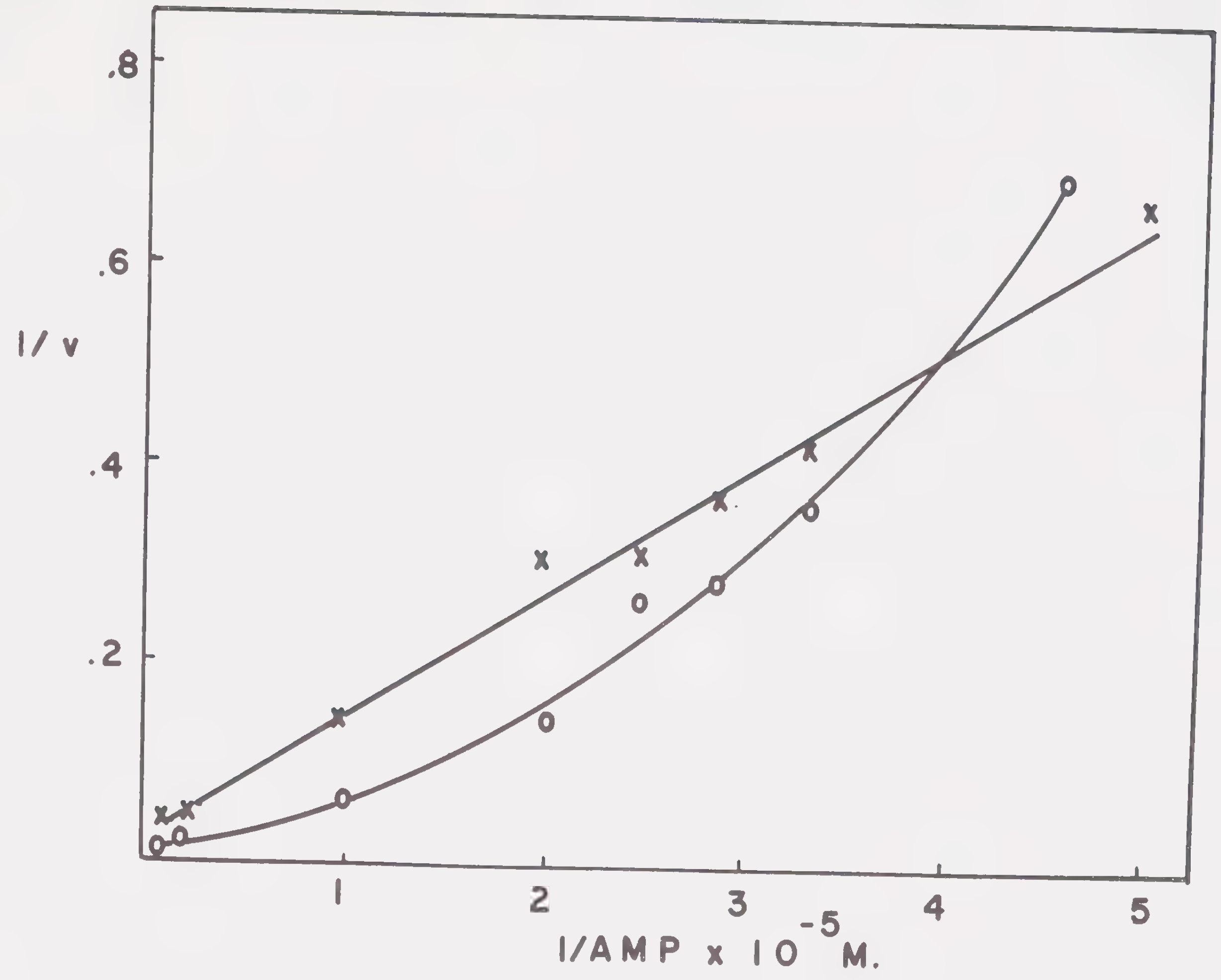
.8
.6
.4
.2
1/ v
1
2
3
4
5
1/AMP x 10^{-5} M.

excess of PAC.

e. Fluorescence Spectra

Ground state electronic spectra have demonstrated metal induced perturbations of the coenzyme. Since the excited state of a molecule is more sensitive to environmental changes, fluorescence data were collected to further elucidate the metal effects on enzyme bound PLP.

The samples absorbed below 0.1 O.D. at the excitation wavelength. Phosphorylase b incubated with a ten molar excess of PAC in 20 mM glycerophosphate, 1 mM DTT pH 6.9 for 12 hr at 25°C was excited at 333 nm. Fluorescence intensity at 535 nm was 21.6% of the emission intensity of native enzyme. Since metal titrations indicate an increase in the 330 nm optical density, PLP quenching induced by PAC is caused either by direct heavy metal effects or via indirect metal modulated conformational change.

Figure 6 denotes the rates of inactivation and PLP fluorescence quenching upon formation of the metalloprotein. Quenching of the 535 nm emission intensity upon excitation at 333 nm preceeds inactivation within the same reaction system, correlating with the previously mentioned metal titration data illustrated in Figure 2.

f. Polarized Light Studies

The extent of gross secondary structural changes in phosphorylase b upon PAC binding was calculated from circular dichroism and optical rotary dispersion data. Enzyme at 5 mg/ml in 30 mM BES, 1 mM DTT and 1 mM EDTA pH 6.8 was incubated with 0.5 mM PAC until 43% inactivated relative to native enzyme. Extensive dialysis of the sample against 5 mM BES, 5 mM EDTA, 1 mM DTT pH 6.8 reversed 2-3% of the inactivation. The metalloprotein was subsequently analyzed via atomic

Figure 6

Time studies of the rate of inactivation and fluorescence quenching upon formation of PAC-phosphorylase *b* complexes. Plot of the fraction of control parameter with respect to peak area or activity *vs*. time. After the addition of 0.5 mM PAC to 2.6 mg/ml phosphorylase *b* in 20 mM glycerophosphate, 1 mM DTT pH 6.9, activities or emission peak areas were assayed at set time intervals.

O——O activity of the metalloenzyme relative to native enzyme

X——X peak area under 535 nm emission peak upon excitation at 333 nm relative to the native enzyme.

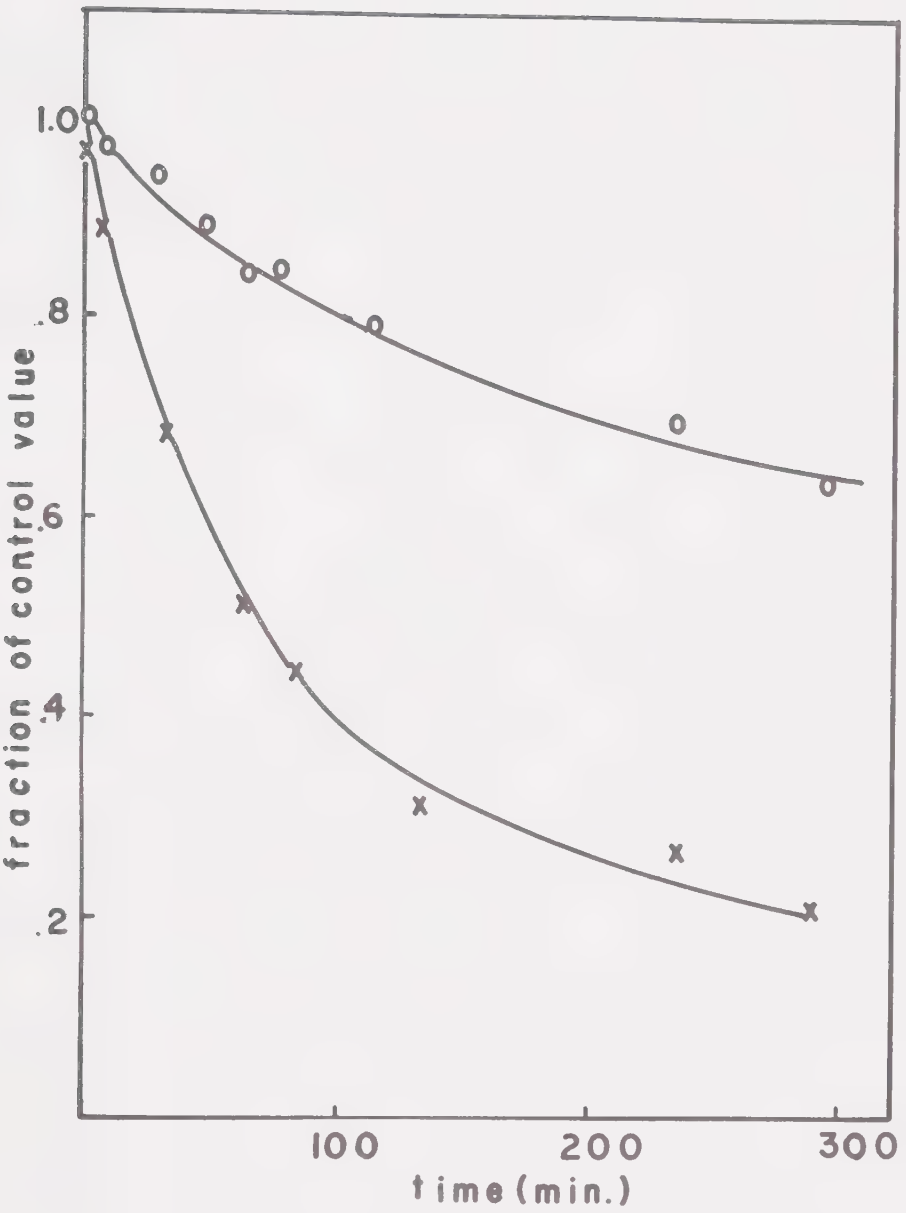
1.00
.8
.6
.4
.2
fraction of control value
100
200
300
time (min.)

absorption to determine the amount of Pt retained. Each mole of monomer incorporates 2.4 moles of Pt. The fraction of protein residing in alpha helical, beta sheet and random coiled structures calculated from both methods is presented in Table 2.

The large discrepancy between the two techniques may be accounted for in part by their inherent differences in resolution. ORD monitors the differences in the refractive indices of L and D plane polarized light as they passed through the sample. Since each transition is spread over a large range of the spectra, resolution is lower relative to CD experiments. The protein's preferential absorption of L or D circularly polarized light causes the CD peak to be centered near the electronic absorption band. Therefore the CD transition are sharper leading to higher data resolution. Previous results have indicated alterations in the PLP pocket upon PAC binding. Although CD and ORD readings were taken at wavelengths corresponding to the peptide backbone, perturbations in the PLP's assymmetry would influence ORD values.

Within experimental error, the metalloprotein exhibits only slight structural differences relative to the native enzyme. However two possibilities must be considered. Drastic conformational changes at a small number of sites in the protein, when averaged over the entire molecule would result in minor alterations of the net secondary parameters. In addition secondary structures in one area of the protein may be disrupted and reformed in another region, causing the overall result to be similar to the unperturbed native state.

g. Sulfhydryl Reactivity

As mentioned in the Introduction, model studies indicated the preferential reactivity of PAC with Cys and Met residues at neutrality.

Table II

Secondary Structural Parameters Obtained from Polarized Light Studies

Fraction	ORD		CD		reference		x-ray structure
	native	PAC-b	native	PAC-b	apo b	native b	(phosphorylase a)
alpha helix	.36	.23	.47	.43	.44[@] .35[*]	.44[@] .31[*]	.38[#]
beta sheet	.28	.30	.37	.42			.25[#]
random coiled	.36	.47	.16	.14			

After inactivation induced by incubation of phosphorylase b at a concentration of 5 mg/ml with 0.5 mM PAC ceased, the metalloprotein was dialyzed to remove excess Pt ions. The ORD and CD spectra were monitored in the resultant complex at wavelengths corresponding to the peptide backbone. Calculations from Yang-Moffat plots and equations derived from model studies (Appendix 2) were used to determine the fraction of alpha helical, beta sheet and random coiled structures.

[@] refers to reference 42 where $\lambda_c = 279$ for the apo enzyme and $\lambda_c = 280$ for the native enzyme

[*] refers to reference 43 where the reduced mean residue rotation at 231 nm was - 4900° for the apo enzyme and - 4300° for the native enzyme

[#] refers to reference 44

Although phosphorylase b contains 9 Cys per monomer, only four of these residues are available for modification in the native state of the enzyme. These four Cys residues may be further subdivided into a fast reacting group containing peptides B_1 and B_2 and a slower reacting group designated A and N. Modification of the former group has negligible effects on the enzyme's activity and quaternary structure, whereas inactivation and monomerization occur upon reaction of the slower group with such sulfhydryl reagents as PCMB, DTNB and iodoacetamide (45). The former two reagents are used to modify the metalloprotein complex.

Phosphorylase b at a concentration of 5.2×10^{-5}M was incubated with 26×10^{-5}M PAC in 30 mM BES pH 6.8 for 2 hr at 30°C. DTNB was added to a ten fold dilution of the native and modified enzyme at zero time. Absorbance was corrected against metal and reagent blanks. Determination of the number of reactive sulfhydryl groups was based on an molar absorbtivity of 13,600 (46). Figure 7 denotes the different rates of Cys modification indicating the perturbation of one of the slow reacting sulfhydryls upon PAC coordination with the enzyme.

An alternate sulfhydryl modification experiment reacted PCMB with with the metalloprotein in 30 mM BES pH 6.8. Reactions containing mole ratios of PAC to monomer of 1, 5, 10 and 0, were incubated at 25°C for 16 hr prior to the addition of 9.38×10^{-5}M PCMB. Once absorption at 255 nm had stabilized, absorbance was recorded. Native enzyme incubated either without PAC of with equimolar concentrations of metal to monomer exhibits the same number of reactive Cys. Increasing the concentration of metal further results in a decreased reactivity of a single sulfhydryl moiety, thus substantiating the DTNB observations.

h. Sedimentation Velocity Profile

Phosphorylase b at a concentration of 2.5 mg/ml was reacted

Figure 7

Sulfhydryl reactivity of PAC-phosphorylase _b_ with DTNB. Plot of the number of reactive sulfhydryl groups per subunit as determined from optical densities at 412 nm and a molar extinction coefficient of 13,600 _vs_. time. The concentration of DTNB used was 0.2 mM, other reaction conditions are described in the text. All optical densities were corrected for reagent and metal interferences.

●——● number of Cys residues reacting per monomer of native enzyme

○——○ number of Cys reacting per subunit in the metalloprotein

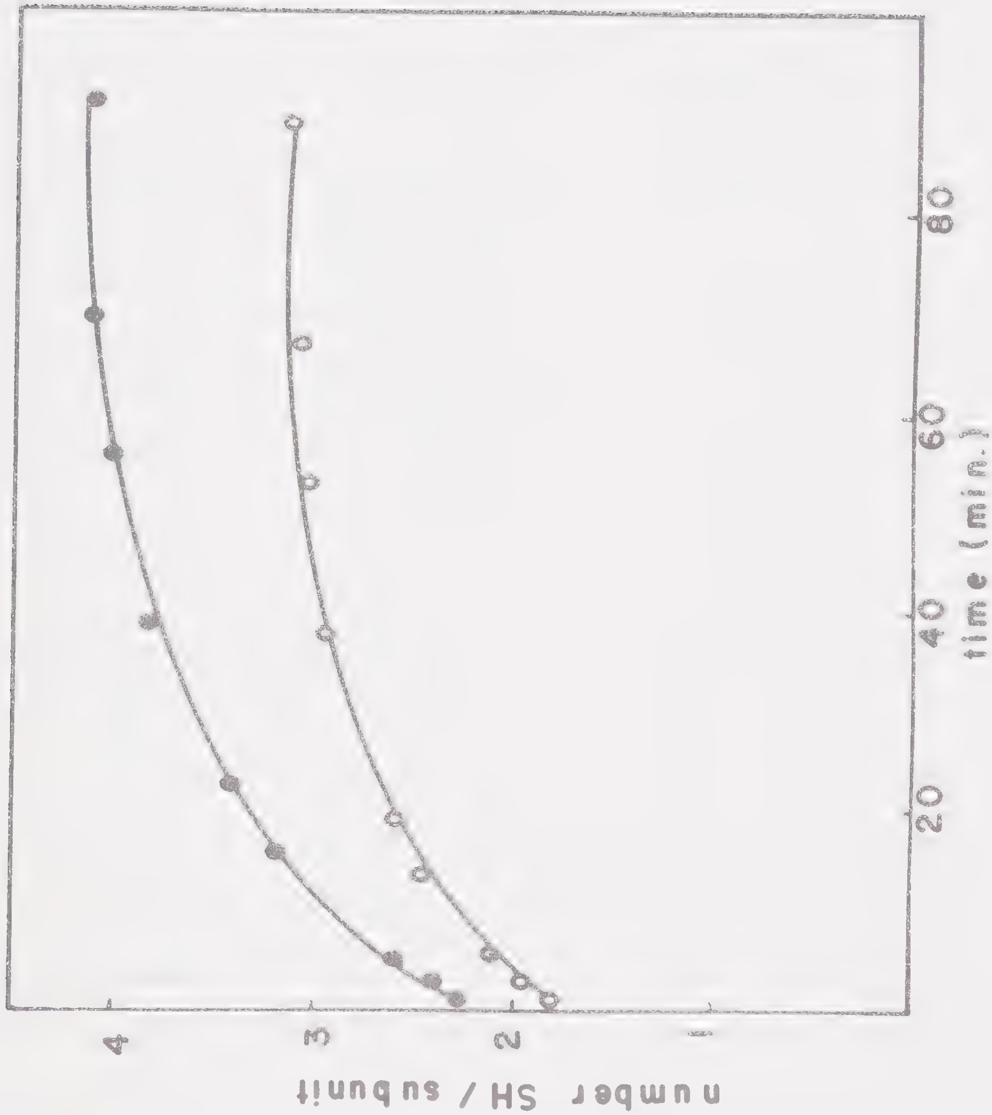
number SH / subunit
1
2
3
4
time (min.)
20
40
60
80

with a ten fold excess of PAC until 50% inactivated relative to the native enzyme. After dialysis against 30 mM BES, 3 mM DTT pH 6.8, the samples were centrifuged at 56,000 rpm at 20°C. In Figure 8, the native enzyme sediments as a dimer with $S_{obs} = 7.86 \times 10^{-13}$ whereas the metalloprotein exhibits peaks at both 5.8 and 7.5×10^{-13}. Two minor peaks are situated at lower S values. Occupation of the platinum site(s) is involved in inducing monomerization of the enzyme.

2. PAC Coordination to Phosphorylase b in the Crystalline State

a. Number of Metal Binding Sites

The number of PAC binding sites per monomer of phosphorylase b in hydrolyzed microcrystals was determined as 2.0 ± 0.4 via atomic absorption and 4.0 ± 0.5 via the QDT / $SnCl_2$ spectrophotometric assay. Reference to Table 3 indicates similarities in the number of PAC binding sites within the solution and the crystalline states of the enzyme. Although the spectrophotometric and atomic absorption methods differed in the absolute number of sites, the correlation between the two physical states within the same method is satisfactory. The possible reactivity of the sulfhydryl groups of quinoxalinedithiol with the amino acids released upon acid hydrolysis of the protein are difficult to correct for, although standard Pt curves contained hydrolyzed native enzyme.

The apparent discrepancy between the number of PAC sites reported from phosphorylase a and phosphorylase b x-ray crystallographic data may be reassessed by an evaluation of the fractional changes in the structural amplitudes expected in the metalloprotein crystal relative to the native enzyme. In 1956, Crick and Magdoff (47) proposed an equation, Appendix 3, which calculated the approximate fractional change in intensity induced by heavy metal interactions with protein molecules.

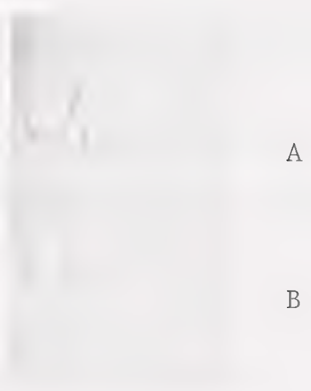

Figure 8

Sedimentation velocity profile of phosphorylase b reacted with PAC. The reaction conditions are outlined in the text. Native phosphorylase b (A) (7.86) sedimented as a single schlieren peak, however in the presence of covalently bound PAC (B) (5.81 to 7.52), the enzyme exhibited 2 major and 2 minor schlieren peaks. The numbers in brackets refer to the peak location in svedburg units at 20°C. The right side of the profile refers to the top of the ultracentrifugation cell.

Table III

Analytical Determinations of the Number of PAC Binding Sites Per Phosphorylase Monomer

Method	Number of PAC Binding Sites			
	Phosphorylase b in solution	Phosphorylase b in microcrystals	Phosphorylase b in macrocrystals	Phosphorylase a in macrocrystals
atomic absorption	2.2 ± 0.1	2.0 ± 0.4		
QDT / $SnCl_2$	4.2 ± 0.5	4.0 ± 0.5		
x-ray difference fourier			1#	2.5*

# one site (reference 35)

* in four sites with a total occupancy approximately equal to 2.5 gram atoms Pt per monomer (reference 17)

Johnson (35) reports the presence of a single PAC site per phosphorylase *b* monomer and a fractional change, ($\overline{\Delta F}/\overline{F}_P$) (100), in structural amplitude of 16.2% with this metal derivative. However, simple calculations from the Crick Magdoff equation predict a fractional change in the order of 9%, or about one half of the experimentally determined parameter. Alternatively, similar calculations from the data published by Fletterick (17), which indicate the presence of 2.5 gram atoms of Pt per monomeric unit, support a fractional intensity change of 15% which compares with the published value of 22%. In summary, these calculations suggest that the number of Pt sites within the phosphorylase *b* monomer exceeded one as the fractional change in structural amplitude reported by Johnson would be compatible with a Pt occupancy of at least two sites.

b. Activity Studies with Crosslinked Crystals

Tetragonal macrocrystals of phosphorylase *b*, with an average surface area of 3.1 mm^2, were soaked in 1 mM PAC for 2 days at 16°C prior to crosslinking with glutaraldehyde. The experiment was also performed in the reverse order with crosslinking preceeding the exposure of the crystal to PAC with similar results. The metalloprotein crystals exhibit cracking and fragmentation relative to control crystals. Duplicate assays give activities of 5.0 ± 0.5 nmol/min/mg and 9.9 ± 0.3 nmol P_i/min/mg for crystals in the absence and presence of PAC respectively. Crystal supernatant solutions express no activity over a four hour incubation, indicating that the crosslinked crystals are not being extensively solubilized by substrate solutions. Although this apparent metal activation contrasts with the observed inhibition of the metalloprotein in solution and in solubilized macrocrystals, it does not necessarily confirm the existence of different Pt binding sites within the

two physical states. Metal induced fracturing of the crystal lattice would not only increase substrate accessability and decrease steric influences on the lengthening of the maltodextrin chain, but would promote enzyme fluidity by increasing the fraction of the protein proximal to the protein solvent interface.

c. Activity Studies with Solubilized Crystals

Uncrosslinked tetragonal macrocrystals of phosphorylase _b_ presoaked with PAC as outlined in Methods, were extensively washed with crystallization buffer to remove excess metal. Incomplete solubilization of these crystals occurs in solvents of high ionic strength or viscosity. Although 0.5 M NaCl dissolves unmodified crystals within 2 hr., only chipping and lateral cracking are evidenced with the metallocrystals after 48 hr at 16°C The supernatant of crystals soaked in 20% glycerol was assayed for activity after 48 hr at 16°C The control exhibits activity in the order of 5 μmol /min/mg whereas PAC-phosphorylase _b_ was completely inactive. These low activities are expected due to glycerol's noncompetitive inhibition of phosphorylase _b_ in the solution state. Calculations at various concentrations of glycerol with the solution enzyme were used to determine values for the K_i intercept of 64 mM and the K_i slope of 50 mM with respect to the substrate glucose-1-phosphate.

The addition of a substrate solution containing 2 mM IMP, 11.5 mM maltoheptaose, 38 mM G-1-P, 10 mM BES, 1 mM DTT pH 6.8, increase crystal dissolution but complete solvation did not occur. Soluble enzyme released from the crystal lattice by this method exhibits activities of 21.4 and 34.8 umol/min/mg. The metalloprotein under analogous conditions exhibits activities of 3.4 and 4.3 umol/min/mg. Therefore the inactivation observed in solution studies is reflected by the metalloenzyme in the crystal state.

C. Discussion

Several parameters are evaluated to assess the extent of correlation between metal binding sites within the two physical states of phosphorylase. Interpolations from x-ray crystallographic data established the immediate protein environment of the metal site in conjunction with its distance from substrate, effector and ligand interaction sites. By comparing the physico-chemical properties expressed by the metalloprotein in solution to the steric restrictions imposed on the site by the crystal lattice structure, differences or similarities in the mode of metal modulation of the enzyme could be assessed. There are however other complicating factors to be considered. Within a crystal, the binding site may include functional groups from more than one enzyme molecule and therefore would be less energetically favourable in solution. In addition, molecular packing within the crystal lattice could sterically block a binding site which would be accessable in the solution state.

The coordinates of the four PAC derivatives within each phosphorylase a subunit obtained from x-ray analyses are referred to in Table 4. Site 1, expressing the highest occupancy, is situated on the apex of a "tower-like" structure consisting of approximately 30 amino acids which extends through the subunit interface at Z = 1/2. The locus of this primary PAC site coincides with the single PAC derivative determined from the 6 A° map of phosphorylase b (35).

An interesting feature of site 1 was the fact that both $Pb(NO_3)_2$ and EMTS coordinate within 2 A° of this locus. The latter metal is retained after crystal washing, indicating covalent bonding with a protein functional group. The affinity of both Pb and mercurial molecules for sulfur ligands suggests the possible proximity of a reactive sulfhydryl

TABLE IV

Coordinates of Metal Derivatives Determined from X-Ray Crystallographic Studies of Phosphorylase

Derivative	Ƶ	Coordinates		
		X	Y	Z
PHOSPHORYLASE A[@]				
PAC 1	78	.155	.360	.342
2	54	.027	.124	.320
3	41	.254	.381	.205
4	22	.291	.338	.205
Gd 1	45	.161	.001	.171
2	27	.043	.142	.305
$Pb(NO_3)_2$ 1	61	.043	.138	.303
2	35	.161	.000	.171
3	26	.491	.411	.102
4	24	.169	.379	.326
$MnCl_2$ 1		.045	.135	.300
2		.150	.400	.320
EMTS 1	73	.026	.088	.391
2	55	.192	.225	.038
3	38	.164	.385	.321
4	24	.202	.010	.450
CH_3Hg 1		.026	.088	.390
2		.192	.225	.038
3		.177	.325	.170
4		.114	.139	.230
PHOSPHORYLASE B[*]				
PAC 1	83	.157	.359	.345
EMTS 1	46	.195	.224	.038
2	63	.028	.088	.385

Note: The lattice constants for tetragonal crystals in space group $P4_32_12$ are a=128.4 ± 0.1 A and c=116 ± 0.1 A . Ƶ was the occupancy factor. [*] refers to reference 35 and [@] refers to reference 17

to PAC site 1. Of the four sulfhydryls, A, N, B_1, B_2, available for modification in native phosphorylase, the latter two are the fastest reacting and exert negligible effects on the integrity of the enzyme's active and alpha aggregation sites (45). Therefore if Cys modification within the crystal parallells the solution enzyme, B_1 and B_2 would exhibit higher site occupancies than A and N and the altered enzyme would remain isomorphous. Chemical modulation of the N site in the case of phosphorylase b or A and N with phosphorylase a induces inactivation and subunit dissociation within the solution state (45). Introduction of similar conformational perturbations within the crystal could conceivably disrupt crystal lattice stabilization forces leading to a decreased quality of x-ray diffraction data. These interpretations were substantiated to some extent from the coordinates reported for EMTS and CH_3Hg derivatives. These metal molecules in both forms of phosphorylase interact at two identical sites which are retained upon washing the crystal with buffer and exhibit high occupancy factors. On this basis the two sites are tentatively allocated to cysteines B_1 and B_2. The coordinates of PAC site 1 did not correlate with these putative fast reacting sulfhydryls, however its proximity to the alternate EMTS and $Pb(NO_3)_2$ sites and the dimer interface suggest possible Pt complexation in the vicinity of the N or the A peptide.

The properties of the protein environment of site 1 are in several aspects compatible with the responses ellicited by PAC interaction with phosphorylase b in the solution state. Modification of the enzyme with a five fold molar excess of PAC reduces the reactivity of one of the slower sulfhydryl groups with DTNB as illustrated in Figure 7. Perturbation of the environment of the N peptide by PAC coordination to phosphorylase may also be inferred from the metal induced inactivation

of phosphorylase b, as alkylation of the A peptide would not be expected to exert this effect.

Although the involvement of the "tower-like" peptide protuberance in the maintenance of dimer integrity has not been established, its realignment induced by PAC or sulfhydryl reagents could promote monomerization which in turn would result in the loss of enzymatic activity. The correlation between subunit dissociation and inactivation are suggested by the fact that the K_m values for G-1-P and AMP within the metalloprotein closely approximated the native enzyme, whereas V_{max} values are significantly altered. From the data concerning subunit interactions, sulfhydryl reactivity and activity, the PAC site occupied in the solution state is compatible with the environment of PAC site 1.

Evidence also exists for the involvement of a second PAC site. The Pt analytical techniques, atomic absorption and QDT/$SnCl_2$, indicate the presence of at least two sites per monomeric unit of phosphorylase b. Reassessment of the number of Pt sites determined from x-ray maps of phosphorylase b as shown in Chapter III 2.a., indicate a second PAC site although the lattice coordinates have yet to be established. The observation that the rate of schiff base formation preceeds inactivation as indicated by the rates of fluorescence quenching, Figure 5, and metal titration curves, Figure 2, is also indicative of a secondary Pt site. Previous studies involving the formation of IAM complexes with phosphorylase (48) demonstrate that the enhancement of 415 nm absorbance and inactivation occur at similar rates, data which contrast with the metalloprotein's characteristics. In addition the loss of the enzyme's allosteric properties upon PAC interaction would not be compatible with metal modulation solely of the N peptide (49).

The next step was to assess the three alternate PAC sites pub-

lished from difference fourier maps of phosphorylase a for their ability to regulate effector cooperativity and the coenzyme pocket. Sites 3 and 4, denoted in Table 4, are situated on the opposite side of the subunit with respect to the active site and the dimer interface. In addition, these loci exhibit low occupancy factors within the crystalline state. Therefore on the basis of site orientation and the enzyme's affinity for PAC, sites 3 and 4 appear initially as unlikely candidates for the alternate Pt site within the solution state. The metals Gd(III), Pb(II) and Mn(II) which coordinate within the protein pocket occupied by PAC site 2, promote tetramerization of the enzyme with the retention of the integrity of the active and the coenzyme sites, properties which contrast with the putative secondary Pt site in solution. Although occupancy data indicate that site 2 is sufficiently reactive with PAC, it is difficult to assess at this time, a possible mode of PAC perturbation which would differentiate its effects from the Gd, Mn or Pb complexes of phosphorylase b. Alternatively, the possibility that the secondary PAC site of the solution enzyme could be sterically blocked within the crystalline state can not, on the basis of these results, be overlooked.

The stability of PAC-phosphorylase b crystals in media of high ionic strength or viscosity is compatible with metal crosslinking. However these crystals retain activity comparable to the native sample, contrasting with the lack of catalytic efficiency expressed by substrate solubilized metalloprotein crystals. If the observed inactivation is based on subunit dissociation, then the energy barrier for monomerization within the crystalline state would be greater than within solution, thus explaining the differential activity responses within the two physical states. In addition the fact that solubilization could occur under

certain conditions supported stabilization of the crystal lattice via "intra" rather than "inter" metal bridging.

In summary, the extension of analogies between PAC sites within the crystalline and the solution states of phosphorylase b is reasonably good for PAC site 1 and more tenuous for the secondary metal locus. One Pt site governs the reactivity of the N or A peptides either via conformational change or direct coordination. The latter proposal appears most likely as the characteristics of the metallo-complex mimicks the properties induced by sulfhydryl modification of phosphorylase b with respect to perturbations of the dimer interface and the active site pocket. Therefore the orientation of PAC site 1 in conjunction with its proximity to the EMTS and $Pb(NO_3)_2$ complies within the parameters of this study with the Pt site occupied in the solution state.

Modulation of allosteric properties and schiff base formation indicate the involvement of a second Pt site. Once the peptide backbone and the coenzyme locus of phosphorylase b have been elucidated, the possible involvement of PAC site 2 in the disruption of the homotropic cooperativity of AMP and the PLP pocket may be reevaluated.

CHAPTER IV

Interactions of Gadolinium Ions with Phosphorylase

A. Introduction

Of the several metal derivatives used in x-ray diffraction studies of phosphorylase, Gd was selected for further investigation due to its inherent paramagnetism and the changes it induced in the physicochemical parameters of the enzyme upon coordination.

Gadolinium is an element of the lanthanide or rare earth family, a transition group possessing 4f orbitals at varying degrees of occupancy. Since the 4f subshell lies spatially and energetically below the 6s, 5p and 4d orbitals, Gd has no significant crystal field stabilization. Consequently its complex formation is highly electrostatic with negligible f orbital direction of ligation via steric forces (50-53). These coordination properties in conjunction with the characteristic lanthanide contraction, enable Gd (.938 A°) to mimic the chemistry of Mn (.80 A°), Ca (.99 A°) and Mg (.66 A°). The numbers in parentheses refer to the respective metal's ionic radius (54).

Although Laporte forbidden f-f transitions indicate alterations in metal-ligand coordination, they can presently be interpreted only qualitatively. Birnbaum _et al_ (55) have suggested the use of difference absorption spectroscopy to characterize specific amino acid - lanthanide interactions. Unfortunately, the hyperfine spectra of Gd solutions, which have low molar extinction coefficients, are centered at 270 nm, thus coinciding with the intense tryptophan/tyrosine band of proteins.

Studies of lanthanide-indole fluorescence indicate a dependence

of quenching potential on the metal's electron capturing ability (56). For example, Eu $4f^6$ and Yb $4f^{13}$ require one electron to complete a stable full or half full subshell. Therefore, they have quenching constants (K_q) in the order of 4.5×10^{-9} and 1.6×10^{-9} M^{-1} sec^{-1}. Analogous experiments with Gd $4f^7$ gave a K_q value of 1×10^{-10} M^{-1} sec^{-1}. Chromophores in the vicinity of Gd would therefore exhibit a decrease in their emission band intensity. Another lanthanide, Tb, possesses inherent fluorescence. Under certain conditions, energy transfer from one or more aromatic residues to the metal causes Tb fluorescence enhancement. Such fluorimetric titration data aid in the characterization of metal associated amino acids and in the determination of the number of metal binding sites and their respective dissociation constants (57).

One of the more dominant techniques for monitoring Gd-macromolecular interactions, nuclear magnetic resonance, utilizes the metal's inherent paramagnetism. The spin of its unpaired electrons generates a magnetic monoment orders of magnitude greater than corresponding nuclear magnetic moments. Fluctuations in the local field generated by these electrons leads to more efficient relaxation of neighbouring nuclei. Under specific conditions, the Solomon-Bloembergen equation expresses the relationship of the various correlation times to the observed relaxation rate (58). The equation consists of two terms. The first, a function of τ_C, denotes relaxation arising from dipole-dipole interactions between the electron spin of the metal, S, and the nuclear spin, I. The second term, τ_e, or scalar interaction, characterizes the effect of transient covalent bond formation between the metal and adjoining nuclei. Actually τ_e and τ_C are the sum totals of the elemental correlation times:

τ_S, τ_M, τ_R.

τ_S : electron-spin correlation time

τ_M : residence time of a nucleus in the first coordination sphere of the metal

τ_R : rotational correlation time

Paramagnetic ions may be classified into two broad groups, the relaxation and the shift probes, depending on which correlation times dominate. The former, comprised of such metals as Mn(II), and Gd (III) possess τ_C values in the order of 10^{-10} to 10^{-11} sec. This dipole-dipole term is governed primarily by τ_R. Shift probes on the other hand have τ_C parameters ranging from 10^{-12} to 10^{-13} sec., times which are representative of very short electron-spin or τ_S relaxation.

Dwek et al (59) have attempted to define the parameters governing H_2O proton relaxation in aquo and small molecular complexes of Gd. To establish that the rapid exchange of metal bound water with bulk solvent existed, they monitored relaxation times at two frequencies, 20 MHz and 35 MHz, over a wide temperature range. Not only did increasing temperatures enhance $1/T_1$, but spin-spin relaxation was about 14% of T_1 at all temperatures studied. Consequently the conditions of fast exchange occurs in this reaction system. Elimination of the scalar term contribution to the Solomon-Bloembergen equation would account for the low values of $1/T_2$ observed. This latter property concurs with observed Gd coordination chemistry, as the unpaired electrons of Gd are shielded by its outer orbitals from ligand contact interactions. The correlation time, τ_C, calculated from their data is in the order of 7×10^{-11} sec. Since τ_M from ^{17}O n.m.r. is approximately 10^{-8} sec. and τ_S from e.s.r. data is 1.5×10^{-10} sec., τ_C appears to be dominated by τ_R as previously proposed.

Reference to the Solomon-Bloembergen equations (58) demonstrates the dependence of $1/T_1$ on the distance separating the unpaired electrons from the nuclei in question. As a result the replacement of water molecules by protein ligands might be expected to cause a decrease in the measured H_2O proton relaxation. In fact, the opposite is observed within Gd-protein complexes (62). Since Gd chelated to small buffering anions free in solution undergoes rapid anistropic motion, while metal ions coordinated to two or more functional groups of a macromolecule rotate at the same rate as that protein chain, the observed enhancement appears to result from a change in the dominant correlation time. Metal ions coordinated to a macromolecule would dominate water proton relaxation primarily by τ_S, whereas τ_R is the major contributing parameter governing relaxation rates within the aquo complexes of Gd (60).

Some of the proteins recently investigated via this technique were pyruvate kinase (61), trypsin (62), concanavalin A (63), Mn-phosphorylase (64), and streptococcal nuclease (63).

B. Results

1. Gadolinium Interactions With Phosphorylase in the Solution State

a. Reaction Conditions

Reaction conditions were chosen to parallel those utilized in crystal studies. The selected buffer, BES, had negligible metal chelation abilities, whereas MES expressed log K_D values in the order of 0.8 for Mg(II) and 0.7 for Ca(II) and Mn(II). Glycerophosphate buffers formed precipitates upon Gd addition. Other reagents, such as EDTA, IMP and AMP sequestered the metal in solution. Metal complexation may be monitored qualitatively through alterations in the hyperfine spectra of Gd.

The selection of hydrogen ion concentration was critical as

insoluble hydroxide adducts were formed at pH values greater than neutrality. To within two tenths of a pH unit, 30 mM BES maintained the hydrogen ion concentration at the initial value in the reaction studied.

b. The Number of Metal Binding Sites

i. Metal Titration Curve

Although Gd complexation with phosphorylase results in various physico-chemical perturbations of the enzyme, only activity and spectral changes were monitored as phosphorylase was titrated with metal.

Figure 9 depicts a typical inactivation curve. With a monomer concentration of 5.62×10^{-5} M, phosphorylase b expresses a 50% loss of activity with a 19 molar excess of Gd after 22 hr. at 25°C. in 30 mM BES. A similar experiment with 8.33×10^{-5} M phosphorylase a exhibits a 50% retention of native activity with a 20 molar excess of metal. Therefore the site(s) responsible for inducing inactivation express the same affinity for Gd ions, within experimental error, with both forms of phosphorylase.

The systems used in the activity studies were also scanned for spectral changes in the characteristic PLP absorption bands. Peak location is identical in both the native and the metalloprotein samples, however the presence of Gd alters peak intensities. Figure 10 outlines the three basic spectral modulations obtained with phosphorylase b. In the presence of approximately equimolar concentrations of metal and monomer, optical densities at both 330 nm and 415 nm increase. Further increases in metal concentration return peak intensities to values approximating the native state. At a molar ratio of 10, the 415 nm peak again increases in intensity until saturation is attained with a molar excess of Gd exceeding 40. In contrast the 330 nm band, Figure 11,

Figure 9

Activity titration curve of phosphorylase b equilibrated with varying concentrations of Gd. Plot of activity in umol /min/mg vs. the ratio of Gd to monomer concentration. Phosphorylase b at a concentration of 5.62 X 10^{-5} M monomer was reacted with varying concentrations of Gd for 22 hr. at 25°C. in 30 mM BES pH 6.8. Substrate solutions contained 75 mM G-1-P, 1 mM AMP and 1% glycogen pH 6.8.

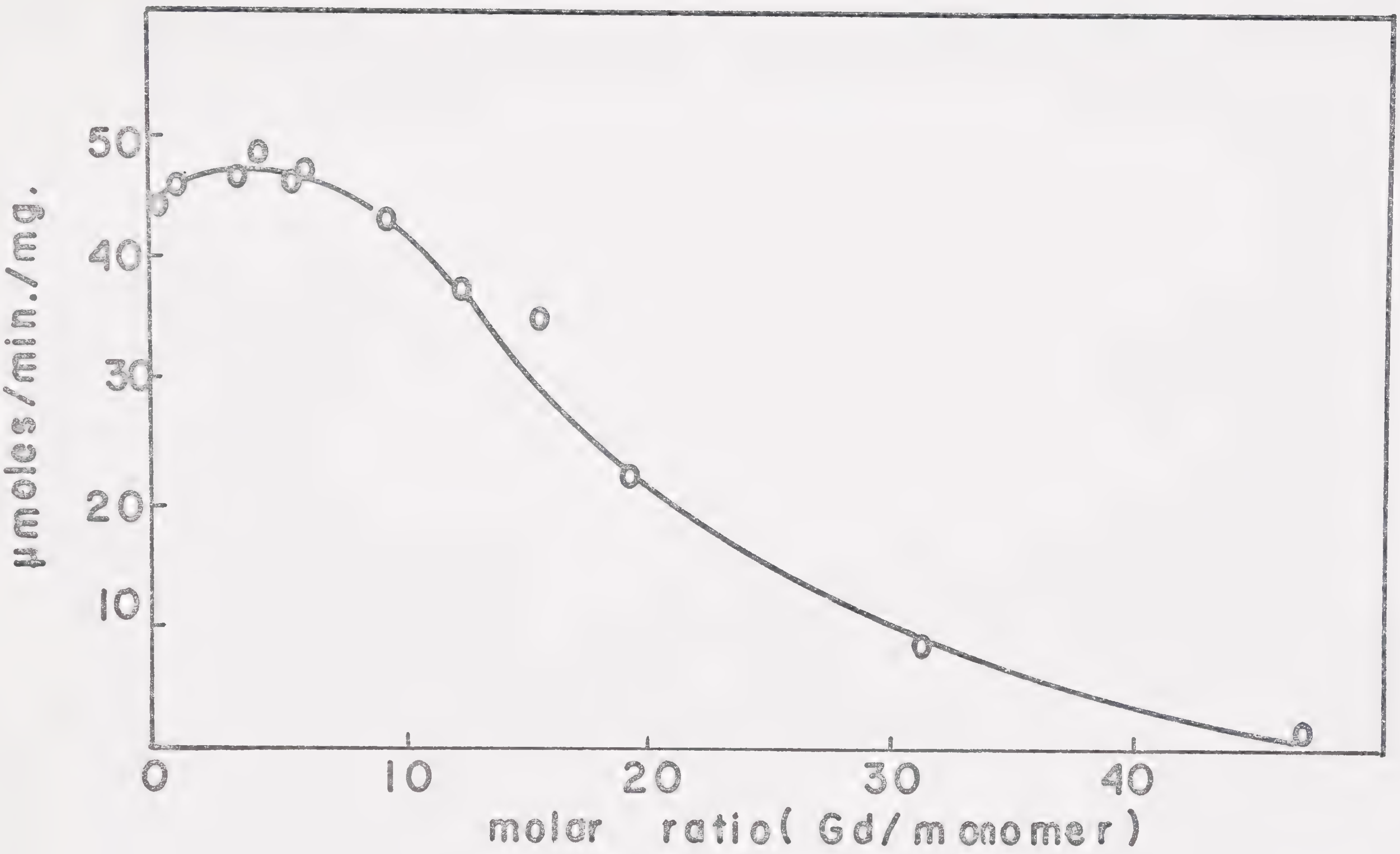
µmoles/min./mg.
50
40
30
20
10
0
10
20
30
40
molar ratio(Gd/monomer)

Figure 10:

Spectral titration curve at 415 nm of phosphorylase b equilibrated with varying concentrations of Gd. Plot of absorbance at 415 nm vs. the molar ratio of Gd to monomer. Phosphorylase b at a concentration of 5.62 X 10^{-5} M monomer was equilibrated with varying Gd concentrations over a period of 22 hr. at 25°C., prior to spectral analysis.

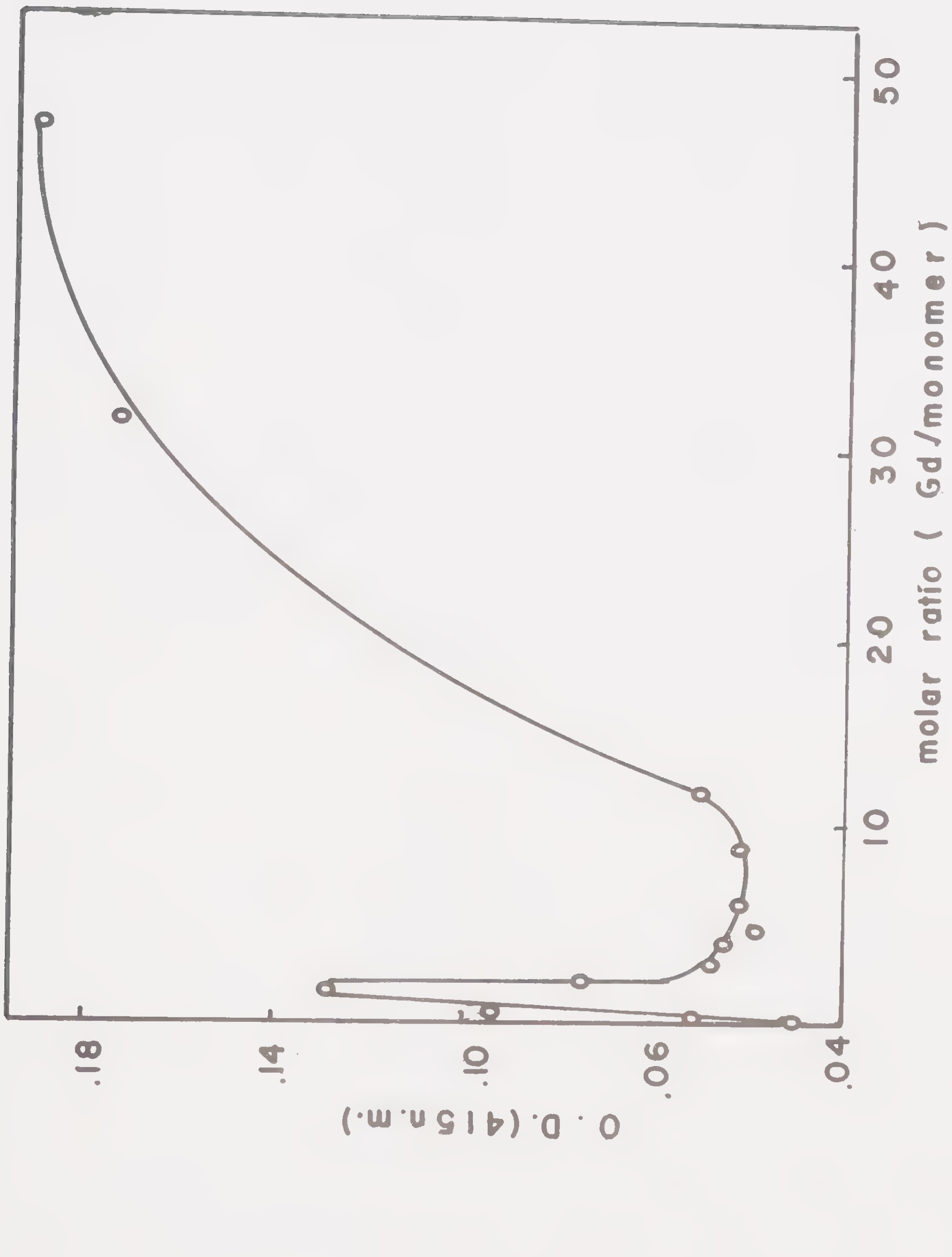
O. D. (415 n.m.)
.18
.14
.10
.06
.04
10
20
30
40
50
molar ratio (Gd/monomer)

Figure 11:

Spectral titration curve at 330 nm of phosphorylase b equilibrated with varying concentrations of Gd. The plot consists of absorbance values at 330 nm vs. the molar ratio of Gd to monomer. Reaction conditions were identical to Figure 10.

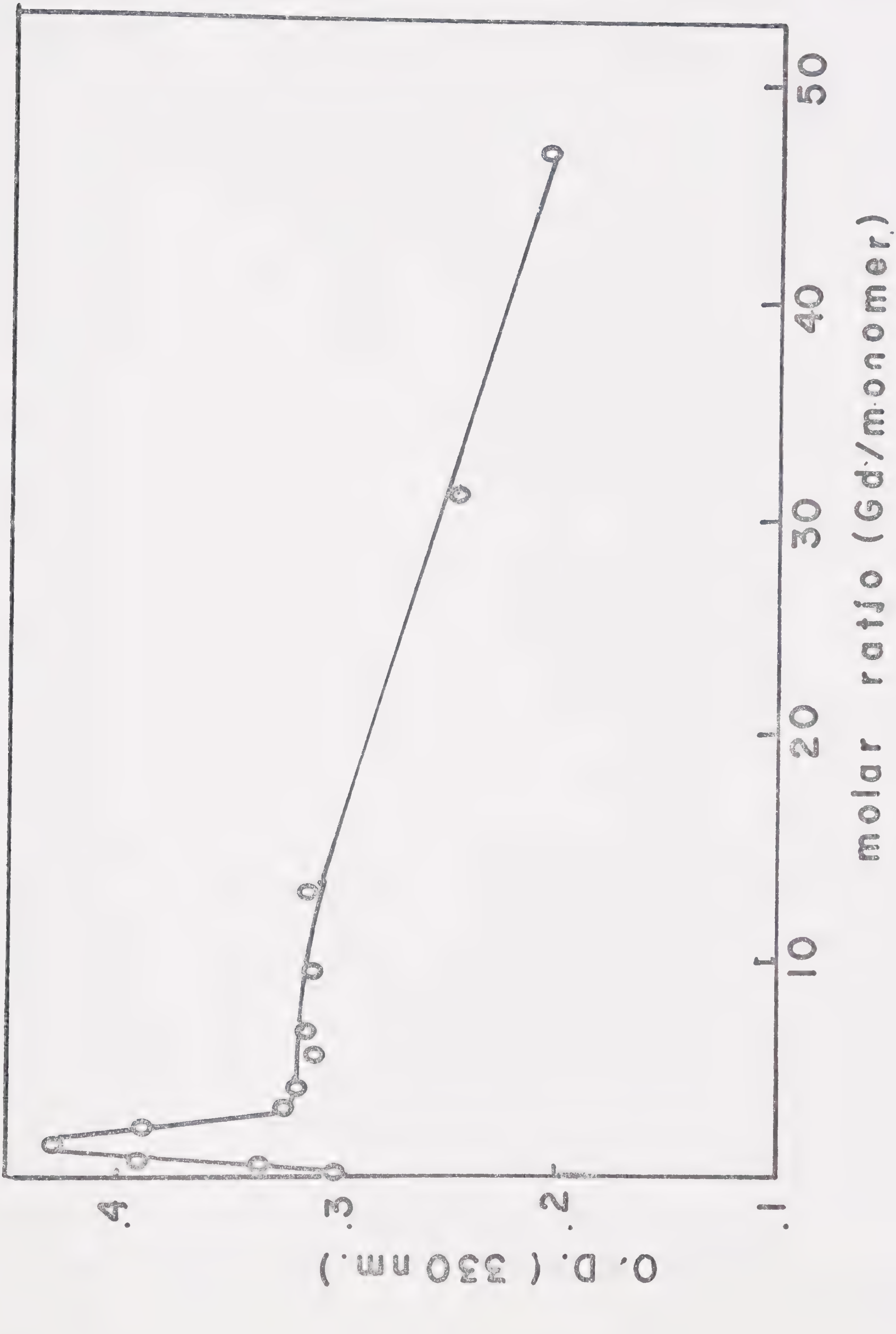
O. D. (330 nm.)
4.
3.
2.
1.
molar ratio (Gd/monomer)
10
20
30
40
50

decreases in optical density only when metal concentrations exceed 5.62×10^{-4} M.

Data obtained from the analogous experiment with phosphorylase a at 5.30×10^{-5} M are less definitive. Optical densities at 415 nm and 330 nm increase to values correlating with the phosphorylase b complex reacted with a 1 to 1.2 molar excess of metal. Further increases in the concentration of Gd induce protein turbidity. However once the concentration of metal exceeded 7.95×10^{-4} M, the metalloprotein remains in solution and exhibits increases in the 415 nm optical density until saturation is attained with a 45 molar excess of metal. Correlating with the Gd-phosphorylase b results, the 330 nm peak intensity decreases within the same range of metal concentrations.

The following sections designate properties observed with equimolar metal to monomer concentrations to the high affinity or primary Gd site and characteristics detected with a greater than 20 molar excess of Gd as definitive of the low affinity site(s).

ii. Water Proton Relaxation

Enhancements, ε^*, were determined at constant phosphorylase b concentrations and varying concentrations of Gd, an M titration, at two frequencies, 40.5 MHz and 270 MHz, at 25°C. Figure 12 demonstrates the marked frequency dependence of water proton relaxation in the presence of the metalloprotein complex. Since τ_S or electron spin relaxation is the correlation time modulated by frequency, these results are indicative of an increased τ_S contribution to spin lattice relaxation. Therefore the rotational correlation time is slower in the metalloprotein relative to the freely tumbling Gd aquo complex as mentioned in the Introduction. In addition Figure 12 depicts the high affinity of metal

Figure 12

Enhancement of water proton relaxation upon Gd titration of phosphorylase *b*. Plot of the observed enhancement calculated via the method outlined in Appendix I *vs*. total Gd concentration. Phosphorylase *b* at a concentration of 14.2 X 10^{-5} M was reacted with Gd at 25°C. for at least 1 hr. prior to the determination of relaxation times.

○——○ observed enhancement at 40.5 MHz

●——● observed enhancement at 220 MHz

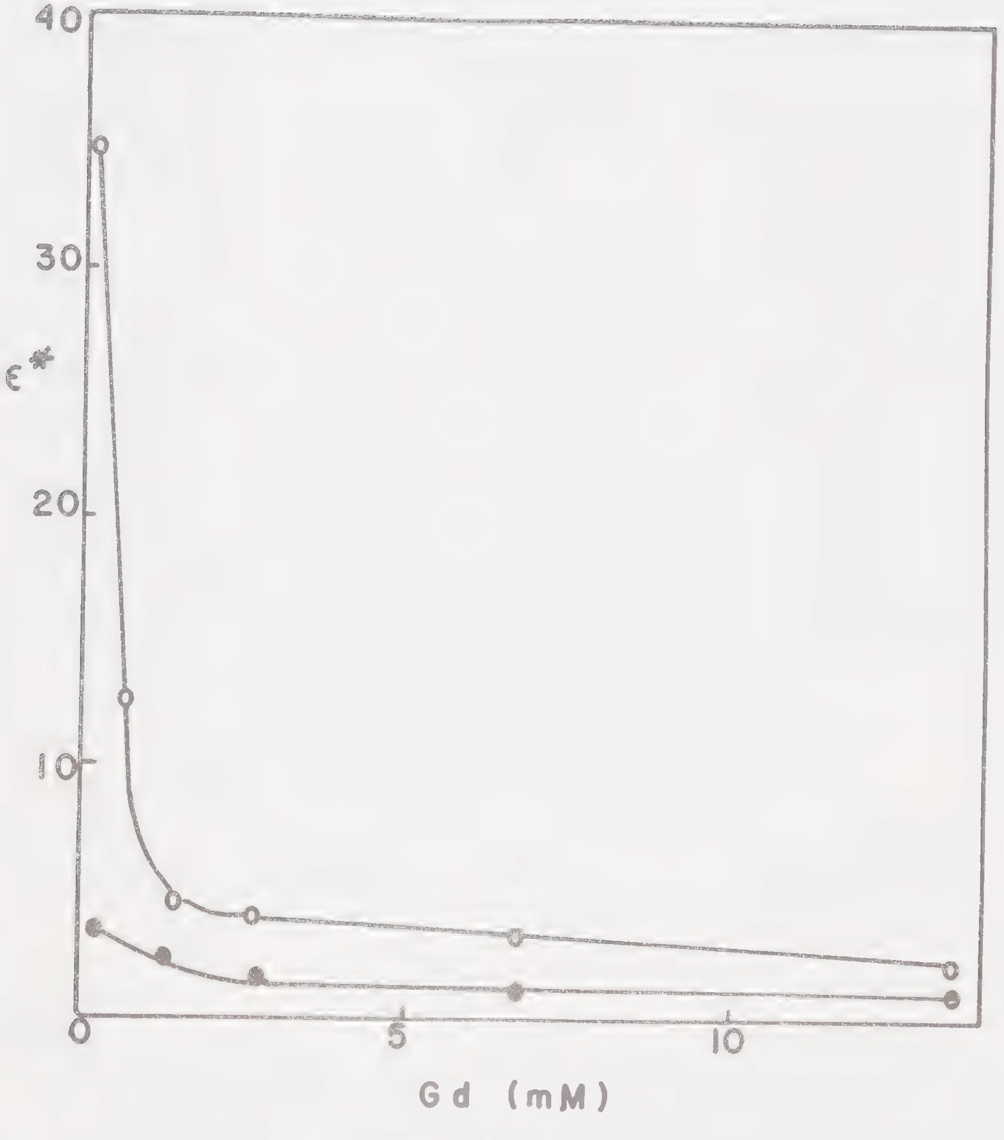
40
30
20
10
0
ε*
0
5
10
Gd (mM)

binding to phosphorylase b since the observed enhancement, ε^*, hasn't plateaued even at a Gd to monomer mole ratio of two.

To ascertain the number of Gd binding sites, n, and their respective dissociation constants, the enhancement of water proton relaxation at metal saturation, ε_B, was required. To obtain this parameter, 50 μM Gd was titrated with enzyme at a frequency of 40.5 MHz and 25°C. At such low concentrations of metal, Gd adsorption to glass became significant. All reaction tubes and pipets were washed in KOH/95% ethanol, 10 mM EDTA and distilled water prior to use. Reciprocal plots of enzyme concentration versus observed enhancement were extrapolated to the y-axis to obtain the approximate value of $1/\varepsilon_B$. Figure 13 depicts the hyperbolic inflection of the curve at a Gd to monomer mole ratio of one. Using the calculations outlined in Appendix 1, approximate values of n and K_D were obtained from Scatchard plots. Assuming n independent and equivalent metal binding site(s), the two following equations were used to fit the three parameters ε_B, n and K_D via iteration.

$$\varepsilon^* = 1 + EM(\varepsilon_B - 1)/M_o$$

$$EM = \frac{((nE_o+M_o+K_o) - ((nE_o+M_o+K_o)^2 - 4nE_oM_o)^{1/2})}{2}$$

where:

EM is the concentration of the Gd-phosphorylase b complex

M_o is the total concentration of Gd

E_o is the total concentration of phosphorylase b monomer

The results indicate 1.02 ± 0.07 Gd binding sites per monomeric unit with an apparent dissociation constant of 1.36 μM ± 0.9 μM and an ε_B of 37.8 ± 0.6.

Figure 13

Enhancement of water proton relaxation upon titration of a constant Gd concentration with phosphorylase *b*. Plot of reciprocal values of observed enhancement *vs*. reciprocal monomer concentration. Gd at a concentration of 50 μM was reacted with enzyme in 30 mM BES, 3 mM DTT pH 6.8 for at least 1 hr. at 25°C. before evaluating $1/T_1$ values.

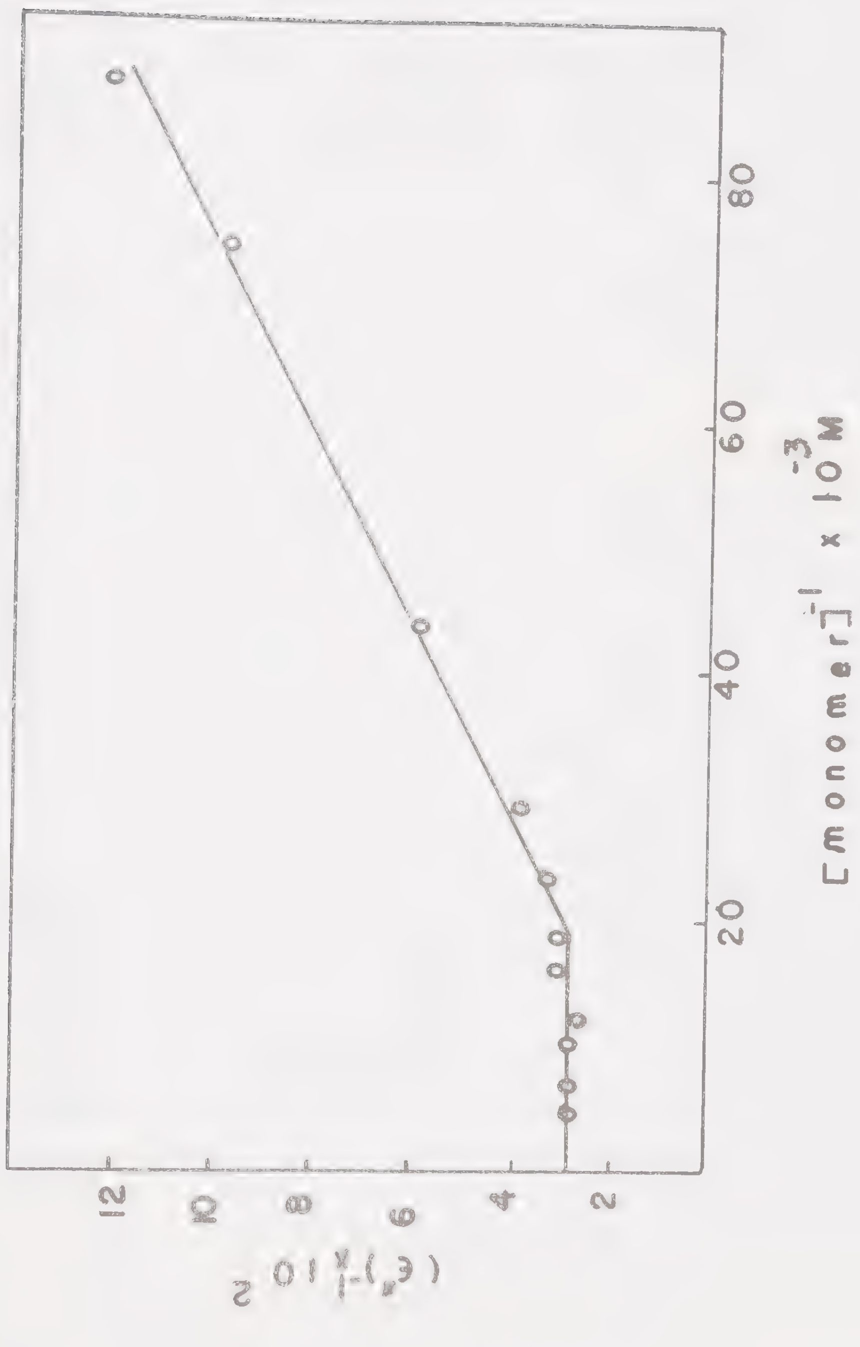
$(\epsilon_r)^{-1}$ x 10^2
12
10
8
6
4
2
20
40
60
80
[monomer]$^{-1}$ x 10^{-3}M

Comparisons of the observed enhancements calculated from both the M and E titrations indicate that the high affinity site is the sole contributor to the observed water proton relaxation enhancement. The metal site(s) expressing a lower affinity as evidenced from previous spectral and activity titrations are either binding very weakly and perhaps nonspecifically or are unavailable for interactions with the bulk solvent as would be the case if the metal was binding within a protein pocket.

c. Perturbations of Phosphorylase Induced upon Gd Occupation of the Low Affinity Site

i. Activity Studies

The addition of a greater than 40 molar excess of Gd to phosphorylase monomer led to rapid inactivation. Figure 14 denotes the relative rates of inactivation and 415 nm peak intensity enhancement as phosphorylase a at 3.7 X 10^{-5} M was reacted with 2.7 mM Gd at 25°C. Although both properties are pseudo first order, the rate of increase in the 415 nm peak intensity preceeds the loss of catalytic activity. This observation could be attributed either to the involvement of at least two unique conformational changes or to the result of a dilution effect. Since activity assays contained protein at a concentration 10^3 times more dilute than the spectral samples, the stability of the electrostatic complexes formed between Gd and the lower affinity metal site of phosphorylase may differ between these two assay systems. In other words, the rates of inactivation and schiff base formation may be the same if the dilution step was eliminated. Unfortunately the validity of this proposal is difficult to establish due to technical complications. Crystal activity assays with phosphorylase a were conducted in the presence

Figure 14

Time study of inactivation and enhancement of 415 nm absorbance values upon reaction of 2.7 mM Gd with phosphorylase *a*. Phosphorylase *a* at a concentration of 3.7×10^{-5} M was reacted in a buffer system containing 30 mM BES, 3 mM DTT pH 6.8. Substrate solutions contained 75 mM G-1-P, 1% glycogen pH 6.8. Absorbance values were read against a buffer reference.

X——X absorbance values at 415 nm

O——O metal induced inactivation

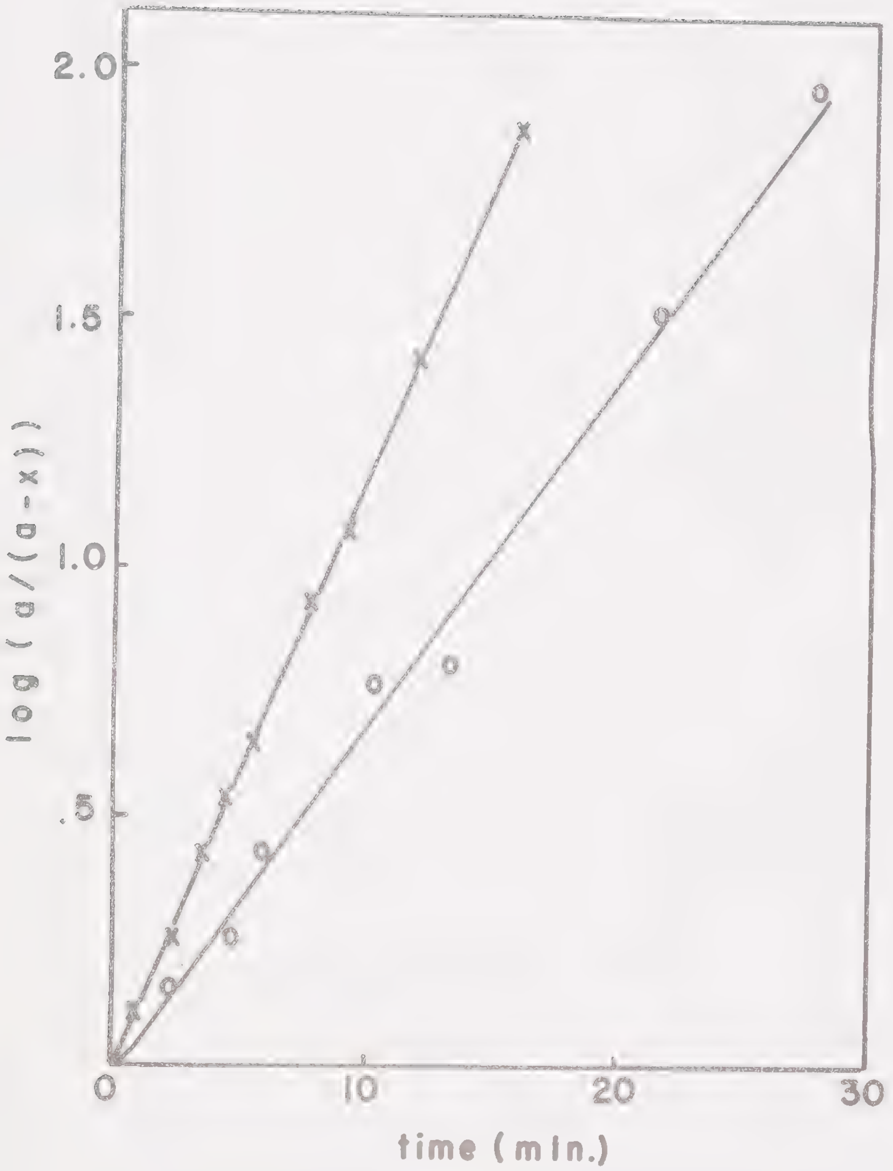
2.0
1.5
1.0
.5
0
10
20
30
log (a / (a - x))
time (min.)

of glucose, therefore inactivation data were collected with the solution form of the enzyme preincubated with a 50 mM concentration of this reagent for 20 min. at 25°C. Although immediate protein turbidity occurs upon the addition of 2 mM Gd, catalytic activity is retained. This observation indicates that the lower affinity Gd site within the glucose stabilized dimer of phosphorylase a is less reactive with metal. The lower occupancy would produce a metalloprotein complex characterized by the titration curves, Figures 10 and 11, in the region where the molar excess of Gd to monomer varied from 1.5 to 10.

Figure 15 indicates the rates of activity and spectral perturbations induced in 3.61×10^{-5} M phosphorylase b upon the addition of 2 mM Gd at 30°C. With respect to kinetic order and the relative rates of inactivation to enhancement of optical densities at 415 nm, the Gd-phosphorylase b complex correlates with its phosphorylase a counterpart.

ii. Coenzyme Characteristics

Visibly, the most significant feature induced in phosphorylase upon occupation of the low affinity Gd site is the production of a yellow colouration of the protein. The following result sections were designed to define the origin and cause of this phenomenon.

iii. Absorption and Fluorescence Spectra

Spectral scans recorded at set time intervals after the addition of 1.7 mM Gd to 3.14 mg/ml of phosphorylase b, Figure 16, evidence an isosbestic point at 362 nm. Peak location coincides within both the native and metalloprotein samples. Therefore Gd occupation of this low affinity site is shifting the PLP tautomer equilibrium in favour of the schiff base structure absorbing at 415 nm.

Figure 15

Time studies of inactivation and 415 nm peak intensity enhancement upon reaction of 2 mM Gd with phosphorylase b. The reaction was conducted in 30 mM BES, 3 mM DTT pH 6.8 with 3.61 X 10^{-5} M phosphorylase b. The substrate solution consisted of 75 mM G-1-P, 1 mM AMP and 1% glycogen pH 6.8.

O——O metal induced inactivation

X——X enhancement of absorbance values at 415 nm

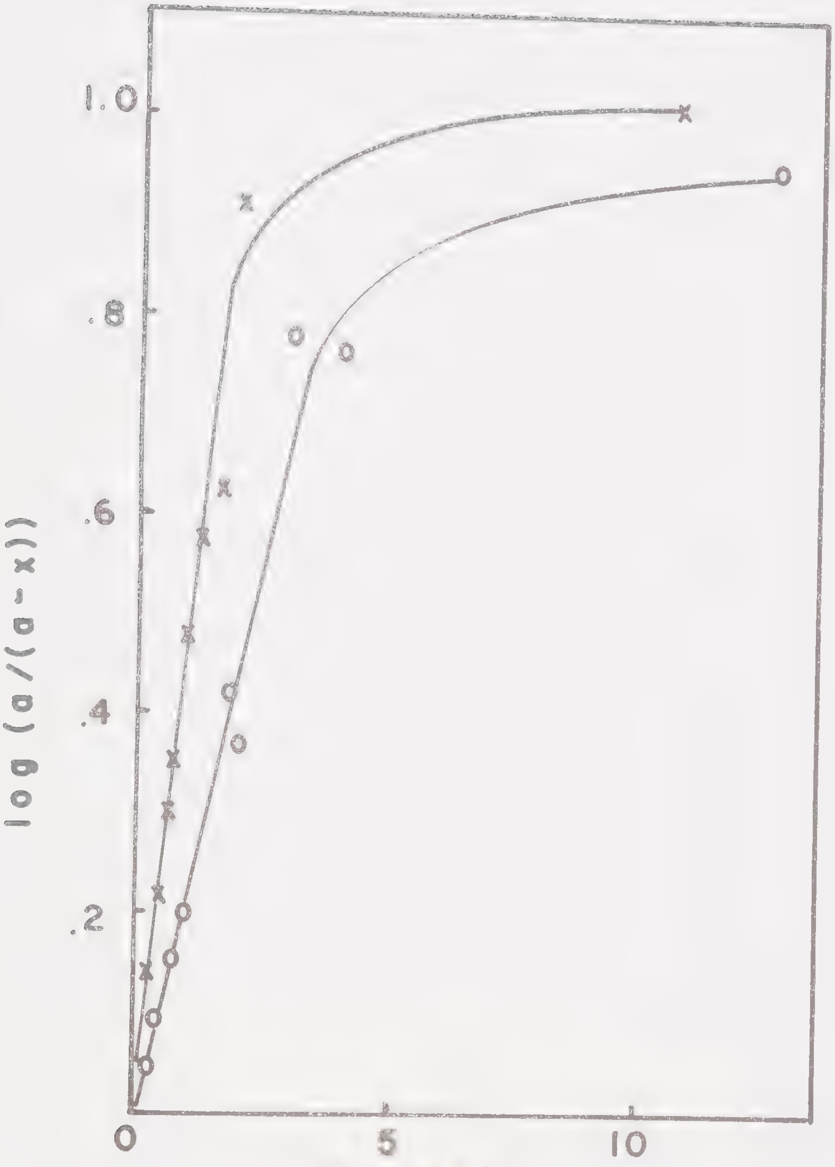
log (a/(a - x))
1.0
.8
.6
.4
.2
0
5
10
time(min)

Figure 16

Spectral scan during the formation of the Gd-phosphorylase b complex. A plot of absorbance vs. wavelength in nm. Phosphorylase b at a concentration of 3.14 mg/ml in 30 mM BES pH 6.8 was reacted with 1.7 mM Gd at zero time. The letters in the spectra refer to the time intervals at which the spectral scan was initiated. The native enzyme sample is denoted by "a" and the metalloprotein samples after 3.5, 8.1 and 28.5 min. reaction times are denoted respectively by "b", "c" and "d". The isosbestic point occurred at 362 nm with a molar extinction coefficient of 2.2×10^3 M^{-1} cm^{-1}.

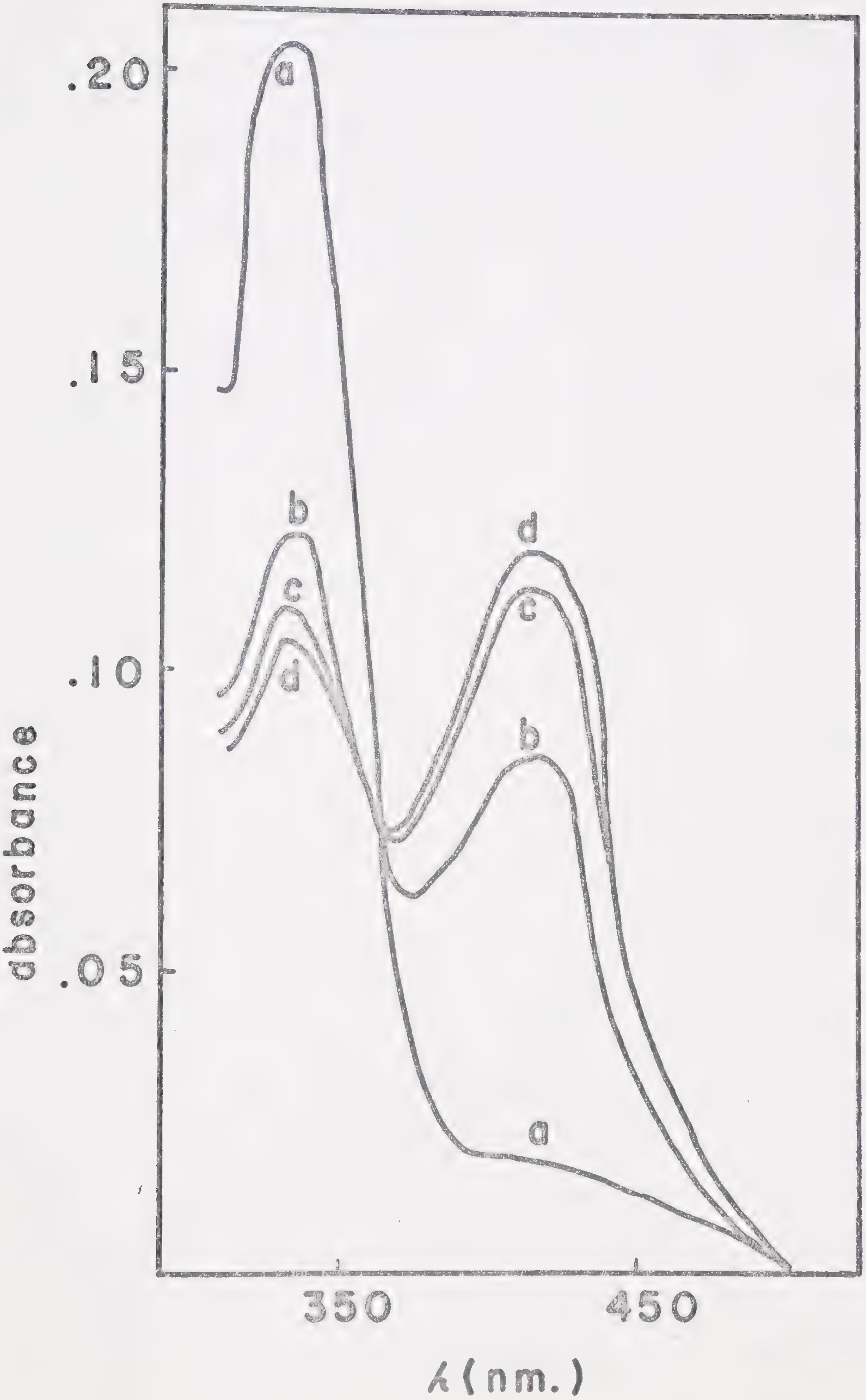
.20
.15
.10
.05
absorbance
350
450
λ (nm.)
a
b
c
d
d
c
b
a

Kinetic studies involving the rate of increase in the 415 nm absorption peak indicate that schiff base formation follows pseudo first order kinetics. The slope of the plot denoted in Figure 17 is $1.73 \pm 0.15 \text{ min}^{-1}/\text{M}^{-5}$. However the decrease in the intensity of the 330 nm absorption peak, under conditions parallel to the 415 nm experiment, is biphasic. Graphs of K_{obs} vs. monomer concentration for each linear segment of the 330 nm plot had slopes of $0.36 \pm 0.07 \text{ min}^{-1}/\text{M}^{-5}$ and $0.16 \pm 0.01 \text{ min}^{-1}/\text{M}^{-5}$. These results suggest that the observed enhancement of schiff base formation upon Gd coordination involves an equilibrium shift between more than two tautomeric species of the coenzyme.

To ascertain whether Gd is stabilizing the schiff base directly via bidentate coordination to the imine nitrogen and the 3' hydroxyl group of PLP (30), fluorescence yields are evaluated. If the metal formed a ground state complex with the coenzyme in order to directly stabilize the schiff base, fluorescence quenching would be expected(56). Fluorescence yields in systems containing either PLP or phosphorylase b in the presence or absence of Gd were calculated by dividing the emission peak area by the absorbance observed at the excitation wavelength. The ratios of this yield in a system containing Gd relative to the native molecule were calculated for PLP and the enzyme in 30 mM BES pH 6.8. With the model, PLP system, excitation at 390 nm in the presence of Gd results in a yield ratio of 0.35 relative to native PLP. In addition the excitation peak is shifted to 400 nm in the presence of Gd. Phosphorylase b in the presence of Gd exhibits a ratio of 1.65 relative to the native enzyme upon excitation at 415 nm. In addition peak locations are not altered in the presence of metal. These prelim-

Figure 17

Rate of alteration of the 415 nm peak intensity upon occupation of the low affinity Gd site in phosphorylase *b*. Plot of the observed rate of increase in the 415 nm absorbance determined from $t^{1/2}$ at various protein concentrations *vs*. monomer concentration. Gd at a concentration of 4.1 mM was reacted with enzyme in 30 mM BES, 3 mM DTT pH 6.8 at 30°C. Spectral readings were recorded against a reagent blank.

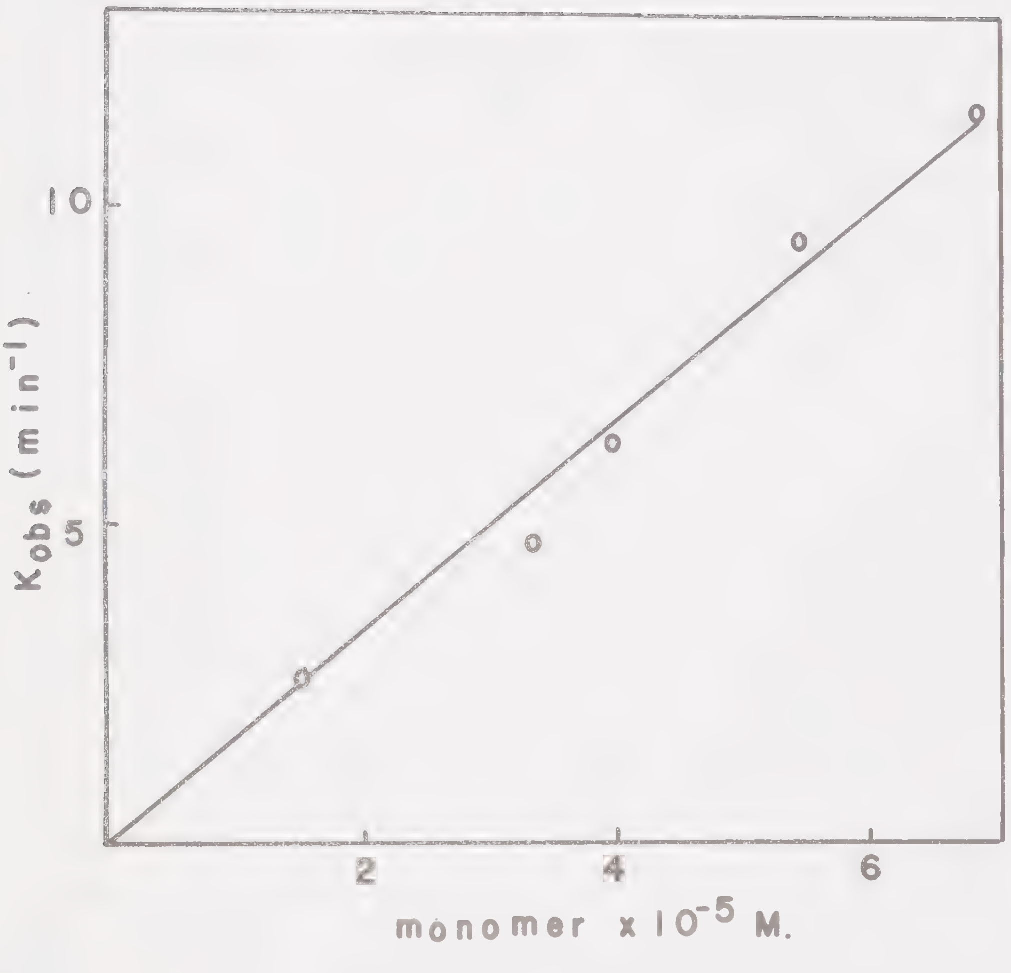
10
5
Kobs (min⁻¹)
2
4
6
monomer x 10⁻⁵ M.

inary results indicate that the low affinity Gd site is not near enough to the coenzyme site to promote fluorescence quenching.

To evaluate this possibility further, the pyridoxal analogue, PLP-Val, was studied in the presence and absence of Gd ions. Previous work with the PLP-Val system in methanol at neutrality and transition metal ions (31) have indicated that some metals are capable of catalyzing and stabilizing schiff base formation (65,66). This phenomenon is evidenced by a blue shift of 26 to 37 nm and a concomitant decrease of the optical density of the ketoimine π_1 band. Interactions of Gd with the PLP-Val complex induce a change in optical density and a blue shift of 12.5 nm in the ketoimine band. Since these parameters are not observed with the Gd-phosphorylase b complex, the absence of direct Gd stabilization of the schiff base may be inferred.

Solvent Accessibility

Data thus far indicate that Gd occupation of the low affinity site induces promotion of schiff base formation indirectly, probably via conformational perturbations. Both models for the structural forms of the coenzyme, as outlined in the Introduction, suggest that the enhancement of the 415 nm peak intensity upon phosphorylase perturbation is due to an increased exposure of the protein bound PLP to solvent molecules. To assess the validity of this proposal in the case of the Gd-phosphorylase complex, the reactivity of the coenzyme within the metalloprotein complex with $NaBH_4$ and NH_2OH was examined.

Phosphorylase b at a concentration of 17 mg/ml was incubated with 3.4 mM Gd in 30 mM BES pH 6.8 until completely inactivated. After chilling the reaction in ice, $NaBH_4$ was added to reduce the double bond of the schiff base. The enzyme obtained after $(NH_4)_2SO_4$ precipitation

and extensive dialysis was assayed for unreduced PLP. Within the sensitivity of the assay, no coenzyme is released from the Gd modified protein, whereas native phosphorylase under the same conditions releases one PLP per subunit.

An alternate approach monitors the reactivity of hydroxylamine with PLP in the metalloprotein complex relative to phosphorylase b perturbed with imidazole citrate (68). Since the protonated hydroxylamine is the reactive species, the resultant internal acid-base catalyzed reaction with PLP is highly pH dependent. The extent of complexation would therefore reflect the microenvironmental pH of the coenzyme site in conjunction with degree of solvent accessability to the PLP pocket. The oxime product of the reaction has a blocked formyl carbon consequently the phenylhydrazine assay of Snell (20) is inapplicable. The extent of the reaction was followed spectrophotometrically against standard PLP-NH_2OH complexes. Phosphorylase b at 13.7 mg/ml was incubated with either 5.7 mM Gd or 0.4 M imidazole for 40 min. at 30°C. prior to the addition of 83 mM NH_2OH and the readjustment of the pH to 5.5 with citrate. Neglecting the fine spectra due to free Gd, peak location of the supernatant solution from the $(NH_4)_2SO_4$ precipitation is identical to the model. Molar extinction coefficients calculated from the models indicate the reaction of one PLP per monomer in the Gd modified protein whereas imidazole citrate perturbation is only 62% as effective. These data indicate a decrease in the hydrophobicity and an increase in the hydrogen ion concentration of the coenzyme's microenvironment within the Gd-phosphorylase b complex.

An observation which further substantiates the opening of the coenzyme pocket was the intensity increase of the 390 nm emission band of 40% reduced phosphorylase b reacted with Gd. Excitation at 330 nm

showed enhanced emission at 390 nm relative to the corresponding peak in 40% reduced enzyme in the absence of metal. Cortijo (69) postulated that the intensity of the 390 nm band was responsive to changes in the microenvironmental pH and hydrophobicity of the coenzyme pocket. Increasing quantum yields in the presence of Gd are indicative of the increased accessibility of the pyridoxamine 5' phosphate to solvent molecules, whereas a blue shift of the 390 nm peak to 384.2 nm reflects a change in pH (70).

Reversibility of Metal Binding

The effect of the dissociation of Gd from the low affinity metal binding site of phosphorylase b was determined via the techniques of EDTA titration, dialysis and gel filtration.

To determine whether Gd forms a one to one complex with EDTA, the decrease in peak intensity of the 230 nm absorption band of EDTA was monitored as the concentration of metal was increased. In 30 mM BES pH 6.8, a plot of the molar extinction coefficient vs. Gd concentration is biphasic with an inflection point at a molar ratio of Gd to EDTA of 1.3. The reverse titration, involving Gd reacted with increasing concentrations of EDTA, plateaus at a molar ratio of 0.98. Since EDTA chelates Gd under these conditions in a one to one complex, the next step was to determine whether EDTA would remove Gd from the low affinity site of the metalloprotein complex. Phosphorylase b at 8 mg/ml was reacted with 6.8 mM Gd in 30 mM BES pH 6.8 until inactivated. By monitoring the change in the 415 nm peak intensity upon titration of the Gd-phosphorylase b complex with EDTA, the extent of metal dissociation from the enzyme could be analyzed. As the concentration of EDTA approached the total concentration of Gd present in the sample, the protein

sample became viscous and turbid with only a slight reinstatement of catalytic activity.

The Gd-phosphorylase b complex prepared for the EDTA titration experiment was passed through a Sephadex G-25 column equilibrated with 30 mM BES pH 6.8. The eluate, which expresses increased viscosity and turbidity relative to the applied sample, lacks the characteristic intense 415 nm peak. In addition only 3 to 4% of the activity is reinstated. Phenylhydrazine assays of the perchloric acid treated eluate indicate the presence of 0.8 PLP per monomer. The protein eluate is unstable and precipitates upon standing at room temperature for 6 hr.

Extensive dialysis of the metalloprotein complex, prepared for the titration experiment, against 30 mM BES, 2.4 mM DTT and 5 mM EDTA at pH 6.8 produced a viscous turbid suspension. Eighty percent of unreduced PLP was bound per subunit.

Results from these three methods indicate that phosphorylase aggregates formed upon occupation of the low affinity site are not easily reversed to the native state upon Gd removal.

iv. Ligand Protection

Several modifiers were preincubated at 30°C with phosphorylase b prior to the addition of 2 mM Gd at zero time. Time studies of inactivation and 415 nm absorption enhancement were monitored relative to the metalloprotein complex in the absence of effectors or substrates to determine the effectiveness of ligand protection.

Manganese binds at two locations on the monomer. The highest affinity site has a K_D of 0.17 mM, while the second is in the range of 5.10 mM (14). At Mn concentrations varying from 0.23 to 2.07 mM there

is no significant change in schiff base formation, but inactivation and intensity decreases in the 330 nm absorption band are slightly slower.

Adenosine, which binds primarily in the glucose-adenine domain outlined in the x-ray crystallographic map (17), at a concentration of 2.88 mM had no effect on Gd induced inactivation, however it did blue shift the 330 nm peak by 10 nm with a slight concomitant increase in both the 415 nm and the 330 nm peak intensities.

Glucose, which activates phosphorylase by promoting dimerization, at a concentration of 50 mM decreases the rate of schiff base formation by 14%. Figure 18 demonstrates the increased lag period preceeding inactivation in the presence of glucose.

Complications arose in determining the effectiveness of AMP, G-1-P and IMP as allosteric regulators of phosphorylase _b_ interactions with Gd. The presence of the phosphate moiety enables all three to chelate Gd as illustrated in Table 5. AMP, an effector required for phosphorylase _b_ activity, promotes enzyme tetramerization under certain conditions. In the presence of 1 mM AMP and one of the following divalent cations, Mn(II), Mg(II), Ca(II), at a concentration of 1 mM, tetramerization of phosphorylase _b_ occurs. Sedimentation velocity data was collected to ascertain whether Gd mimicked these metal cations in this respect. Figure 19 shows the dimeric state of the enzyme sedimenting at 8.44×10^{-13}, whereas the reaction of the native enzyme with 2 mM Gd produces an adduct which sediments as multiple schlieren peaks with a leading edge at 11.28×10^{-13} and a trailing edge at 4.78×10^{-13}. However phosphorylase _b_ preincubated with 1 mM AMP or 5 mM ATP prior to the addition of 2 mM Gd produces a metallocomplex which sediments as a tetramer, $S_{20,obs}$ 13.13×10^{-13}. Another interesting feature of these

Figure 18

Protection study involving Gd induced inactivation of phosphorylase *b* with 50 mM glucose. Plot of the log of the reciprocal fraction of active enzyme *vs.* time. Glucose at a concentration of 50 mM was preincubated with 15.8 mg/ml phosphorylase *b* in 30 mM BES, 3 mM DTT pH 6.8 for 30 min. at 30°C. prior to the addition of 5 mM Gd at zero time. Hedrick substrate solutions were used in the activity assays.

○——○ formation of the metalloprotein complex in the absence of glucose

●——● formation of the metalloprotein complex in the presence of glucose

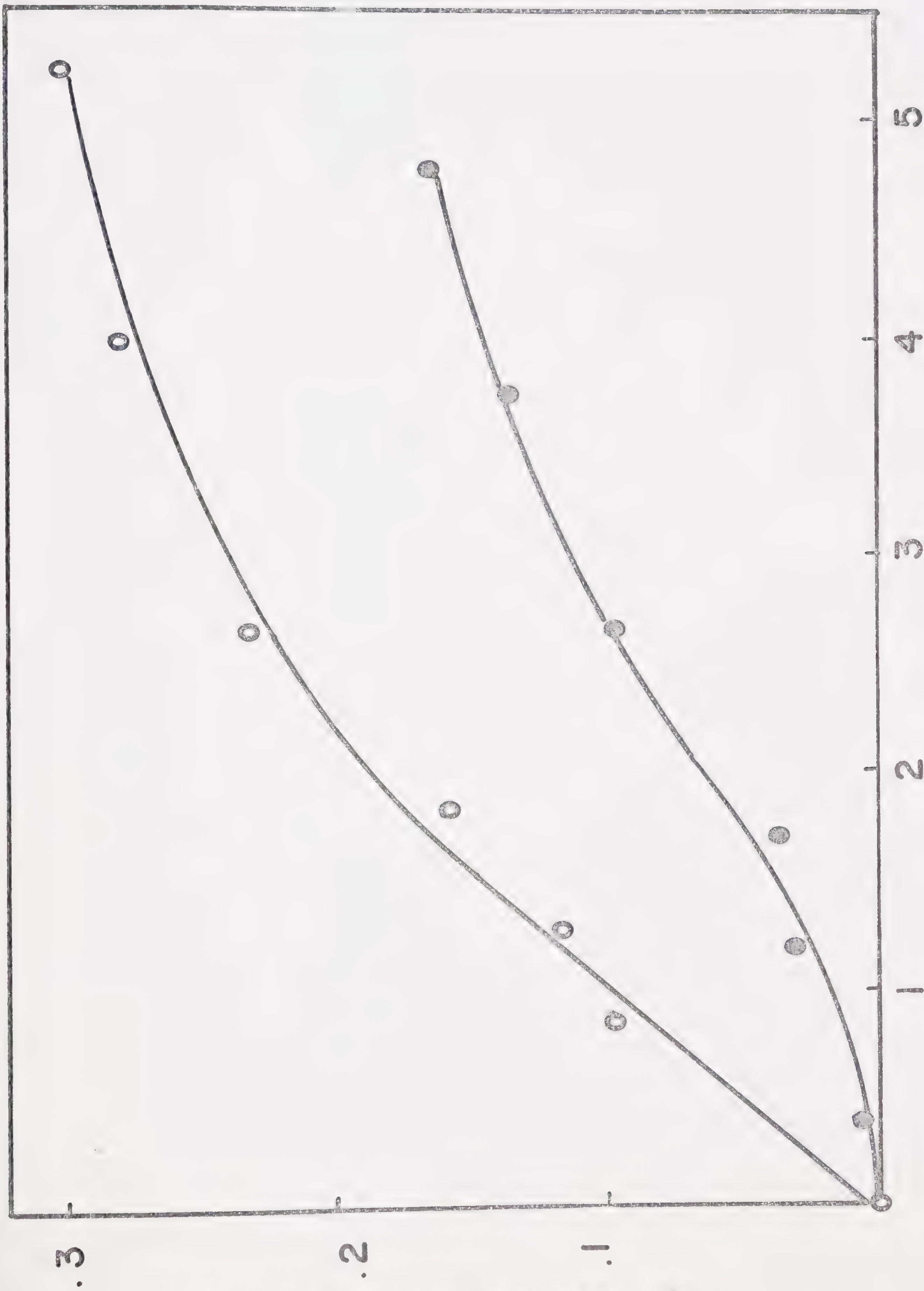
.3
.2
.1
log(100/%control activity)
1
2
3
4
5
time (min.)

Figure 19

Sedimentation velocity study of nucleotide complexes of phosphorylase b reacted with 2 mM Gd. The numbers in brackets refer to the peak locations in svedburg units at 20°C. Phosphorylase b at a concentration of 20 mg/ml was reacted with 5 mM ATP for 20 min. at 30°C. (A) (7.64), prior to the addition of 20 mM Gd (B) (14.2). Under these buffer conditions, 30 mM BES pH 6.8, phosphorylase b at 5.3 mg/ml exhibited the same schlieren peak location both in the presence and absence of 1 mM AMP (C) (8.44). The addition of 2 mM Gd to the native enzyme resulted in the schlieren profile (D) (4.78, 8.04, 10.59, 11.28), while AMP-phosphorylase b-Gd complexes sedimented as depicted in E (13.13).

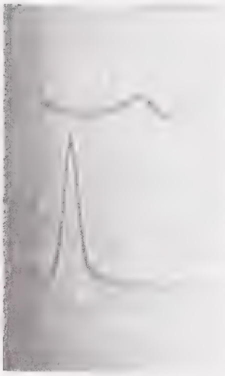

B

A

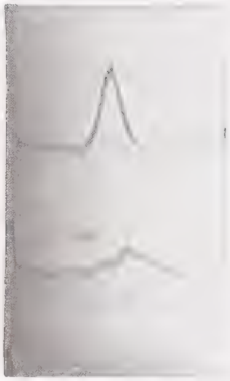

C

D

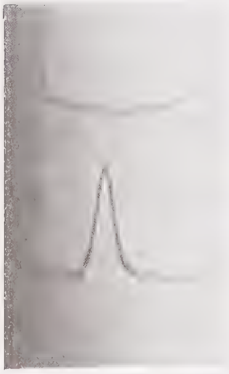

E

latter complexes is their retention of catalytic activity, Figure 20, although immediate protein turbidity occurs upon exposure of the nucleotide-enzyme complexes to Gd ions. IMP at a concentration of 10 mM exerts effects analogous to those obtained with AMP and ATP upon interaction with the enzyme.

The substrate, glucose-1-phosphate, which binds in close proximity to AMP at the active site as evidenced from both x-ray (17) and n.m.r. (16) data, protects phosphorylase b from Gd induced inactivation without the concomitant promotion of protein turbidity.

Possible interpretations of AMP, ATP, IMP and glucose-1-phosphate protection are evaluated in the Discussion.

v. Sulfhydryl Reactivity

Native phosphorylase possesses two fast and two slower reacting sulfhydryl groups per monomer (45). Incubation of the enzyme with 1 mM AMP protects one of the slower groups, while the presence of 20 mM G-1-P enhances its reactivity with sulfhydryl reagents (14). Since modification of one of the slow reacting sulfhydryls led to inactivation and altered subunit interactions, the question arose as to whether Gd perturbation of phosphorylase is centered at this group.

The reactivity of the metalloprotein was studied with both PCMB and DTNB. Concentrations of phosphorylase b varied from 5.4 to 54 μM were incubated with mole ratios of Gd to monomer of 0 or 1.5 or 20 for 8 hr. at 25°C. in 30 mM BES pH 6.8. PCMB was added at a concentration of 9.4×10^{-5} M to a 19 fold dilution of the metalloprotein at room temperature. Peak intensities at 255 nm were recorded once optical density readings had stabilized. Figure 21 demonstrates that metal coordination to phosphorylase induces dramatic increases in sulfhydryl

Figure 20

Protection study involving Gd induced inactivation of phosphorylase *b* in the presence of nucleotides and glucose-1-phosphate. Plot of the log of the reciprocal fraction of active enzyme *vs.* time. Phosphorylase *b* at a concentration of 3.21 X 10^{-5} M monomer was preincubated with either 1 mM AMP, or 5 mM ATP, or 10 mM IMP or 12.3 mM glucose-1-phosphate in 30 mM BES, 3 mM DTT pH 6.8 at 30°C. for 20 min. Gd at a concentration of 1.9 mM was added at zero time to the enzyme. Aliquots removed at set time intervals were assayed for activity using the method of Hedrick (23).

●——● inactivation of native phosphorylase

O- - -O inactivation in the presence of 5 mM ATP

O+ + +O inactivation in the presence of 1 mM AMP

O——O inactivation in the presence of 10 mM IMP or 12.3 mM glucose-1-phosphate

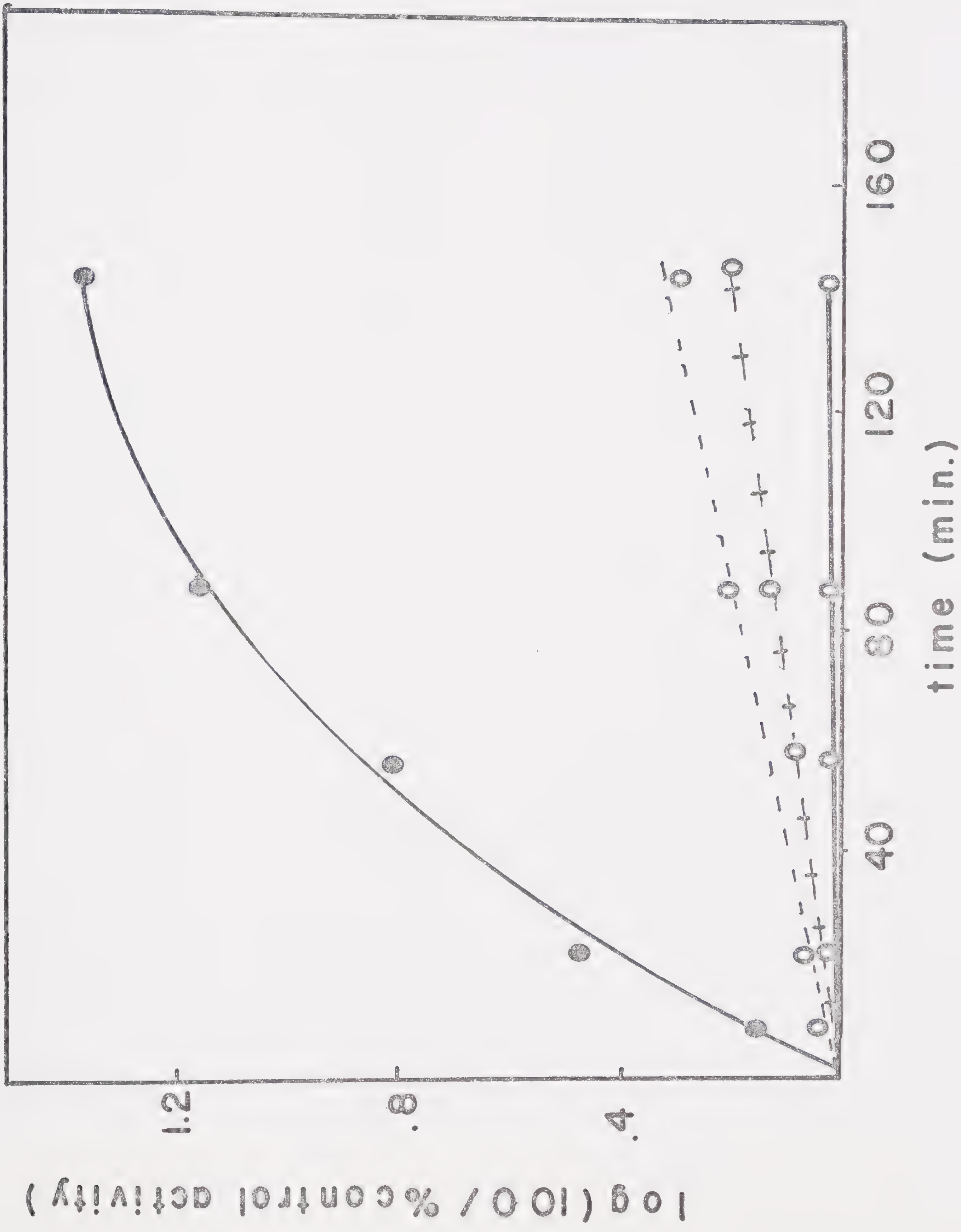
1.2
.8
.4
log (100 / % control activity)
40
80
120
160
time (min.)

Figure 21

Sulfhydryl reactivity of Gd-phosphorylase b with PCMB. A plot of the absorbance readings at 255 nm *vs*. monomer concentration. Reaction conditions are outlined in the text.

O——O enzyme reacted with a 20 molar excess of Gd. The slope was 0.14 absorbance units / M X 10^{-7}.

●——● native enzyme. The slope was 0.01 absorbance units / M X 10^{-7}.

X——X enzyme reacted with an equimolar concentration of Gd. The slope was 0.01 absorbance units / M X 10^{-7}.

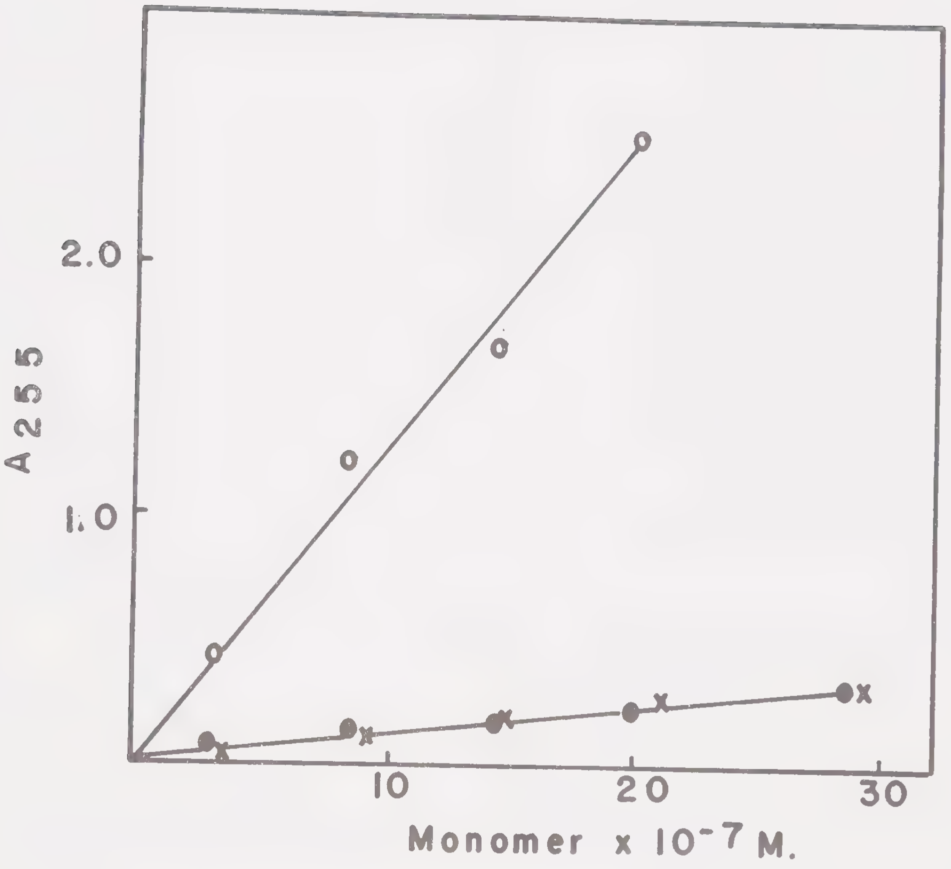

2.0
1.0
A 255
10
20
30
Monomer x 10⁻⁷ M.

reactivity. The number of modified residues within the metalloprotein was difficult to establish since the observed molar absorbtivity of 3×10^4 led to an unrealistically high value.

Phosphorylase b at a concentration of 23.6×10^{-5}M monomer was incubated with 5 mM Gd at 30°C until completely inactivated. Modification of Cys residues was initiated by the addition of 0.5 mM DTNB to a 90-fold dilution of the metalloprotein. Although a previous experiment had indicated no change in peak intensity at 412 nm between Cys-DTNB complexes in the presence or absence of Gd, the number of sulfhydryl groups modified in the metalloprotein appeared to be 24 Cys per monomer. Since only 9 Cys residues per subunit have been determined via amino acid analyses this result is unrealistic. However, only 4 Cys per monomer were modified in the native enzyme under similiar reaction conditions.

d. Perturbation of Phosphorylase Induced Upon Gd Occupation of the High Affinity Site

Evidence from the previously outlined metal titrations, Figures 10 and 11, suggest the presence of a high affinity site in both phosphorylases a and b. Further verification of the latter case is obtained from water proton relaxation calculations, Figure 13.

i. Activity and Spectral Studies

Although the catalytic efficiency of this particular metalloprotein parallells the native enzyme, Figure 9, the characteristic absorption spectra of the coenzyme is modified. Figure 22 depicts the rate of alterations of the 415 nm and the 330 nm absorbance values upon

Figure 22

Time studies of changes in the 330 nm and 415 nm peak intensities upon occupation of the primary Gd site. Plot of the fraction of native phosphorylase b absorbance *vs.* time. Gd at a concentration of 9.1 X 10^{-5} M was added to an equimolar concentration of enzyme at zero time. The buffer system which consisted of 30 mM BES, 3 mM DTT pH 6.8 was used as an optical reference.

O——O enhancement of absorbance at 415 nm

X——X enhancement of absorbance at 330 nm

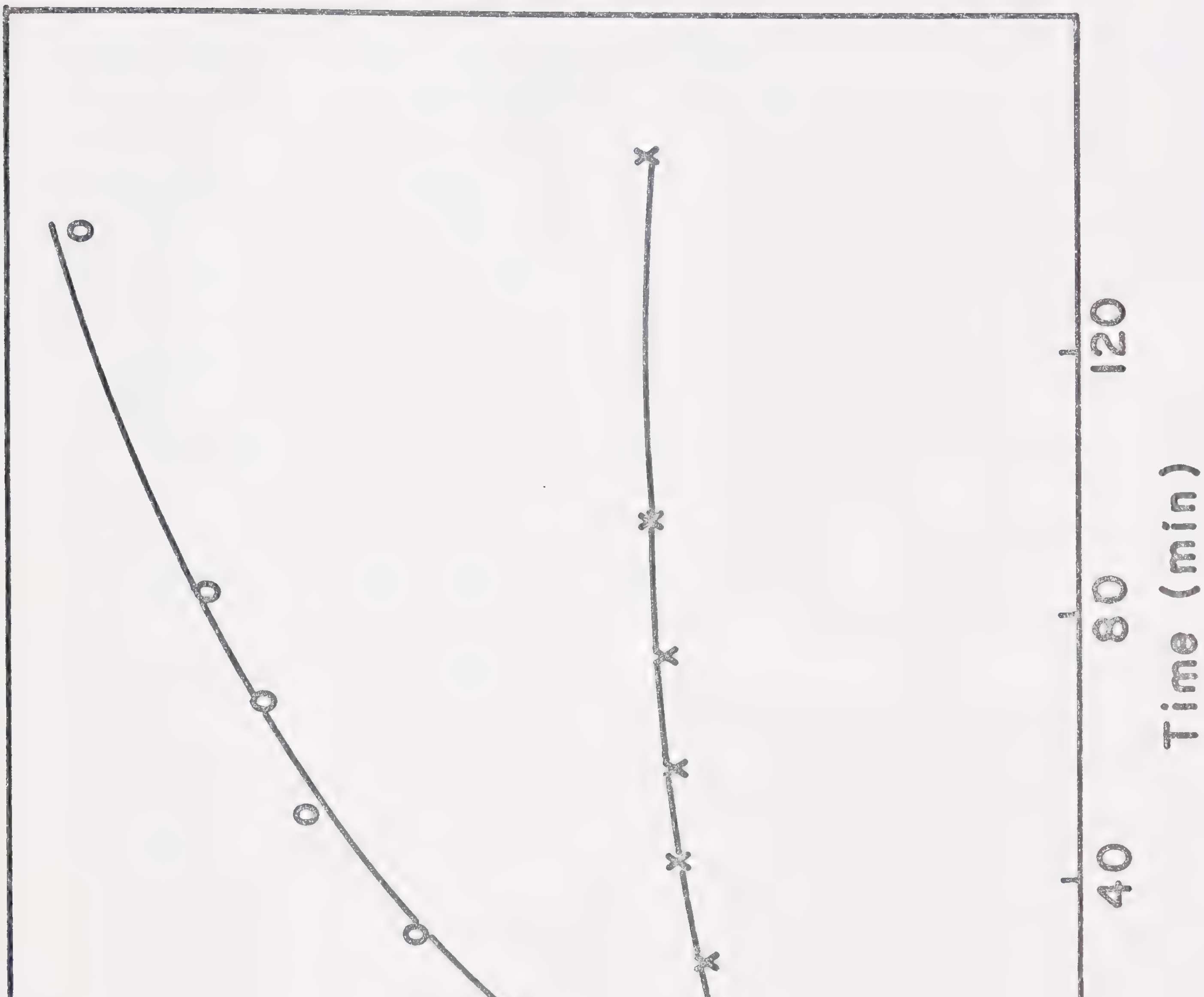
Fraction of Control Value
1
2
3
Time (min)
40
80
120

the reaction of monomer phosphorylase b and Gd at the same concentrations, 9.1×10^{-5} M, at 25°C.

However these absorption changes are complicated, to some extent, by the fact that Gd occupation of the high affinity site induces slight protein turbidity. To assess the significance of this light scattering effect on peak intensities at the coenzyme's characteristic wavelengths, the plot denoted in Figure 23 was examined. Curvature of a double log plot of the change in absorbance vs. wavelength, attributes the enhancement of the 415 nm peak intensity to a shift in the equilibrium of the coenzyme tautomers rather than to protein turbidity (73, 74). Absorbance values at 415 nm characteristic of this metalloprotein are reversed upon the addition of 1 mM AMP and 14 mM G-1-P, indicating that the ternary enzyme complex is capable of re-establishing the integrity of the coenzyme pocket.

ii. Sedimentation Velocity Studies

To assess whether the metalloprotein's characteristics are due to alterations of subunit interactions, sedimentation velocity data was collected with phosphorylase b at 3.8 mg/ml in 30 mM BES, 3 mM DTT pH 6.8 reacted with an equimolar concentration of Gd. The native enzyme sedimented at 8.5×10^{-13} whereas the metalloprotein expresses a value of 9.6×10^{-13}, as illustrated in Figure 24. Preincubation of the enzyme with 1 mM AMP prior to metal addition results in the same schlieren patterns with phosphorylase b-AMP and the Gd-phosphorylase b-AMP complexes sedimenting at 8.5 and 9.6×10^{-13} respectively. Wang et al (72) under different buffer conditions obtains S values in the order of 8.3×10^{-13} for native phosphorylase b and 9.7×10^{-13} in the presence of 1 mM AMP. These results confirm metal alterations of sub-

Figure 23

Log plot of the change in absorbance with wavelength of phosphorylase b reacted with an equimolar concentration of Gd. Phosphorylase b at 8.3 X 10^{-5} M was reacted with an equimolar concentration of Gd at 25°C for 20 hr in 30 mM BES, 3 mM DTT. Absorbance values for the native and metallo forms of the enzyme were determined against a buffer blank.

X——X native enzyme

O——O metalloenzyme

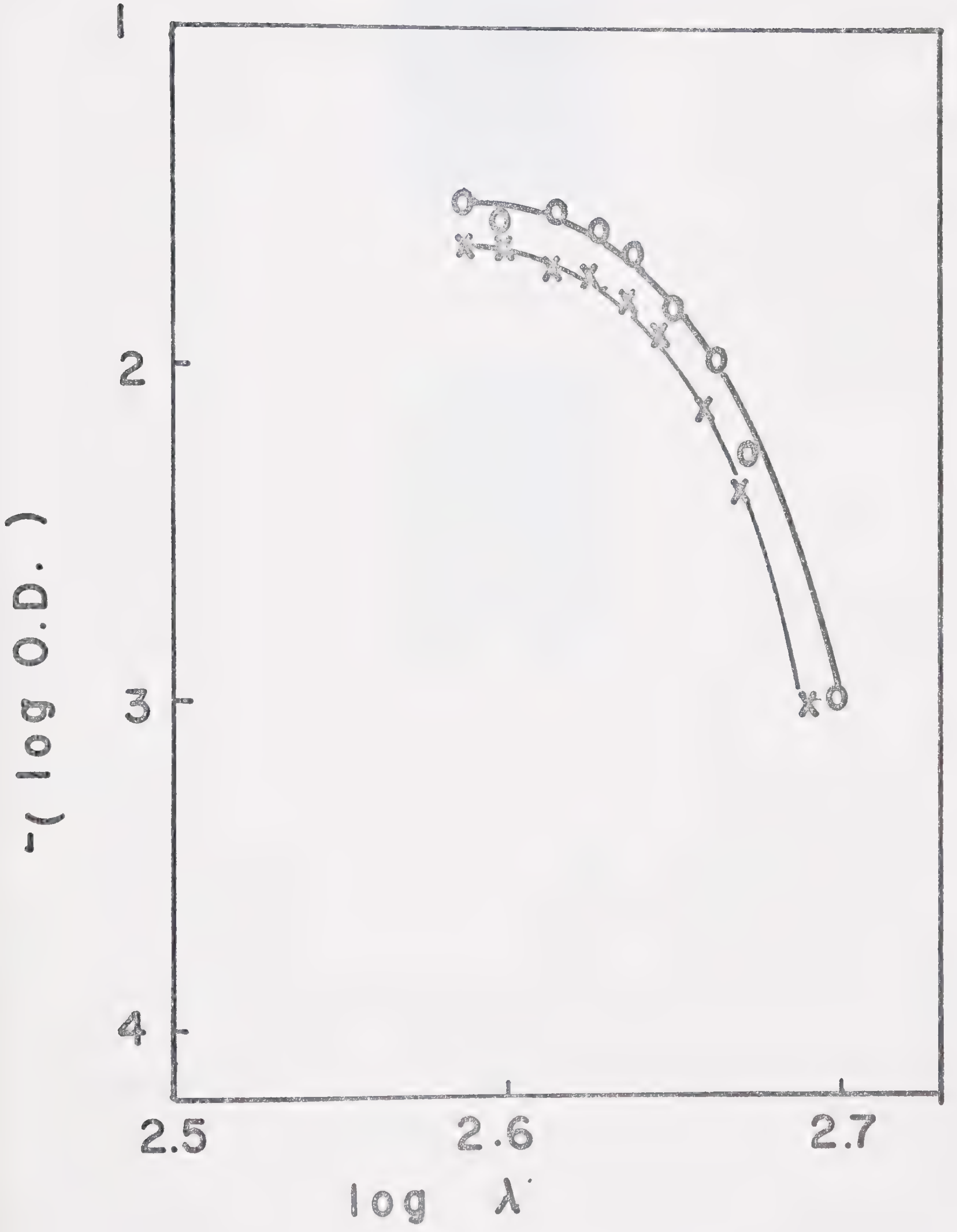
1
2
3
4
2.5
2.6
2.7
log λ
-(log O.D.)

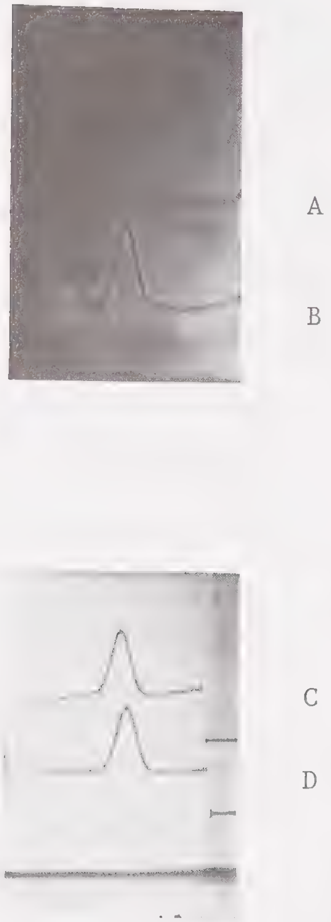

Figure 24

Sedimentation velocity study of phosphorylase b in the presence and absence of 1 mM AMP reacted with an equimolar concentration of Gd. The buffer system, which contained 3.8 mg/ml of the enzyme, consisted of 30 mM BES, 3 mM DTT pH 6.8. Native phosphorylase b (A) and the AMP-phosphorylase b complex (B) sedimented as single schlieren peaks (8.52). In the presence of an equimolar concentration of Gd, the native complex sedimented as illustrated in D (9.64) and the AMP-phosphorylase b complex formed the schlieren peak C (9.61). The numbers in brackets refer to the schlieren peak location in svedburg units at 20°C.

unit interactions are not influenced by the binding of the effector , AMP, to the active site of the phosphorylase b subunit.

Conversely the Gd site appears to exert negligible influences over AMP binding to phosphorylase as the homotropic effects of AMP are retained unaltered in the metalloprotein. A reciprocal plot of velocity vs. AMP concentration was obtained with 9.2×10^{-5} M phosphorylase b incubated with an equimolar concentration of Gd for 2 hr. at 30°C., prior to activity analyses. The substrate used contained 75 mM G-1-P and 1% glycogen pH 6.8. The sigmoidicity of the plot corresponds with the native enzyme and calculated K_m and V_{max} values are also comparable.

iii. Coenzyme Characteristics

Reaction of the metalloprotein with $NaBH_4$ reduces the absorption intensity at 415 nm to native values. This would indicate that the enhancements in absorbance at this wavelength are due to an increased solvent accessability of the coenzyme pocket.

To determine the proximity of the high affinity Gd site to the coenzyme, the peak width and chemical shift of the phosphorous resonance peaks of PLP within the native and the metalloenzyme were examined. Phosphorous resonance peaks corresponding to the coenzyme, Figure 25, consists of at least two components exhibiting chemical shifts of 108 Hz and 492 Hz relative to a phosphoric acid reference. The difference in the chemical shifts between the two major resonances of 384 Hz corresponds within experimental error to the analogous parameter reported by Busby et al (75). Although estimates of the total linewidths are complicated by the low signal to noise ratio, the $\Delta\nu_T$ of

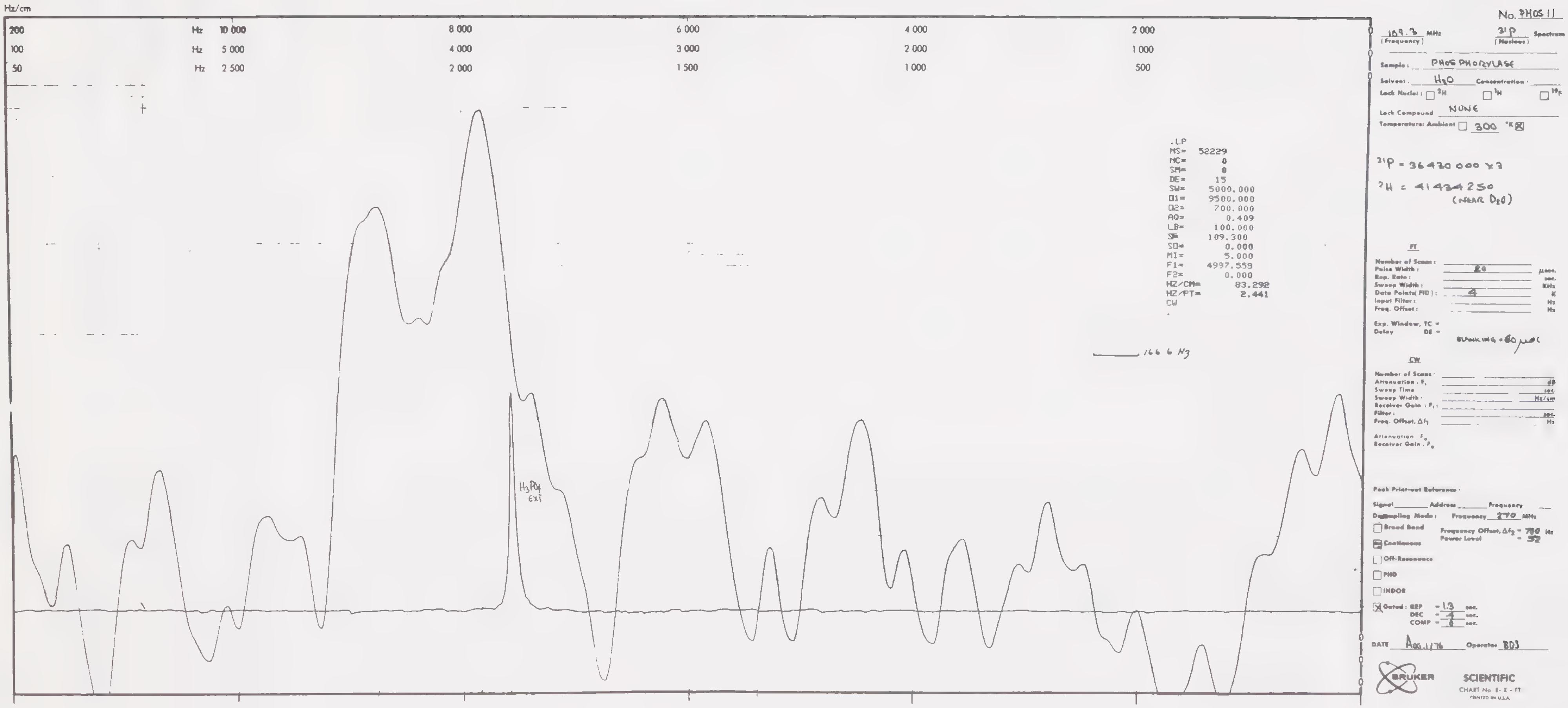

```
.LP
NS=   52229
NC=       0
SM=       0
DE=      15
SW=     5000.000
O1=     9500.000
O2=      700.000
AQ=        0.409
LB=      100.000
SF=     109.300
SO=        0.000
MI=        5.000
F1=     4997.559
F2=        0.000
HZ/CM=        83.292
HZ/PT=         2.441
CW
.
```

No. PHOS 11

109.3 MHz (Frequency) 31P (Nucleus) Spectrum

Sample: PHOSPHORYLASE

Solvent: H_2O Concentration:

Lock Nuclei: ☐ ^2H ☐ ^1H ☐ ^{19}F

Lock Compound NONE

Temperature: Ambient ☐ 300 °K ☒

$^{31}P = 36\,430\,000 \times 3$

$^2H = 41\,434\,250$ (NEAR D_2O)

FT

Number of Scans:

Pulse Width: 20 µsec.

Rep. Rate: sec.

Sweep Width: KHz

Data Points (FID): 4 K

Input Filter: Hz

Freq. Offset: Hz

Exp. Window, TC =

Delay DE =

BLANKING = 60 µsec

CW

Number of Scans:

Attenuation: F_1 dB

Sweep Time sec.

Sweep Width: Hz/cm

Receiver Gain: F_1:

Filter: sec.

Freq. Offset, Δf_1 Hz

Attenuation F_0

Receiver Gain, F_0

Peak Print-out Reference:

Signal ______ Address ______ Frequency ___

Decoupling Mode: Frequency 270 MHz

☐ Broad Band

☒ Continuous

☐ Off-Resonance

☐ PHD

☐ INDOR

☒ Gated: REP = 1.3 sec.
DEC = .4 sec.
COMP = .8 sec.

Frequency Offset, Δf_2 = 780 Hz

Power Level = 32

DATE Aug. 1/76 Operator BDS

BRUKER SCIENTIFIC

CHART No. B-X-FT

PRINTED IN U.S.A.

Figure 25

Phosphorous n.m.r. spectra of native phosphorylase b within the solution state. Reaction conditions were previously described in Methods (B-7).

675 Hz parallells the line broadening expected at a frequency bracketed by the values published for spectra at 36.4 MHz and 129 MHz (75).

Upon the addition of Gd, Figure 26, the ratio of the intensities of the two major peaks decreases from 0.94 to 0.85 and $\Delta\nu_T$ increases to 1016 Hz. However the chemical shifts of P^{31} in the metalloprotein complex coincide with the values of the native enzyme.

At 109.3 MHz, the primary factor regulating linewidth is the anistropy of the phosphorous group with a minor contribution due to dipolar relaxation. Therefore enhancements of $\Delta\nu_T$ reported for the Gd-phosphorylase b complex may be attributed either to changes in the chemical shift anistropy due to metal induced conformational alterations of the coenzyme's environment or to the proximity of the paramagnetic ion to the P^{31} nucleus. Differentiation between these two modes of interaction requires higher spectral resolutions. It was interesting to note, however, that visible and ultraviolet spectral analyses in conjunction with the increased accessability of the schiff base to $NaBH_4$ reduction would suggest from both structural models of the coenzyme (see Introduction), an increased accessability of PLP to solvent molecules. If the hydrophobicity of the pocket coordinating the coenzyme is in fact decreased, the phosphate group may experience fewer steric restraints on its degree of orientational freedom, a property which would contrast with the $\Delta\nu_T$ observed in the P^{31} spectra.

iv. Reversibility of Metal Binding

The addition of an equimolar concentration of EDTA to phosphorylase b at 6.6×10^{-5} M preincubated with an equal concentration of Gd at 30°C for 2.5 hr results in a slow reversal of the metalloprotein's characteristic spectra to native values. After three hours,

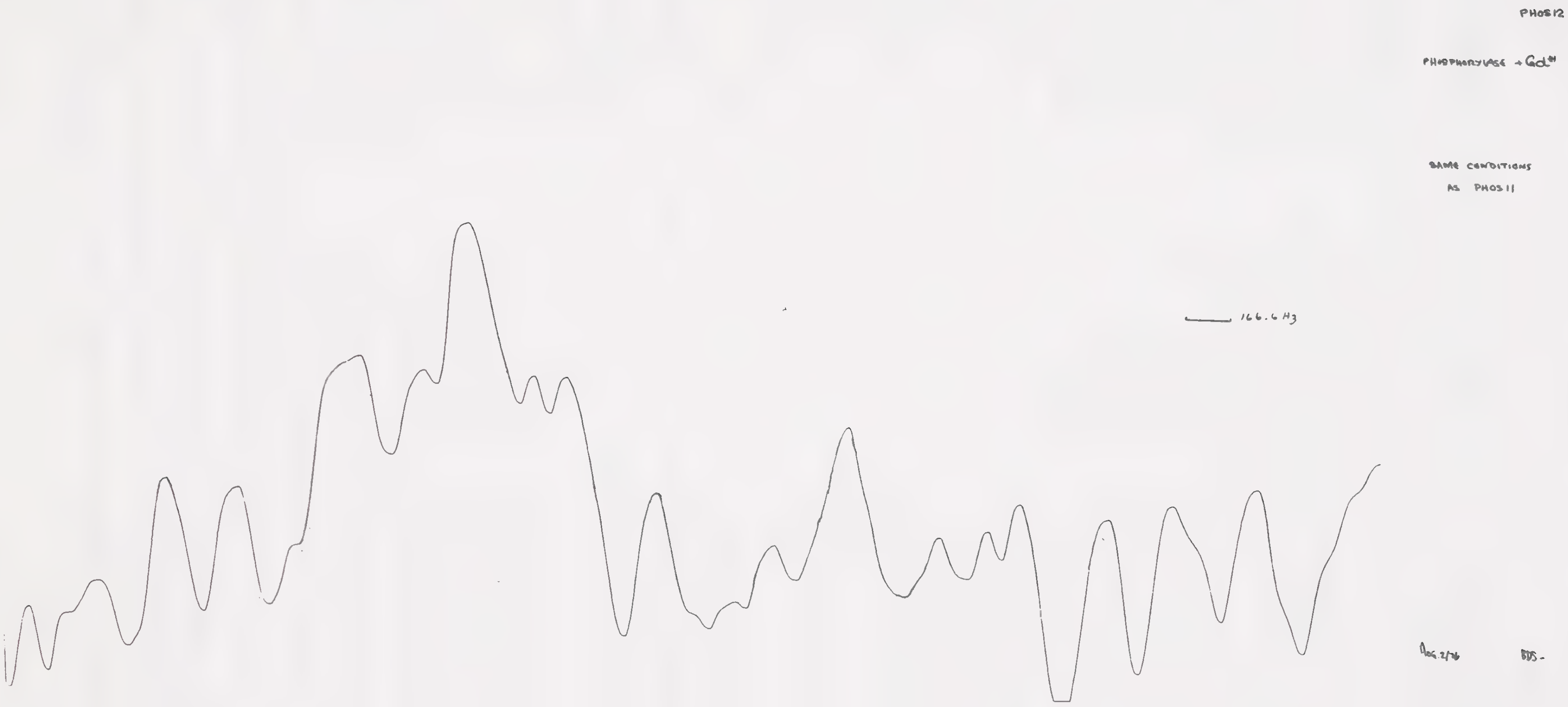

Figure 26

Phosphorous NMR spectra of phosphorylase b upon occupation of the primary Gd site within the solution state. Reaction conditions were outlined in Methods (B-7).

the conversion as evidenced by this method is virtually complete.

v. Sulfhydryl Reactivity

To obtain further information regarding metal induced conformational changes, the reactivity of the metalloprotein's sulfhydryl groups with DTNB and PCMB were evaluated. A one to one mole ratio of monomer to Gd was incubated for 2.2 hr at 25°C before the addition of 0.45 mM DTNB or 1×10^{-5} M PCMB. Samples were diluted 90 fold in 30 mM BES to eliminate possible metal interference with the sulfhydryl reagents. The native and the metallo forms of phosphorylase b are modified at the same rate and to the same extent with both PCMB, Fig. 21, and DTNB, thus confirming only localized metal induced conformational changes.

2. Gadolinium Interactions with Phosphorylase in the Crystalline State

a. Activity Studies with Crosslinked Crystals

Previous sections dealt with the metal induced inactivation of phosphorylase in solution. Analogous studies were conducted with tetragonal crystals of the enzyme to ascertain whether Gd promoted similar effects within this state.

Substrate solutions or crystal buffers, containing Gd concentrations exceeding 10 mM, solubilized microcrystals of phosphorylase. Therefore the tetragonal microcrystals were crosslinked with glutaraldehyde prior to activity assays or to exposure to saturating concentrations of Gd. Microcrystals of phosphorylase a incubated for 2 days in either 10 mM or 40 mM Gd were diluted ten fold in substrate at zero time. Aliquots were removed and assayed for P_i release as described in Methods. Linear regression analyses of the rate of P_i production are clearly indicative of metal induced inactivation. In the absence of Gd,

the crystals express activities in the order of 7.62 ± 0.16 nmol /min/mg, whereas in the presence of 10 mM or 40 mM Gd the activities are respectively 5.26 ± 0.12 and 0.052 ± 0.003 nmol /min/mg.

Analogous experiments with crystals of phosphorylase b are less conclusive as the presence of IMP in the crystal buffer served to sequester Gd ions, Table 5. Consequently the concentration of free Gd is not adequate to provide significant occupation of the low affinity Gd site responsible for inducing inactivation of the enzyme.

C. Discussion

The extent of correlation between Gd binding sites in the two physical states of phosphorylase is assessed by comparing the physicochemical characteristics of the metalloprotein within the solution state with the protein environment of the metal sites determined from x-ray crystallographic maps of phosphorylase a. Coordinates determined by Fletterick et al (17) for the heavy metal derivatives of phosphorylase at 6 A° resolution, Table 4, demonstrate Gd occupation of two unique sites per monomeric unit. Although Gd replacement under the conditions of their experiment is not isomorphous, the diffraction data are interpretable. However, prolonged incubation of the crystal with Gd concentrations exceeding 10 mM induces major disruptions of the crystal lattice (79). Therefore allocations of weaker, alternate Gd sites are unavailable from the direct interpretation of x-ray maps of the enzyme.

Analyses of Scatchard plots, obtained from water proton relaxation data with the solution form of the metalloprotein, demonstrate the existence of a single, unique Gd site per subunit with an apparent K_D of 1.4 μM. In addition the absence of further increases in the ε^* parameter upon titration of phosphorylase with Gd indicate that this metal site is the sole contributor responsible for relaxation enhancement and is therefore highly accessible to solvent contact. Extending these characteristics to the crystalline state of the Gd-phosphorylase a complex, it appears that Gd site 1, which exhibits both a high occupancy factor and coordinates situating it on the protein solvent interface, correlates with the solution form of the metalloprotein in this respect. However a recent difference fourier analysis of a phosphorylase a crystal soaked in a Mg free buffer which contained 0.1 mM Gd,

indicates occupancy of Gd site 2 in preference to Gd site 1 (77). In other words, the absence of M_g competition with Gd ions for the protein increases the Gd binding potential of the second metal locus. If the K_D of 5.10 mM reported by Birkett (14) for the second Mn site of phosphorylase b is correct, then the high affinity Gd site, which in solution expresses a K_D of 1.4μM, should be able to effectively displace the Mg ion during the 24 hr. soaking period. The solution studies with the Gd-phosphorylase complex were conducted in the absence of 10 mM Mg, therefore an apparent discrepancy exists between the solution and the crystal results.

Modulation of the enzyme's characteristics examined in this study upon occupation of the primary Gd site in solution include perturbations of both subunit interactions and the equilibrium between tautomeric structures of the coenzyme. However observations regarding the retention of catalytic efficiency, AMP homocooperativity and sulfhydryl reactivity within the metalloprotein at levels which parallelled the native enzyme, suggest the induction of only localized protein perturbations upon Gd coordination. The maintenance of active site integrity would be compatible with Gd sites 1 and 2 as these loci are situated within the crystal lattice more than 20 A° removed from the G-1-P coordinates.

Incubation of phosphorylase with an equimolar concentration of Gd also induces the formation of a modified dimer in the case of phosphorylase b both in the presence and absence of 1 mM AMP and enhances tetramer formation with phosphorylase a. It was interesting to note that Wang (74) observed identical perturbations of the quaternary structure when 1 mM AMP was incubated with the two enzyme forms. The

slight turbidity incurred upon Gd occupation of the primary site could be attributed either to the involvement of Gd in the initiation of enzyme crystallization or to the formation of a less stable adduct upon Gd modulation of the alpha aggregation site relative to the effector AMP. If site 1 were equivalent to the high affinity site defined from solution studies, then alterations of subunit interactions would be attributed to conformational changes centered at a locus 30 A° removed from the metal site. Gadolinium site 2 however is situated nearer the dimer interface. In addition the metals $MnCl_2$ and $Pb(NO_3)_2$ coordinated within angstroms of this Gd 2 locus. Kent (10) demonstrated that phosphorylase b preincubated with 1 mM AMP formed tetramers in the presence of these two divalent cations. However in the absence of effector molecules, subunit interactions remained in the native form. If Gd effects parallelled those induced by Mn and Pb ions at site 2, then it would be difficult to rationalize the observed modification of dimer interaction in a one to one complex of Gd to phosphorylase b in the absence of AMP. These observations suggest a closer correlation between the high affinity Gd site in the solution state with Gd site 1 of the crystalline state.

The shift in equilibrium in favour of the molecular species of PLP absorbing at 415 nm, as an equimolar concentration of Gd to monomer is added, appear to be due to an increased solvent accessability of the coenzyme pocket, as the reaction of the metalloenzyme with $NaBH_4$ led to a reduction in the absorbance at 415 nm. However incubation of this metalloprotein with 1 mM AMP and 14 mM G-1-P serves to reverse the spectral band intensity at 415 nm to that characteristic of the native enzyme. Difficulties arose in correlating these coenzyme results with the

environment of Gd sites 1 and 2 as the locus of PLP within the crystal lattice has yet to be established. Phosphorous n.m.r. spectra were recorded to provide some information concerning the proximity of Gd to PLP. With respect to chemical shifts and $\Delta\nu_T$, the native enzyme correlates with the P^{31} spectra reported by Busby (75) for the coenzyme of phosphorylase b. Discrepencies between their work and the results of Feldman (9) were originally attributed to differences in enzyme concentration and perhaps AMP contamination of the sample. The significance of the former parameter was discounted as this study was conducted at protein concentrations parallelling those used by the German group. Therefore the basis for these different results has yet to be resolved.

A positive aspect of the P^{31} study is the fact that Gd interaction with phosphorylase b exerts subtle effects on the spectra of the coenzyme. Previous work by Barry (78) and Tanswell (79) had demonstrated the effect of the isotropic broadening probe, Gd, on nuclear relaxation. Therefore direct coordination of this lanthanide ion to the phosphorous nucleus would decrease the resonance peak intensities to noise levels. Since this property is not observed, the enhancement of $\Delta\nu_T$ is attributed either to metal induced conformational changes or to Gd complexation centered at a locus less than 20 A° away from the PLP site. Differentiation between these two modes of interaction is difficult to ascertain due to the poor quality of the spectra.

On the basis of spectral titration and protection studies obtained with the solution form of the enzyme, the existence of a second Gd site is proposed. Spectral analyses indicates the reversal of the enhanced PLP absorption peaks induced by the high affinity Gd site to native values with phosphorylase b. This property may be attributed

to a reinstatement of the coenzyme pocket's conformation to a state approximating the native enzyme. The apparent K_D of this second site as evidenced from spectral titration curves (Figures 10 and 11) is approximately 6.0 μM, therefore this metal locus would be sufficiently occupied under the conditions of the n.m.r. experiment to exert paramagnetic effects on water proton relaxation. The absence of altered ε_B values after saturation of the high affinity Gd site was attained would therefore be due to a shielding of the metal's primary coordination sphere from water proton contact. To summarize the observations concerning the second Gd site thus far, this metal locus, which is protected by protein folding from the bulk solvent, exhibits a high affinity for Gd ions. Gadolinium occupation of this site returns the equilibrium of the coenzyme's tautomeric structures to a state characteristic of the native enzyme and in addition this metalloprotein retains activity.

Additional confirmation of an alternate Gd site may be inferred from effector and substrate protection studies. In the presence of a 75 molar excess of Gd to monomer, phosphorylase is inactivated and its subunit interactions are disrupted. However, preincubation of phosphorylase b with AMP, IMP and ATP at respective concentrations of 1 mM, 10 mM and 5 mM protect the enzyme from Gd induced inactivation and cause immediate protein turbidity upon the addition of a 75 molar excess of the metal. Sedimentation velocity studies indicate that the nucleotide-phosphorylase b-Gd complexes formed tetramers. Under the same reaction conditions, the substrate, G-1-P, prevents inactivation without the concurrent induction of protein turbidity. The disparity between the modes of effector and substrate modulation of the enzyme's affinity for Gd at the low affinity site may be attributed either to

differing effects on the subunit interaction sites or on the allosteric states of the enzyme or on the metal chelation ability of the phosphate functional groups. The former two possibilities may be eliminated on the basis of the following previously published data. Under the experimental conditions of this study, AMP, IMP, G-1-P and glucose had no discernable effect on the subunit interactions of native phosphophosphorylase _b_, whereas ATP promotes monomerization (85). Allosteric interpretations, using the nomenclature previously defined (8), would indicate that the R', I and IMP-phosphorylase _b_ states of the enzyme express a lower affinity for Gd relative to the T state. However at concentrations wherein the substrate exerts virtually complete protection, G-1-P binds only weakly to the T state. Therefore the protection of phosphorylase _b_ from Gd effects at high concentrations of the metal, appears to be due to the ability of phosphate to sequester Gd ions, Table 5. Consequently Gd chelation by ATP, IMP, AMP and G-1-P would prevent significant occupation of the Gd site(s) responsible for inducing subunit dissociation and inactivation, whereas the Gd site number 2 would be capable of coordinating metal ions at these concentrations.

The previously mentioned sedimentation velocity studies of the nucleotide-phosphorylase _b_-Gd complexes imply that Gd occupation of the second metal site promotes tetramerization of the enzyme in the presence of AMP, IMP and ATP. This observation in conjunction with the retention of the integrity of the active and coenzyme sites, suggests strong similarities between this locus and the divalent cationic site characterized by Kent (10). Of the two Gd sites published by Fletterick (17) for phosphorylase _a_, Gd site 2 exhibits properties which align most satis-

Table V

Complexation of Effectors and Substrates with Phosphorylase _b_, Mn and Gd

Ligands	Dissociation Constant (mM)			Concentration of Ligand (mM)
	phosphorylase _b_[a]	Mn[b]	Gd[c]	
AMP	0.2 (0.3)	3.5		0.5, 1.0, 2.0
G-1-P	50	34		12.3
ATP	0.7	0.032[c]	0.0001	5.0
IMP	1.0	5.0		10.0
glucose		negligible		50.0

The column on the extreme right indicates the ligand concentrations used in the protection studies involving the low affinity Gd site. The superscripts "a", "b", and "c" refer respectively to references 80, 14 and 81.

factorily with the observed characteristics of the secondary Gd locus within the solution state of phosphorylase.

Crystallographic and proton relaxation data failed to discern the weaker site(s) of Gd interaction with phosphorylase. Since spectral and activity studies of phosphorylase b in solution equilibrated with varying concentrations of Gd indicate a fifty percent occupancy of this site at a metal concentration of 1.5 mM, Gd coordination to the protein would be too weak to affect ε_B significantly. Additional verification of the weak interaction of Gd with this site was obtained from the previously outlined ligand protection studies.

Occupation of the low affinity Gd site(s) upon incubation of the solution form of the enzyme with concentrations of metal exceeding 1.5 mM, is characterized by polydisperse schlieren peaks, loss of enzymatic activity, increases in the peak intensities at 415 nm, loss of AMP homocooperativity and enhanced reactivity of Cys residues with DTNB and PCMB.

The loss of catalytic activity may be a direct result of the perturbation of subunit interactions, as x-ray maps of phosphorylase have situated the active site in close proximity to the dimer interface. It was interesting to note that phosphorylase crystals incubated with a 10 mM or greater concentration of Gd also express significant conformational changes. Metalloprotein crystals, uncrosslinked with glutaraldehyde, are solubilized within a few hours. The crosslinked crystals of phosphorylase a, used in activity assays, exhibit fracturing of the crystal lattice structure and losses of activity upon exposure to saturating Gd concentrations. Both lines of evidence suggest that the Gd induced changes of the protein's conformation are capable of disrupting

crystal lattice stabilization forces.

Modulation of the PLP pocket in phosphorylase solutions containing a 20 or greater molar excess of Gd to monomer are not due to the direct stabilization of the schiff base via Gd coordination between the phenolic group of the pyridoxal ring and the imine nitrogen. This conclusion was based on the absence of fluorescence quenching and spectral peak shifts within the metalloprotein. The opposite characteristics are observed with the metallocomplexes of pyridoxal derivatives. Therefore, occupation of the lowest affinity site by Gd induces conformational repercussions at the coenzyme pocket. The PLP site within the metalloenzyme experiences increased contact with the bulk solvent, as evidenced by the complete reduction of the schiff base with $NaBH_4$ and the increased reactivity of PLP with NH_2OH. Although an isosbestic point is observed Figure 16, the rate of peak intensity increases at 415 nm preceeds the loss of optical density at 330 nm. These data suggests that the protein bound PLP consists of an equilibrium mixture involving more than two molecular structures of the coenzyme and that Gd promotes the formation of the schiff base tautomer which absorbs at 415 nm.

The specificity of the low affinity Gd site is difficult to establish on the basis of the preceeding data. However analogies between the protein characteristics expressed upon carbodiimide modification (84) and Gd coordination suggest that the site of modulation may be centered at identical functional groups. Incorporation of 1-1.4 ^{14}C-glycinate ethyl ester molecules per subunit upon carbodiimide activation of phosphorylase in solution, indicate that the perturbation of a unique site is responsible for alterations of the active, coenzyme and subunit interaction sites.

Bibliography

1. Graves, D.J., Wang, J.H. (1972). In "The Enzymes" (P.D. Boyer, ed.), vol. 7, p. 435. Academic Press, New York and London.
2. Engers, H.D., Bridger, W.A., Madsen, N.B. (1969). J. Biol. Chem. 244, 5936.
3. Huang, C.Y., Graves, D.J. (1970). Biochem. 9, 660.
4. Chignell, D.A., Gratzer, W.B., Valentine, R.C. (1971). J. Biol. Chem. 236, 1082.
5. Seery, V.L., Fischer, E.H., Teller, D.C. (1970). Biochem. 9, 3591.
6. Honikel, K.O., Madsen, N.B. (1973). Can. J. Biochem. 51, 344.
7. Johnson, G.F., Tu, J.I., Bartlett, M.L.S., Graves, D.J. (1970). J. Biol. Chem. 245, 5560.
8. Madsen, N.B., Avramovic-Zikic, O., Lue, P.F., Honikel, K.O. (1976). Molecular and Cellular Biol. 11, 35.
9. Feldman, K., Helmreich, E.J.M. (1976). Biochem. 15, 2394.
10. Kent, A.B., Krebs, E.G., Fischer, E.H. (1958). J. Biol. Chem. 232, 549.
11. Honikel, K.O., Madsen, N.B. (1972). J. Biol. Chem. 247, 1057.
12. Radda, G.K. (1970). FEBS Lett. 11, 295.
13. Buc, H. (1967). Biochem. Biophys. Res. Commun. 28, 59.
14. Birkett, D.J., Dwek, R.A., Radda, G.K., Richards, R.E., Salmon, A.G. (1971). Eur. J. Biochem. 20, 494.
15. Kasvinsky, P., Madsen, N.B. (1976). J. Biol. Chem. (in press).
16. Busby, S.J.W., Radda, G.K. (1976). In "Current Topics in Cellular Regulation" (B.L. Horecker, R.R. Stadman, eds.), vol. 10, p. 90.

Academic Press, New York and London.

17. Fletterick, R.J., Sygusch, J., Murray, N., Madsen, N.B., Johnson, L.N. (1976). J. Mol. Biol. 103, 1.

18. Fischer, E.H., Krebs, E.G. (1962). In "Methods in Enzymology" (S.P. Colowick, N.O. Kaplan, eds.), vol. 5, p. 69. Academic Press, New York and London.

19. Krebs, E.G., Love, D.S., Bratvold, G.E., Trayser, K.A., Meyer, W.L., Fischer, E.H. (1964). Biochem. 3, 1022.

20. Wada, H., Snell, E.E. (1965). J. Biol. Chem. 236, 2089.

21. Graves, D.J., Sealock, R.W., Wang, J.H. (1965). Biochem. 4, 290.

22. Barry, C.D., North, A.C.T., Glasel, J.A., Williams, R.J.P., Xavier, A.V. (1971). Nature (London) 232, 236.

23. Green, A.A., Cori, G.T. (1943). J. Biol. Chem. 151, 21.

24. Hedrick, J.L., Fischer, E.H. (1965). Biochem. 4, 1337.

25. Hu, H., Gold, A.M. (1975). Biochem. 14, 2224.

26. Buc, M.H., Buc, H. (1968). In "Symposium on Regulation of Enzyme Activity and Allosteric Interactions" Oslo, July, 1967. Academic Press, New York and London.

27. Lowry, O.H., Rosebrough, A. (1951). J. Biol. Chem. 193, 265.

28. Ross, E., Schatz, G. (1973). Analytical Biochem. 54, 304.

29. Janota, H.F., Ayres, G.H. (1964). Analytical Chem. 36, 138.

30. Allan, J.E. (1962). Spectrochim. ACTA 18, 259.

31. Matsushima, Y., Martell, A.E. (1967). J. Am. Chem. Soc. 89, 1322.

32. Adler, A.J., Greenfield, N.J., Fasman, G.D. (1973). In "Methods in Enzymology" (C.H.W. Higgs, S.W. Timasheff, eds.), vol. 27, p. 675. Academic Press, New York and London.

33. Chen, Y., Yang, J.T., Chau, K.L. (1974). Biochem. 13, 3350.

34. Carr, H.Y., Purcell, E.M. (1954). Physics Rev. 94, 630.

35. Johnson, L.N., Madsen, N.B., Mosley, J., Wilson, K.S. (1974). J. Mol. Biol. 90, 703.

36. Belluco, U. (1974). In "Organometallic and Coordination Chemistry of Platinum" (P.M. Maitlis, F.G.A. Stone, R. West, eds.), p. 19, Academic Press, New York and London.

37. Thompson, A.J., Williams, R.J.P., Resolva, S. (1972). Structure and Bonding 11, 1.

38. Morris, C.R., Gale, G.R. (1973). Chemico-Biol. Interactions 7, 305.

39. Haake, P., Turley, P.C. (1967). J. Am. Chem. Soc. 89, 4611.

40. Wade, M., Tsernglou, D., Hill, E., Webb, L. (1974). Biochem. Biophys. Acta 322, 124.

41. Wyckoff, H.W. (1967). J. Biol. Chem. 242, 3750 and 3984.

42. Hedrick, J.L. (1966). Arch. Biochem. Biophys. 114, 216.

43. Johnson, G.F., Graves, D.G. (1966). Biochem. 5, 2906.

44. Fletterick, R.J., Sygusch, J. (1976). J. Biol. Chem. (in press).

45. Battell, M. (1968). MSc Thesis, U. of Alberta.

46. Ellman, G.L. (1959). Arch. Biochem. Biophys. 82, 70.

47. Crick, F.H.C., Magdoff, B.S. (1956). ACTA Crystallography 9, 901.

48. Avramovic-Zikic, O., Smillie, L.B., Madsen, N.B. (1970). J. Biol. Chem. 245, 1558.

49. Kastenschmidt, L.L., Kastenschmidt, J., Helmreich, E. (1968). Biochem. 10, 3590.

50. Moeller, T. (1965). Chem. Rev. 65, 1.

51. Birnbaum, E.R., Gomez, J.E., Darnall, D.W. (1970). J. Am. Chem. Soc. 92, 5287.

52. Darnall, D.W., Birnbaum, E.R. (1970). J. Biol. Chem. 245, 6484.

53. Freeman, A.J., Dimmond, J.O., Watson, R.E. (1966). In "Quantum Theory of Atoms and Molecules, and the Solid State" (P. Löwden, ed.) Academic Press, New York and London.

54. Handbook of Chemistry and Physics (1971-72). The Chemical Rubber Co., 52nd Edit.

55. Birnbaum, E.R., Darnall, D.W. (1973). Bioinorg. Chem. 3, 15.

56. Ricci, R.W., Kilichowski, K.B. (1974). J. Phys. Chem. 78, 1953.

57. Sherry, A.D., Cottam, G.L. (1973). Arch. Biochem. Biophys. 156, 665.

58. Dwek, R.A. (1973). In "Nuclear Magnetic Resonance in Biochemistry" Clarendon Press, Oxford.

59. Dwek, R.A., Morallee, K.G. (1971). Eur. J. Biochem. 21, 204.

60. Reuben, J. (1971). Biochem. 10, 2834.

61. Dwek, R.A., Jones, R. (1974). Eur. J. Biochem. 47, 271.

62. Reuben, J. (1974). Biochem. 13, 1777.

63. Furie, B., Eastlake, A., Schechter, A.N., Anfinsen, C.B. (1973). J. Biol. Chem. 248, 5821.

64. Dwek, R.A., Radda, G.K. (1972). Eur. J. Biochem. 29, 509.

65. Martell, A.E. (1963). In "Chemical and Biological Aspects of Pyridoxal Catalysis" (E.E. Snell, P.M. Fasella, A. Braunstein, A.R. Fanelli, eds.), p. 13, Pergamon Press.

66. Smith, J.W. (1970). In "The Chemistry of Carbon Nitrogen Double Bonds" (S. Patai, ed.), p. 235, Interscience, New York.

67. Peterson, S.A., Sober, H.A. (1954). J. Am. Chem. Soc. 76, 169.

68. Shaltiel, S., Hedrick, J.L., Fischer, E.H. (1966). Biochem. 5, 2108.

69. Shaltiel, S., Cortijo, M. (1972). Eur. J. Biochem. 29, 134.

70. Radda, G.K. (1971). In "Current Topics in Bioenergetics" (D.R. Sandai, ed.), p. 81, Academic Press, New York and London.

71. Kriss, E.E. (1965). Ukr. Khim. Zh. 31, 328.

72. Black, W.J., Wang, J.H. (1968). J. Biol. Chem. 243, 5892.

73. Schneider, A.S. (1973). In "Methods in Enzymology" (C.H.W. Higgs, S.W. Timasheff, eds.), vol. 27, p. 774, Academic Press, New York and London.

74. Donovan, J.W. (1969). In "Physical Principles and Techniques of Protein Chemistry" (S.J. Leach, ed.), vol. A, p. 164, Academic Press, New York and London.

75. Busby, S.J.W., Gadian, D.G., Radda, G.K., Richards, R.E., Seeley, P.J. (1975). FEBS Letters 55, 14.

76. Honikel, K.O., Madsen, N.B. (1973). Can. J. Biochem. 51, 357.

77. Fletterick, R.J. personal communication.

78. Barry, C.D., Glasel, J.A., Williams, R.J.P., Xavier, A.V. (1974). J. Mol. Biol. 84, 471.

79. Tanswell, P., Thornton, J.M., Korda, A.V., Williams, R.J.P. (1975). Eur. J. Biochem. 57, 135.

80. Madsen, N.B. (1972). Molecular Basis of Biological Activity 1, 13.

81. Valentine, K.M., Cottam, G.L. (1973). Arch. Biochem. Biophys. 158, 346.

82. Van Holds, K.E. (1971). In "Circular Dichroism and Optical Rotary Dispersion" p. 203-220, Prentice-Hall Inc.

83. Eisenberg, D. (1970). In "The Enzymes" (P.D. Boyer, ed.), vol. I, p. 38, Academic Press, New York and London.

84. Avramovic-Zikic, O., Breidenbach, W.C., Madsen, N.B. (1974). Can. J. Biochem. 52, 146.

85. Devincenzi, D.L., Hedrick, J.L. (1970). Biochem. 9, 2048.

APPENDIX I

Calculations for Water Proton Relaxation Data

a. Observed Enhancement (ε^*)

$$\varepsilon^* = (1/T^*_{1P} - 1/T_{1P})/(1/T^*_{1M} - 1/T_1)$$

where $1/T^*_{1P}$ is the observed relaxation in the presence of Gd and protein,

$1/T_{1P}$ is the observed relaxation in the presence of protein,

$1/T_{1M}$ is the observed relaxation in the presence of Gd and buffer,

$1/T_1$ is the observed relaxation in the buffer.

b. Scatchard Plot

i. Relation of ε^* to the concentrations of free and bound Gd may be expressed as:

$$M_t \varepsilon^* = M_f \varepsilon_f + M_B \varepsilon_B$$

where M refers to the concentration of metal in molarity,

ε refers to relaxation enhancement,

the subscripts: f refers to unbound metal ions,

B refers to metal coordinated to protein,

t refers to the total metal concentration.

ii. Providing conditions of fast exchange exist $T^*_{1M} << \tau_M$ (60) then ε_f is equal to one.

iii. Once the concentrations of free and bound metal are determined from equation i, K_D and n may be determined from:

$$K_D = ((nE_f)(M_t - M_B))/M_B$$

by setting $x_B = M_B/M_t = (nE_f/(K_D + (nE_f))$

then $x_B/M_f = n/K_D - x_B/K_D$

where E refers to the concentration of phosphorylase monomer in molarity.

APPENDIX II

Calculations for Polarized Light Data

a. Optical Rotary Dispersion Calculations (82)

The fraction (f) of alpha helical, beta sheet and random coiled structures were determined from the following equations:

$$f_a = (b_o)_{ex}\,(630°)^{-1}$$

$$f_b = ((a_o)_{ex} + 325)\,(1050_o °)^{-1}$$

$$f_r = 1 - (f_a + f_b)$$

where the subscripts a refer to alpha helix,
b refer to beta sheet,
r refer to random coil,
ex refer to experimentally determined values from Yang Moffat plots.

The constants were derived from model studies (82).

	alpha helix	beta sheet	random coil
a_o	0°	400°	650°
b_o	-630°	0°	0°

b. Circular Dichroism Calculations (32)

The following equations were solved for the fractions of alpha helix (f_a) and beta sheet (f_b) using experimentally determined ellipticity factors (θ); where the subscript refers to the wavelength (nm) examined.

1. $\theta_{210} + 2200 = -24200\ f_a - 5990\ f_b$
$\theta_{215} - 500 = 26500\ f_a - 9330\ f_b$

2. $\theta_{210} + 2200 = -24200\ f_a - 5990\ f_b$

$\theta_{225} - 260 = -28960\ f_a + 1280\ f_b$

3. $\theta_{215} - 500 = -26500\ f_a - 9330\ f_b$

$\theta_{220} - 1670 = -30970\ f_a - 7380\ f_b$

4. $\theta_{215} - 500 = -26500\ f_a - 9330\ f_b$

$\theta_{225} - 260 = -28960\ f_a + 1280\ f_b$

5. $\theta_{220} - 1670 = -30970\ f_a - 7380\ f_b$

$\theta_{225} - 260 = -28960\ f_a + 1280\ f_b$

APPENDIX III

The Crick Magdoff Equation for Approximating the Fractional Change in Intensity Expected upon Heavy Atom Binding to a Protein Molecule

1. $$\frac{\text{rms } \Delta I}{(I)} = ((2N_H)/N_P)^{1/2}(f_H/f_P) = \frac{2 \text{ rms } \Delta F}{F}$$

where $\frac{\text{rms } \Delta I}{I}$ refers to the root mean square of the fractional intensity produced upon stoichiometric binding of heavy atoms to a protein molecule,

N_H refers to the number of heavy atom sites per protein molecule,

N_P refers to the number of atoms per protein molecule,

f_H refers to the number of electrons per heavy atom,

f_P refers to the number of electrons per protein monomer,

F is equivalent to $I^{1/2}$

2. Equation interpretation for phosphorylase-PAC complexes

Enzyme form	N_H	N_P	f_H*	f_P*	rms $\Delta F/F$
PHOSPHORYLASE _b_	1.0	8000	80	7	9%
PHOSPHORYLASE _a_	2.5	8000	80	7	15%

* reference 83

APPENDIX IV

Summary of the Properties of Metallocomplexes of Phosphorylase b

Enzyme Form	Native		Gd - b			PAC - b
	b	a				
Metal Sites			1	2	3	
Solution Properties						
Number of Sites			1	1	≥ 1	2-4
Apparent K_D			1.4 μM	6.0 μM	1.5 μM	covalent
Catalytic Activity	yes		yes	yes	no	no
Coenzyme Pocket	closed		slightly open	closed	open	open
Coenzyme Absorption Wavelength (nm)	330 > 415		415 peak increased	330 > 415	415 > 330	415 peak increased
Reactive Sulfhydryls B_1,B_2 A,N	2 2		2 2	2 2	9	2 1
Aggregation State	dimer	dimer and tetramer	modified dimer	tetramer	polydisperse M.W.	monomer
$S_{20,obs} X 10^{-13}$	8.6	8.6; 12.3	9.6	12.6	4.8 → 11.3	5.8
Ligand Protection			reversal with EDTA		AMP, ATP, G-1-P, IMP chelate Gd	AMP, Gd, G-1-P have no effect

Enzyme Form	Native		Gd - b			PAC - b
	b	a				
Metal Sites			1	2	3	
Other	metal requirement for crystallization .		site exposed to solvent; does not bind at PLP site.	no change in ε_B .	irreversible effect; does not bind at PLP site; disrupts AMP cooperativity.	415 nm peak increase preceeds inactivation.
Crystal Properties						
Catalytic Activity	active, K_M values approximate the solution state, however, V_{max} values are much lower.				crosslinked a inactive.	crosslinked b active, solubilized b is inactive.
Other	IMP and Mg are required for b crystallization, glucose and Mg are required for a crystallization.				promotes solubilization of uncross-linked crystals.	stabilizes crystal lattice structure.

B30170